Collective Dynamics in Infinite Networks of Pulse-Coupled Phase Oscillators

Diploma thesis
for the acquisition of the academic degree
Diplom-Physik (Dipl.-Phys.)

Friedrich-Schiller-Universität Jena
Faculty for Physics and Astronomy

by Stilianos Louca
born March 17, 1986 in Jena

Supervisor: Dr. Fatihcan M. Atay (Max Planck Institute for Mathematics in the Sciences)

Reviewers: Prof. Dr. Gerhard Schäfer (Friedrich-Schiller-Universität)
Dr. Fatihcan M. Atay

July 11, 2012

Abstract

In this thesis I study networks of identical pulse-coupled phase oscillators in the thermodynamic limit, that is, with the network size tending to infinity. Two models are considered in which oscillators are distributed on a separable metric space, according to a finite Borel measure. The first model is an evolution equation for the oscillator phase field, the second model is a continuity equation in the oscillator phase distribution. Both models are examined with respect to the existence and local stability of synchrony, i.e. all oscillators having one common, time-dependent phase. Continuing, all-to-all pulse-coupled networks of phase oscillators with additive white noise are examined, in the limit where pulses tend to Dirac distributions. This is done using a Fokker-Planck equation for the oscillator phase density. Particular interest is devoted to stationary states (i.e. time-independent phase densities), their existence, uniqueness, stability and bifurcation behaviour at a changing noise strength.

Zusammenfassung

In dieser Diplomarbeit befasse ich mich mit Netzwerken identischer pulsgekoppelter Phasenoszillatoren im thermodynamischen Grenzfall, das heißt im Übergang zu unendlich großen Netzwerken. Es werden zwei Modelle betrachtet in denen Oszillatoren auf einem separablen metrischen Raum gemäß eines endlichen Borelmaßes verteilt sind. Das erste Model ist eine Evolutionsgleichung im Phasenfeld, das zweite Model ist eine Kontinuitätsgleichung für die Phasenwahrscheinlichkeitsverteilung. Beide Modelle werden hinsichtlich Existenz und lokaler Stabilität synchroner Lösungen untersucht, das heißt in denen alle Oszillatoren die gleiche Phase aufweisen. Anschließend werden Netzwerke vollständig und gleichmäßig (*all-to-all*) gekoppelter Phasenoszillatoren mit additivem weisen Rauschen untersucht, im Grenzfall dass Oszillatorpulse die Form von Dirac-Distributionen annehmen. Dies geschieht unter Verwendung einer Fokker-Planck Gleichung für die Phasenwahrscheinlichkeitsverteilung. Spezielles Interesse ist stationären Zuständen (das heißt zeitunabhängigen Verteilungen) gewidmet, insbesondere hinsichtlich Existenz, Eindeutigkeit, Stabilität und Bifurkationsverhalten bei veränderlicher Rauschstärke.

Preface

The present thesis presents the results of my research at the Max Planck Institute for Mathematics in the Sciences in Leipzig, from September 2011 to May 2012. I had the luck to be supervised by Dr. Fatihcan Atay, coordinator of the research group "Dynamical Systems and Network Analysis".

I worked on so-called *networks of pulse-coupled phase oscillators*. These represent dynamical systems, composed of several simpler interacting units, each one possessing a stable limit cycle. Under certain assumptions on their limit cycles and coupling, these units can be approximated by so-called *phase oscillators*, that is, one-dimensional systems completely described by a single circular coordinate, their *phase*. Any interaction between them is therefore described by changes of their phase, either continuous or discontinuous in time. Such networks have seen increased attention in the last 50 years. They bear a great potential for the understanding of many naturally occurring complex systems, whose observed collective behaviour can not be traced back to the dynamics of their individual components. Prominent examples include neuronal networks and in particular parts of the central nervous system (Chawanya et al. 1993, Wang 1995), the interaction of cardiac pacemaker cells (Jalife & Antzelevitch 1979), coupled Josephson junctions (Wiesenfeld et al. 1998, Trees et al. 2005), the synchronization of flashing fireflies (Winfree 2001) and crowd synchrony on the Millennium Bridge (Strogatz et al. 2005, Eckhardt et al. 2007).

Numerous approaches exist for modelling the interaction of phase oscillators. One of them is the so-called Winfree model (Winfree 1967), in which each oscillator phase advances at a speed additively modulated by a so-called *stimulus*. The latter is a weighted sum of scalar-valued *pulses*, each one depending on the current phase of a distinct oscillator in the network. The contribution of the stimulus to a particular oscillator phase speed is weighted by a so-called *infinitesimal phase response* (*curve*), short iPRC, itself depending on the current oscillator phase. My research focused on limits of this model as the network size tends to infinity. This simplification allows for alternative descriptions and gives access to the application of techniques that would not be available in the finite case.

Chapter 1 starts with a short introduction to the historical development of the vast and exciting field of oscillator networks. I then describe the generalizations and limits of the Winfree model treated in the thesis. Certain existence and uniqueness theorems for solutions to initial value problems for the considered models are also presented in the first chapter. They are more of a mathematical interest and can be safely skipped. Chapter 2 addresses the question of synchrony in networks of identical oscillators, i.e. solutions corresponding to all oscillators sharing a common time-dependent phase. Sufficient conditions are given for their existence as well as local stability. The coupling topology of the network and the oscillator iPRCs are of central importance in these conditions. In chapter 3 I look at so-called *all-to-all spike-coupled* networks of identical oscillators, extended by additive white noise. It turns out that in such networks, stationary states (i.e. time-independent solutions in the statistical sense) display a rich bifurcation behaviour and play a central role in the network dynamics. Chapter 4 presents conclusions and closing remarks. Many rather technical proofs are moved to the appendix, so as not to obscure the true essence of this thesis. The interested reader will also find there some elaborations on the examined models. The appendix is not self-contained and should be read

within the context of the section referring to it.

The reader should be familiar with the basic terminology of dynamical systems and bifurcation theory, measure theory, topology, functional analysis and Fokker-Planck equations. I occasionally make use of Banach lattices and positive operators, but having experience in the latter is not essential for the comprehension of this work. Understanding the applied numerical methods requires some basic knowledge of standard quadrature schemes, optimization algorithms and solvers for ordinary differential equations. I refer the reader to Meiss (2007) and Michel et al. (2008) for an introduction to dynamical systems. I refer to Bogachev (2006) on measure theory and to Kelley (1955) on basic topology. I refer to Lax (2002) and Brézis (2010) on functional analysis and spectral operator theory. I refer to Risken (1996) and Frank (2005) on Fokker-Planck equations. I refer to Schaefer (1974) and Zaanen (1997) on Banach lattices and positive operators. I refer to Burden & Faires (2001) for an overview of standard numerical analytical techniques.

This work was conducted with the support of the Max Planck Institute for Mathematics in the Sciences. Most of it is due to be published in peer reviewed journals at some later time (Louca & Atay n.d.*a*, Louca & Atay n.d.*b*). I would like to express my deepest gratitude to Dr. Fatihcan Atay for his numerous and invaluable advices. I would also like to thank Prof. Gerhard Schäfer at my university in Jena for his unyielding support. Finally, I thank Yulia Titova for proofreading this thesis.

Contents

Notation

I use the symbol $\mathbb{K}$ for either $\mathbb{R}$ or $\mathbb{C}$. I denote $\mathbb{R}_+ := [0,\infty)$ and $\mathbb{N}_0 := \mathbb{N} \cup \{0\}$. For any $\lambda \in \mathbb{C}$, I write λ^* for its complex conjugate, $\Re(z)$ or $\mathrm{Re}(z)$ for its real part and $\Im(z)$ or $\mathrm{Im}(z)$ for its imaginary part. For any set A let 1_A denote its indicator function. For any real interval $J \subseteq \mathbb{R}$ I write $|J| := \sup J - \inf J$. When referring to derivatives of functions on the boundary of J, I shall mean the appropriate one-sided derivatives. For any topological space Q I shall denote its Borel σ-algebra by $\mathscr{B}(Q)$. I will always assume the space to be endowed with that σ-algebra. For two Banach spaces E, F let $\mathcal{L}(E,F)$ denote the space of bounded, linear operators from E to F and abbreviate $\mathcal{L}(E) := \mathcal{L}(E,E)$. For any set R and any function $f : R \times E \to F$ I shall say that $f(r,x)$ *is of class* $o(x)$ *as* $x \to 0$ *uniformly in* $r \in R$, if $\sup_{r\in R} \|f(r,x)\| \in o(\|x\|)$ as $\|x\| \to 0$. For any linear operator $\mathcal{H}$ on some normed space I will write $\sigma(\mathcal{H})$ for its spectrum, $\sigma_{\mathrm{p}}(\mathcal{H})$ for its point spectrum, $r(\mathcal{H})$ for its spectral radius and $\|\mathcal{H}\|$ for its operator norm. The symbol Id denotes the identity operator. For vectors $\{v_i\}_{i\in I} \subseteq V$ in a $\mathbb{K}$-vector space V I write $\mathrm{span}_{\mathbb{K}}\{v_i : i \in I\}$ for their linear hull.

I denote measure spaces as tuples $(M, \mathscr{M}, \mu)$, with $\mathscr{M}$ being a σ-algebra over the set M and μ being a (positive) measure on the *measurable space* $(M, \mathscr{M})$. For $1 \leq q \leq \infty$ I write $L^q(\mu)$ for the complex L^q-space defined on $(M, \mathscr{M}, \mu)$ and $\|\cdot\|_{L^q(\mu)}$ for the corresponding norm. I write $L^q(M)$ for $L^q(\mu)$ if the measure μ is clear from the context. By default I assume on $\mathbb{R}^n$ the Lebesgue measure and on S^1 the normalized Haar measure. For any measurable function $f : M \to \mathbb{K}$ I denote $\mu(f) := \int_M d\mu\, f$. For any σ-finite measure space $(M, \mathscr{M}, \mu)$ and measurable functions $f, g : M \times M \to \mathbb{K}$, I write $f * g : M \times M \to \mathbb{K}$ for the *convolution* of f and g, defined as $(f * g)(x,y) := \int_M d\mu(z)\; f(x,z) \cdot g(z,y)$.

For any metric space X and $x \in X$ I denote by $B_\varepsilon(x)$ the closed ball of radius $\varepsilon \geq 0$ and centre x. The symbol 'd' will be used to denote the metric on the space in the given context. For any subset $A \subseteq X$ I write $\mathrm{diam}\, A := \sup_{x,y\in X} d(x,y)$ for the *diameter* of A. For any function $f : X \to Y$ between two metric spaces X, Y let its *modulus of continuity* $\omega_f : \mathbb{R}_+ \to [0,\infty]$ be defined by

$$\omega_f(\varepsilon) := \sup\{d(f(x_1), f(x_2)) : x_1, x_2 \in X,\ d(x_1,x_2) \leq \varepsilon\}\,.$$

I identify the circle S^1 with the quotient group $\mathbb{R}/\mathbb{Z}$. For $\Theta \in \{S^1, \mathbb{R}\}$ and any $f : \Theta \to \mathbb{K}$ I shall denote by $\mathrm{diam}\, f := \mathrm{diam}\, \mathrm{supp}\, f$ the diameter of its support. For any set R and mapping $f : R \times \Theta \to \mathbb{K}$, I shall denote by $\mathrm{supp}_\Theta f$ the closure of $\bigcup_{r\in R} \mathrm{supp}\, f(r,\cdot)$ in Θ and $\mathrm{diam}\, f := \mathrm{diam}\, \mathrm{supp}_\Theta f$. For any two $\vartheta_1, \vartheta_2 \in S^1$ I shall denote by $[\vartheta_1, \vartheta_2]$ the circular arc between ϑ_1 and ϑ_2 (inclusive), covered as one traverses S^1 from ϑ_1 to ϑ_2 in the positive sense. By convention $[\vartheta_1, \vartheta_1] := \{\vartheta_1\}$. The symbol Π_{c} shall denote the canonical projection of real values to the quotient group $\mathbb{R}/\mathbb{Z} = S^1$. Note that Π_{c} is a covering map for S^1. For any function f defined on S^1 I call the composition $f \circ \Pi_{\mathrm{c}}$ its *pullback* on $\mathbb{R}$. I will often abbreviate $f(\Pi_{\mathrm{c}}(\vartheta))$ (where $\vartheta \in \mathbb{R}$) with $f(\vartheta)$, the distinction should be clear from the context. For $f : S^1 \to \mathbb{K}$ I denote by $\mathcal{F}_n(f) := \int_{S^1} d\varphi\; f(\varphi) e^{-i2\pi n\varphi}$ its n-th Fourier component.

For measurable spaces $(M, \mathscr{M}), (N, \mathscr{N})$ I shall denote by $\mathcal{M}(M,N)$ the class of measurable functions $f : M \to N$. For any metric space Y I denote by $\mathcal{M}_{\mathrm{b}}(M,Y)$ the class of measurable, bounded functions $f : M \to Y$, endowed with the supremum metric $d_\infty(f_1,f_2) := \sup_{x\in M} d(f_1(x), f_2(x))$. For topological spaces P, Q, I denote by $\mathcal{C}(P,Q)$ the class

of continuous functions $f : P \to Q$ and by $\mathcal{C}_{\mathrm{b}}(P, Y)$ the class of continuous, bounded functions $f : P \to Y$, endowed with the supremum metric. I denote by $\mathcal{C}_{\mathrm{u}}(X, Y)$ the class of uniformly continuous functions $f : X \to Y$ between two metric spaces X, Y. By $\mathcal{C}_{\mathrm{u,b}}(X, Y)$ I denote the class of bounded, uniformly continuous functions from X to Y, endowed with the supremum metric. For $k \in \mathbb{N}_0$ I denote by

$$\mathcal{C}^k_{\mathrm{zm}}(S^1) := \left\{ f \in \mathcal{C}^k(S^1, \mathbb{C}) : \int_{S^1} d\varphi \; f(\varphi) = 0 \right\}$$

the class of complex, k-times continuously differentiable functions on S^1 with *zero mean*. For any smooth manifold $\mathcal{X}$ I write $\mathcal{C}^k(\mathcal{X}, \mathbb{R}_+)$ for the class of real, k-times continuously differentiable functions on $\mathcal{X}$ with non-negative values. $\mathcal{C}^1(\mathbb{R}, \mathcal{C}_{\mathrm{b}}(P, S^1))$ shall stand for the class of functions $f \in \mathcal{C}(\mathbb{R}, \mathcal{C}_{\mathrm{b}}(P, S^1))$, $(t, p) \mapsto f(t, p)$ for which there exists a mapping $\dot{f} \in \mathcal{C}(\mathbb{R}, \mathcal{C}_{\mathrm{b}}(P, \mathbb{R}))$, called the *time-derivative* of f, and an *error term* $F : \mathbb{R} \times P \times \mathbb{R} \to \mathbb{R}$, such that

$$f(t + \varepsilon, p) = f(t, p) + \dot{f}(t, p) \cdot \varepsilon + F(t, p, \varepsilon)$$

for every $t, \varepsilon \in \mathbb{R}, p \in P$ and $\sup_{p \in P} \|F(t, p, \varepsilon)\| \in o(\varepsilon)$ as $\varepsilon \to 0$ for every $t \in \mathbb{R}$. The class $\mathcal{C}^1(\mathbb{R}, \mathcal{M}_{\mathrm{b}}(M, S^1))$ is defined in a similar way.

For any finite sequence of topological spaces $Q_1, .., Q_n$ I assume the cartesian product $Q_1 \times \cdots \times Q_n$ to be endowed with the product topology. For any finite sequence of metric spaces $(X_1, d_1), .., (X_n, d_n)$ I assume the cartesian product $X_1 \times \cdots \times X_n$ to be endowed with the product metric $d((x_1, .., x_n), (y_1, .., y_n)) := \sum_{i=1}^n d_i(x_i, y_i)$. Similarly, for any finite sequence of normed spaces $(V_1, \|\cdot\|_1), .., (V_n, \|\cdot\|_n)$ I assume the direct product $V_1 \times \cdots \times V_n$ to be endowed with the product norm $\|(v_1, .., v_n)\| := \sum_{i=1}^n \|v_i\|_i$. For any finite sequence of measurable spaces $(M_1, \mathscr{M}_1), .., (M_n, \mathscr{M}_n)$ I assume on $M_1 \times \cdots \times M_n$ the product σ-algebra $\mathscr{M}_1 \otimes \cdots \otimes \mathscr{M}_n$. I remind the reader that for separable metric spaces $X_1, .., X_n$ the equality $\mathscr{B}(X_1 \times \cdots \times X_n) = \mathscr{B}(X_1) \otimes \cdots \otimes \mathscr{B}(X_n)$ holds (Bogachev 2006, Theorem 6.4.2).

By *solutions* to ordinary differential equations on Banach spaces or smooth manifolds I always mean strong solutions. Let W be a Banach space or a smooth, complete manifold with tangent bundle TW and let $\mathrm{v} : \mathbb{R} \times W \to TW$, $(t, w) \mapsto \mathrm{v}(t, w) \in T_w W$ be a time-dependent vector field on W. I will call a family $(U(t, t_o))_{t, t_o \in \mathbb{R}}$ (or $(U(t, t_o))_{t \geq t_o}$) of mappings $U(t, t_o) : W \to W$ the *flow generated by* v *on* W, whenever $U(t, t_o)(v)$ is the unique solution to the initial value problem

$$U(t_o, t_o)(w) = w, \qquad \frac{d}{dt} U(t, t_o)(w) = \mathrm{v}(t, U(t, t_o)(w))$$

for all $t, t_o \in \mathbb{R}$ (or $t \geq t_o$) and $w \in W$. I will say the flow is *autonomous* if $U(t, t_o)$ only depends on the difference $(t - t_o)$. For $t_1, t_o \in \mathbb{R}$ I refer to $U(t_1, t_o) : W \to W$ as the *propagator from time* t_o *to* t_1 *induced* by the vector field v or by the differential equation $\dot{w}(t) = \mathrm{v}(t, w(t))$. Throughout the text I will make use of the abbreviations 'ODE' for 'ordinary differential equation' and 'EOM' for 'equation of motion'. If not stated otherwise, the symbols "ϑ" and "φ" will be used for real or circular variables. On the other hand, the symbols "θ" and "ϕ" shall be used for functions depending on at least one parameter (such as time), typically mapping into S^1 or $\mathbb{R}$. An overview of used symbols and abbreviations can also be found on page 74.

Chapter 1

Introduction

1.1 Historical background

Over the last 50 years, an increasing number of biological and physical systems displaying collective behavioural patterns has been modelled by networks of coupled oscillators. Examples include the synchronization of flashing fireflies (Winfree 2001), the interaction of cardiac pacemaker cells (Jalife & Antzelevitch 1979), the seemingly spontaneously arising activity coherence in the visual cortex (Sompolinsky et al. 1991, Chawanya et al. 1993, Wang 1995), crowd synchronization on the Millennium Bridge (Strogatz et al. 2005, Eckhardt et al. 2007), large arrays of coupled Josephson junctions (Wiesenfeld et al. 1998, Trees et al. 2005), diffusion coupled chemical oscillators (Kuramoto & Arakai 1984) and Wireless sensor networks (An et al. 2011). To a great part, these oscillators represent dynamical systems with stable limit cycles (i.e. one-dimensional, periodic attractors), coupled so weakly that after any coupling-induced distortion they quickly return to their attractor, albeit with a certain phase shift. This *weak coupling* property, illustrated in figure 1.1, permits a reduction of their dimensionality to a single circular coordinate, a so-called *phase*. In periodically spiking neurons, the phase is typically determined by timing of the action potential (Galán et al. 2005, Smeal et al. 2010). For isolated oscillators the oscillator phase can, after an appropriate coordinate transformation, be assumed to be of periodicity 1 and advance uniformly in time at an *intrinsic* frequency $\omega > 0$.

Any short, weak perturbation of such a so-called *phase oscillator*, is expressed as a long-term phase shift along the limit cycle with respect to the unperturbed dynamics. In the context of stable limit cycles, such perturbations induce transitions between the surrounding *isochrons*, the latter being hypersurfaces of constant phase. See (Guckenheimer 1975, Kuramoto & Arakai 1984) and (Winfree 2001) for more mathematical details on isochrons. The function mapping the phase at which the perturbation takes place to the phase shift it induces, is called the *phase response curve* (short, PRC) to that particular perturbation (Winfree 2001, Granada et al. 2009). The exact nature of considered perturbations depend on the oscillator model at hand and the natural system it describes. In neuronal oscillators for example, perturbations may take the form of presynaptic action potentials, inducing a change in the membrane potential of postsynaptic neurons (Kandel et al. 2000, Smeal et al. 2010). See figure 1.2 for an appropriate illustration. PRCs hide any intrinsic dynamics of oscillators and are of a phenomenological nature, often accessible to experimental verification in naturally occurring oscillators. I refer to the excellent work of Winfree (2001) for more details on PRCs, possible PRC measurement techniques and numerous examples of measured PRCs in animal circadian rhythms. PRCs have also been measured in excitable neurons (Jalife & Antzelevitch 1979, Tateno & Robinson 2007, Cui et al. July 2009) and cardiac pacemakers (Levy et al. 1970, Jalife & Moe 1979, Jalife et al. 1983). Despite or because of their simplicity, phase reduced oscillator models turned out to be very useful in understanding the behaviour of many of the systems mentioned in the first paragraph, a

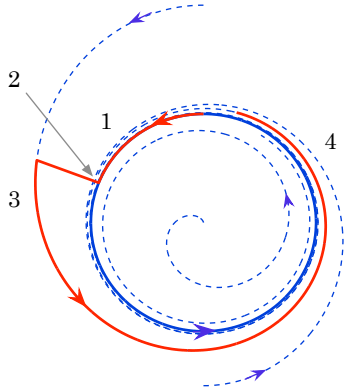

Figure 1.1: On the definition of phase oscillators, here as an approximation of two-dimensional dynamical systems with a stable limit cycle (full, blue curve). The dashed curves around the limit cycle give the system's phase portrait on the phase plane. The full red curve represents the system's trajectory before and after an external perturbation (taking place at point 2) of the limit cycle. Note the different parts of the trajectory: (1) Shortly before the perturbation the system lies on the limit cycle. (3) Right after the perturbation the system has a non-trivial distance to the limit cycle. (4) After a while the system has settled again on the limit cycle, possibly with a certain phase shift.

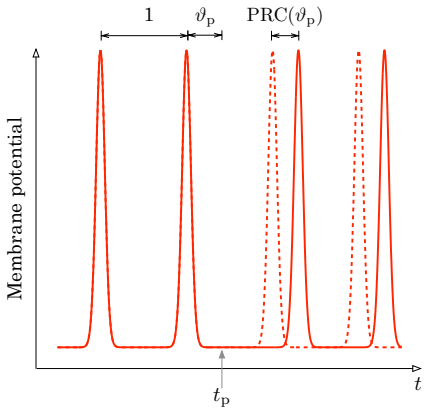

Figure 1.2: On the definition of the PRC of phase oscillators, illustrated on the (hypothetical) example of a neuron firing at frequency 1. The oscillator phase $\theta(t)$ is identified with $(1-t)$, where t is the time needed for the next spike to occur if the neuron is until then unperturbed. At time t_p (phase ϑ_p) an external stimulus (e.g. a presynaptic action potential) perturbs the neuron and results in a delay of the next spike. This delay translates into a negative phase shift PRC(ϑ_p) along the corresponding limit cycle. The full curve represents the evolution of the neuron membrane potential in time, the dashed curve the hypothetical membrane potential in the unperturbed case.

prominent example being the spontaneous occurrence of synchrony. Nowadays, these models have branched into a rich research field of their own, at the intersection of, among others, dynamical systems theory and statistical physics (Strogatz & Stewart 1993, Strogatz 2000). Their study is driven not only by mathematical curiosity, but also the hope that their understanding might shed light on phenomena observed in real systems. Furthermore, they increasingly demonstrate that even suspiciously oversimplified models, can reproduce some of the complex behaviour seen in nature (Smeal et al. 2010).

Winfree (1967) and Swade (1969) suggested that certain perturbations of naturally occurring phase oscillators, may be described as a temporary frequency modulation due to incoming *stimuli* $\mathbf{S}(t) \in \mathbb{R}^n$ from the environment. They introduced a so-called *sensitivity function* (or *velocity*

response curve) $\boldsymbol{\psi} : S^1 \to \mathbb{R}^n$ and postulated the dynamics

$$\dot{\theta}(t) = \omega + \boldsymbol{\psi}(\theta(t)) \cdot \mathbf{S}(t) \tag{1.1}$$

for the phase $\theta(t)$ of stimulated oscillators. Of course this already presumes that environmental influences or modelled oscillator interactions can be *encoded* in a real, time-dependent vector $\mathbf{S}(t)$ to begin with. The phase response curve $\mathrm{PRC}_{\mathbf{S}}$ to any stimulus $\mathbf{S}$ with support in $[0, \varepsilon]$, is given by the convolution

$$\mathrm{PRC}_{\mathbf{S}}(\vartheta) := \int_0^{\varepsilon} dt\ \boldsymbol{\psi}(\theta(t)) \cdot \mathbf{S}(t), \qquad \vartheta \in S^1, \tag{1.2}$$

where $\theta(t)$ solves the initial value problem $\theta(0) = \vartheta$, $\dot{\theta}(t) = \omega + \boldsymbol{\psi}(\theta(t)) \cdot \mathbf{S}(t)$. Kuramoto & Arakai (1984, §3.2 & §5.2) give a derivation of such dynamics using a perturbation analysis around stable limit cycles. They assume that stimuli distort the (multidimensional) oscillator dynamics as an additive term in the full equation of motion. The sensitivity function can in certain cases be seen as a limit of PRCs corresponding to infinitesimally short stimuli (Ermentrout & Kopell 1990). More precisely, let $(S_\varepsilon)_{\varepsilon>0} \subseteq \mathcal{C}(\mathbb{R}, \mathbb{R}_+)$ be a family of stimuli such that $\sup_{\varepsilon>0} \|S_\varepsilon\|_\infty < \infty$, $\|S_\varepsilon\|_{L^1(\mathbb{R})} > 0$ and $\operatorname{supp} S_\varepsilon \subseteq [0, \varepsilon]$ for every $\varepsilon > 0$. Then provided $\psi \in \mathcal{C}(S^1, \mathbb{R})$, one easily finds that $\mathrm{PRC}_{S_\varepsilon}(\vartheta) / \|S_\varepsilon\|_{L^1(\mathbb{R})} \to \psi(\vartheta)$ as $\varepsilon \to 0$, uniformly in $\vartheta \in S^1$. This is why sensitivity functions are also called *infinitesimal phase response curves* (short, iPRC). Contrary to PRCs which generally depend on the exact shape and duration of the incoming stimulus, the iPRC provides with an intrinsic description of an oscillator's reaction to environmental perturbations. Note that the existence of an iPRC at the base of all possible PRCs, is usually a mathematical postulate for naturally occurring oscillators, a simplification making the study of their interaction more accessible to analytical methods. Nonetheless, the validity of this assumption can be tested, and in the positive case the shape of the iPRC can be calculated, by applying suitable deconvolution methods to measured PRCs (Netoff et al. 2005, Galán et al. 2005, Preyer & Butera 2005, Kiss et al. 2005, Schultheiss et al. 2010, Ota et al. 2011). Note that the existence of an iPRC follows if one assumes PRCs to depend linearly and sufficiently smoothly on incoming stimuli, which in turn can be interpreted as a weak coupling condition. The interested reader will find a more detailed elaboration in appendix A.1.1.

For systems of multiple interacting oscillators, encoding the influence of the entire system on an individual oscillator in a real-valued stimulus is not always trivial. For certain Hodgkin-Huxley neuron models with voltage-dependent chemical coupling, the dynamics of two connected phase-reduced oscillators have been shown (Ermentrout & Kopell 1990, §2.1) to take the form

$$\dot{\theta}_1(t) = \omega_1 + \psi(\theta_1(t)) \cdot I(\theta_2(t)), \qquad \dot{\theta}_2(t) = \omega_2 + \psi(\theta_2(t)) \cdot I(\theta_1(t)), \tag{1.3}$$

for a suitable, model-specific iPRC $\psi : S^1 \to \mathbb{R}$. The term $I(\theta_k(t)) \geq 0$ (with $i, k = 1, 2$, $i \neq k$) is given by the current synaptic conductance from the presynaptic neuron k to the postsynaptic neuron i, and increases with the presynaptic potential. Electrophysiological experiments on olfactory mitral cells of mice (Galán et al. 2005) and abdominal ganglia neurons of Aplysia (Preyer & Butera 2005) have revealed a similar coupling through synaptic interactions, driven by presynaptic potentials of connected neurons.

The dynamics (1.3) suggest a generalization to networks of N so-called *pulse-coupled* phase oscillators with phases $\theta_1, .., \theta_N$ and intrinsic frequencies $\omega_1, .., \omega_N > 0$, satisfying

$$\dot{\theta}_i(t) = \omega_i + \psi(\theta_i(t)) \cdot \sum_{j=1}^{N} G_{ij} \cdot I(\theta_j(t)), \qquad i \in \{1, .., N\}. \tag{1.4}$$

The functions $\psi : S^1 \to \mathbb{R}, I : S^1 \to \mathbb{R}$ represent the oscillator iPRC and *pulse* respectively. $G \in \mathbb{R}_+^{N \times N}$ is the *coupling matrix* and the weighted sum in (1.4) the *stimulus* perturbing the i-th

oscillator. Its additive character is justified by the linearity assumption implied by the existence of an iPRC. Such a coupling scheme presumes that pulses *fired* by a certain oscillator j are of a similar shape for all *receiving* oscillators i, at most scaled by a scalar value G_{ij}. In neuronal networks G_{ij} could, for example, represent the synaptic strength of the presynaptic neuron j to the postsynaptic neuron i. In systems where oscillators are thought of as being spatially distributed, G_{ij} may decrease with the distance of the oscillator pair i, j. Model (1.4), henceforth referred to as *Winfree model* (Winfree 1967), has recently seen increased attention (Ariaratnam & Strogatz 2001, Ariaratnam 2002, Goel & Ermentrout 2002, Quinn et al. 2007, Giannuzzi et al. 2007, Basnarkov & Urumov 2009), which mainly focused on the mathematically tractable case $G_{ij} = 1/N \ \forall i, j$ (*all-to-all coupling*), $\psi(\vartheta) = -\psi_o \sin\vartheta$ and $I(\vartheta) = 1 + \cos\vartheta$.

It should be mentioned that the latter case takes, in the limit of weak coupling ($|G| \ll 1$) and almost identical intrinsic frequencies ($|\omega_i - 1| \ll 1$), the form

$$\dot{\theta}_i(t) = \omega_i + \frac{\psi_o}{2N} \sum_{j=1}^{N} \sin\left(\theta_j(t) - \theta_i(t)\right), \qquad i \in \{1, .., N\}. \tag{1.5}$$

This limit is known as the *Kuramoto model* (Kuramoto 1975, Kuramoto & Arakai 1984), and can be derived (see for example Ariaratnam 2002, §2) using averaging theory (Guckenheimer & Holmes 1990). Despite its simplicity, it displays rich synchronization behaviour, which is probably one of the reasons it has been far more thoroughly studied than the original Winfree model. The reader is referred to the review by Acebrón et al. (2005) on the Kuramoto model.

Explicitly solving the Winfree model (1.4) for large N quickly becomes a difficult task. Unfortunately, many physical systems modelled by coupled oscillators are so large that even modern supercomputers would not be able to simulate their dynamics within practical time scales. A prominent example is the human central nervous system, estimated to consist of over 10^{14} neurons (Drachman 2005). Such large scale systems may on the other hand be best described by alternative models, where the number of oscillators is taken to be infinite per se. Such models often allow for different analytical and computational techniques not only for their explicit solution, but also their qualitative understanding. Of course, any involved simplifications carry the implicit hope that the interesting behavioural patterns of the real, typically discrete system are not lost on the way.

For all-to-all coupled networks of identical oscillators ($\omega_i = \omega \ \forall i$), an often considered transition of (1.4) in the *thermodynamic limit* (i.e. as $N \to \infty$) is to the *continuity equation*

$$\partial_t \rho(t, \vartheta) = -\partial_\vartheta \left\{ \rho(t, \vartheta) \cdot \left[\omega + \psi(\vartheta) \cdot \int_{S^1} d\varphi \ I(\varphi) \cdot \rho(t, \varphi) \right] \right\}, \tag{1.6}$$

describing the evolution of the probability density $\rho(t, \vartheta)$ at time $t \in \mathbb{R}$ of an oscillator being at phase $\vartheta \in S^1$ (Ariaratnam 2002, Giannuzzi et al. 2007). This equation is analogous to the Boltzmann equation in kinetic gas theory. In view of the equivalence of oscillators, one typically identifies the network state with the phase density $\rho(t, \cdot)$ itself. An advantage of such density-oriented models is the intrinsic statistical interpretation of oscillator states. This is an important aspect in large natural systems, where the behaviour of individual oscillators fades from view against the macroscopic, *average* collective system behaviour. It should be noted that the above cited articles on (1.6) in fact consider networks of oscillators with non-identical intrinsic frequencies, described by a probability density $\rho(t, \omega, \vartheta)$ both in the frequency ω and phase ϑ. Such networks have been shown to exhibit a rich phase diagram with respect to the coupling strength and frequency variance (Ariaratnam & Strogatz 2001, Giannuzzi et al. 2007).

When modelling natural systems it is meaningful to include in the model the effects of noise, representing unknown perturbations and non-zero temperature effects on oscillators. This is typically done by introducing an additive term $\sqrt{2D} \cdot \xi_i(t)$ to the equation of motion (1.4), with $D \geq 0$ and the stochastic process $\xi_i(t)$ representing white noise with mean $\langle \xi_i(t) \rangle = 0$

and covariance $\langle \xi_i(t), \xi_j(t') \rangle = \delta_{ij}\delta(t-t')$. The once noise-free, deterministic Winfree model for all-to-all coupled, identical oscillators then takes the form of a *Langevin equation* (Risken 1996, §4.4)

$$d\theta_i(t) = \left[\omega + \psi(\theta_i(t)) \cdot \frac{1}{N}\sum_{j=1}^{N} I(\theta_j(t))\right] dt + \sqrt{2D} \cdot dW_i(t) \tag{1.7}$$

in the stochastic processes $\theta_1, .., \theta_N$ on S^1, with $W_1, .., W_N$ being independent Wiener processes. Accordingly, the continuity equation (1.6) becomes a non-linear *Fokker-Planck equation* (Kolmogoroff 1931, Risken 1996, Frank 2005)

$$\partial_t \rho(t,\vartheta) = -\partial_\vartheta \left\{ \rho(t,\vartheta) \cdot \left[\omega + \psi(\vartheta) \cdot \int_{S^1} d\varphi \; I(\varphi) \cdot \rho(t,\varphi)\right]\right\} + D \cdot \partial_\vartheta^2 \rho(t,\vartheta) \tag{1.8}$$

in the density $\rho(t,\vartheta)$, with the diffusion coefficient D being interpreted as the network's *temperature*.

Continuity equations and Fokker-Planck equations similar to (1.6) and (1.8) have already been considered as thermodynamic limits of the Kuramoto model (1.5) with great success (Kuramoto & Arakai 1984, Sakaguchi 1988, Strogatz & Mirollo 1991). For the latter, path-integral derivations have been given both for the continuity-equation (Bonilla 1987, Bonilla et al. 1992) as well as the Fokker-Planck equation (Acebrón et al. 2005, Appendix A). Crawford & Davies (1999, Appendix B) have given an alternative derivation, by assuming that oscillator phases stay statistically independent for all times $t \geq 0$, provided they were such at time $t = 0$. This assumption of *propagation of chaos* (Hollinger 1962, Dawson 1983), turns out to be essential for extracting an autonomous differential equation for the *one-oscillator* density $\rho(t,\vartheta)$, from an a priori coupled hierarchy of equations for joint oscillator-phase densities of all possible degrees. That hierarchy closely resembles the famous BBGKY hierarchy for the n-particle distributions in kinetic gas theory (see for example Wilmanski 2008, §7.2). The interested reader may find a similar justification for the Fokker-Planck equation (1.8) in appendix A.1.2.

1.2 Models examined in this thesis

In this thesis I examine three classes of infinite networks of coupled phase oscillators, all of which are generalizations or thermodynamic limits of the Winfree model introduced above. In the first two models, oscillators are distributed on some abstract finite Borel measure space $(X, \mathscr{B}(X), \mu)$, over a separable metric space X with Borel σ-algebra $\mathscr{B}(X)$. Accordingly, the oscillator index $i \in \{1, .., N\}$ is replaced by a coordinate $x \in X$, the coupling matrix becomes a coupling kernel $G : X \times X \to \mathbb{R}_+$ and the phase vector $(\theta_i)_{i=1}^N$ becomes a phase field $(\theta(x))_{x\in X}$. All oscillators are assumed to be identical and noise-free. The Winfree model (1.4) then changes to

$$\dot\theta(t,x) = \omega + \psi(\theta(t,x)) \cdot \int_X d\mu(y) \; G(x,y) \cdot I(\theta(t,y)) \tag{1.9}$$

in the time-dependent phase field $\theta(t) \in \mathcal{M}_{\mathrm{b}}(X, S^1)$. The measure μ can be seen as a fixed *oscillator distribution* on X, similar to the continuous neuron distribution often assumed in neural field theory (Beurle 1956, Griffith 1963). The space X itself may represent any topology typically of interest, simple examples being the n-dimensional sphere S^n, the $\mathbb{R}^n$ or the n-dimensional torus $\mathbb{T}^n$. The second model is a, perhaps not so obvious, generalization of the continuity equation (1.6). At each point $x \in X$ an infinite number of all-to-all pulse-coupled phase oscillators is assumed, whose phase distribution is described by a probability density $\rho(t,x,\cdot)$. The latter shall satisfy the continuity equation

$$\partial_t \rho(t,x,\vartheta) = -\partial_\vartheta \left[\rho(t,x,\vartheta) \cdot \mathrm{v}(t,x,\vartheta,\rho(t))\right], \tag{1.10}$$

with the *velocity field* v being given by

$$\mathrm{v}(t,x,\vartheta,\rho(t)) := \omega + \psi(\vartheta)\cdot\int_X d\mu(y)\; G(x,y)\int_{S^1} d\varphi\; I(\varphi)\cdot\rho(t,y,\varphi). \tag{1.11}$$

The right hand side of (1.11) is to be understood as follows: At each point $y \in X$ oscillators fire a mean pulse $\int_{S^1} d\varphi\; I(\varphi)\cdot\rho(t,y,\varphi)$, which contributes additively with a weight $G(x,y)$ to the total stimulus perturbing oscillators at point $x \in X$. The model (1.9) shall be referred to as the *field model*, as opposed to the *fluid model* (1.10). Analogous models have been considered as thermodynamic limits of the Kuramoto model (and generalizations of it), taking X as the real line, the two-dimensional plane or S^1 (Shiogai & Kuramoto 2003, Laing 2009, Lee et al. 2011). In the simple case where X is a finite set and μ on it the counting measure, (1.9) becomes the original Winfree model (1.4) (for identical oscillators). Similarly, (1.10) can then be interpreted as a system of coupled continuity equations for finitely many interacting networks, each one comprising infinitely many, identical, all-to-all pulse-coupled phase oscillators. Such models can be of particular relevance for natural systems consisting of several *loosely coupled* clusters, each one of them comprising a large number of strongly interacting oscillators. An alternative interpretation of the fluid model and its connection to the field model are presented in section 1.3. Note that while the question of existence and uniqueness of solutions to initial value problems in the field model (1.9) is rather trivial (Deimling 1977, Appell et al. 2000), this is by far not the case for the fluid model (1.10), where the right hand side consists of a non-linear differential operator. Section 1.4 addresses this issue and gives some existence and uniqueness results for solutions to the fluid model, at least in certain function classes and for certain initial values. Both the field and fluid models are studied in chapter 2 with respect to synchrony, i.e. solutions corresponding to all oscillators sharing one common, time-dependent phase. Sufficient conditions for its existence and local stability are given. These will involve the connection topology defined by the coupling kernel as well as the structure of the oscillator iPRC and pulse. The presented results generalize findings of Goel & Ermentrout (2002) on the original, finite Winfree model (1.4).

Following up in chapter 3, infinite networks of all-to-all pulse-coupled identical phase oscillators with additive white noise are studied, in the limit that oscillator pulses approximate Dirac distributions (so-called *spikes*). This will be done by looking at the Fokker-Planck equation

$$\partial_t\rho(t,\vartheta) = -\partial_\vartheta\Big[\rho(t,\vartheta)\cdot[\omega+\psi(\vartheta)\cdot\rho(t,0)]\Big] + D\cdot\partial_\vartheta^2\rho(t,\vartheta) \tag{1.12}$$

in the oscillator-phase probability density $\rho(t,\vartheta)$, obtained by formally replacing $I(\varphi)$ in (1.8) with $\delta(\varphi)$. Such an approximation may be particularly meaningful for certain neuronal oscillators, as action potentials of periodically firing neurons can be of significantly shorter duration than the firing periods themselves. For example, the inhalation of odour molecules has been found to trigger oscillations of the local field potential of mitral cells in the olfactory bulb of rats, within the frequency range $20-80$ Hz and with spikes lasting just about 2 ms (Desmaisons et al. 1999, Lagier et al. 2004). Note that to arrive at (1.12), the limit of Dirac pulses is taken *after* the limit of an infinite network size. The case where oscillator phases in finite networks discontinuously *jump* due to connected spiking oscillators has been extensively studied in the literature (see for example the article of Goel & Ermentrout (2002) and the citations therein). By taking the limit of Dirac pulses after the thermodynamic limit, one obtains a well-behaved partial differential equation instead of a discontinuous ordinary one.

For the study of (1.12) it will mainly for simplicity be assumed that $\psi(0) = 0$, though most analytical results can be extended to more general iPRCs. Many iPRCs derived from biophysical neuron models or determined through experiments on real neurons satisfy this assumption (Ermentrout 1996, Preyer & Butera 2005, Ota et al. 2011). I will address questions of existence, uniqueness and stability of *stationary probability densities* (or *stationary states*), that is,

time-independent solutions to the Fokker-Planck equation (1.12). Related research has already been conducted on the original noise-free model (1.6) for some special iPRC and pulse shapes (Ariaratnam 2002, Basnarkov & Urumov 2009). As it turns out, both the iPRC shape and noise level have a strong influence on the emerging behavioural patterns. Most analytical findings are supplemented to a considerable extent by numerical analysis. The latter is applied to two special iPRC families, which qualitatively resemble many of the iPRCs measured in natural oscillators, including neuronal ones. As numerical simulations reveal, the local stability of stationary states is strongly linked to the attractors and the long term dynamics of the network. In view of possible applications to neuronal networks, special interest is devoted to the network stimulus $\rho(t,0)$ (corresponding to the mean network pulse), its time evolution and its dependence on the network parameters in case of stationarity.

1.3 Connecting the field and fluid models

The two models (1.9) and (1.10) are related in a way that might not be apparent at first sight. In theorem 2.4.4 it is shown that the stability of network synchrony in the fluid model is, under additional assumptions, implied by the stability of synchrony in the corresponding field model. In fact, the proof of that theorem will reveal that the mean oscillator phase solves, within the context of the fluid model and up to an error of order $o(\sup_{x\in X} \operatorname{diam} \rho(t,x,\cdot))$, the field equation (1.9). One can thus interpret the field model as a limit of the fluid model as oscillator densities $\rho(t,x,\cdot)$ approach at each point x a Dirac distribution. As shown below, this link works in both ways. I present a heuristic interpretation of the fluid model as a statistical approximation of the field model. The idea is to consider the density $\rho(t,x,\cdot)$ as a description for the oscillator phase distribution *in the proximity* of x, in the same way as the local velocity of a moving fluid in fact represents the average velocity of nearby fluid particles. Of course, the density $\rho(t,x,\cdot)$ would preserve much more information than just the local average.

For simplicity, let us consider X in this section to be a compact metric space and μ a finite, strictly positive Borel measure on X. As a reminder, a strictly positive Borel measure on some topological space is a measure assigning to every non-empty open set a strictly positive value. Let us also assume the following *homogeneity condition*: The limit

$$\lim_{\varepsilon\to 0^+} \frac{\mu(B_\varepsilon(x))}{\mu(B_\varepsilon(y))} =: \mathscr{N}(x,y) \tag{1.13}$$

exists in $(0,\infty)$ for all $x,y \in X$, is approached uniformly in x,y and the mapping $\mathscr{N}: X\times X \to (0,\infty)$ is continuous. A simple example of such a space would be the n-sphere $X = S^n$ (as boundary of the unit ball in $\mathbb{R}^{n+1}$). Let $\omega > 0$, $\psi, I \in \mathcal{C}(S^1,\mathbb{R})$ and $G \in \mathcal{C}(X\times X,\mathbb{R})$. Let $\mathrm{v}: X\times S^1 \times \mathcal{M}(X,S^1) \to \mathbb{R}$ be defined as

$$\mathrm{v}(x,\vartheta,\theta) := \omega + \psi(\vartheta)\cdot \int_X d\mu(y)\; G(x,y)\cdot I(\theta(y)). \tag{1.14}$$

Note that $\|\mathrm{v}(x,\cdot,\cdot) - \mathrm{v}(\tilde{x},\cdot,\cdot)\|_\infty \to 0$ as $d(x,\tilde{x}) \to 0$. Let $\theta \in \mathcal{C}^1(\mathbb{R}, \mathcal{M}_\mathrm{b}(X,S^1))$ satisfy the field equation

$$\dot{\theta}(t,x) = \mathrm{v}(x,\theta(t,x),\theta(t)). \tag{1.15}$$

For any $\varepsilon > 0$ and $(t,x) \in \mathbb{R}\times X$ let $\rho_\varepsilon(t,x,\cdot) \in \mathcal{L}(\mathcal{C}_\mathrm{b}(S^1,\mathbb{R}),\mathbb{R})$ stand for the non-negative, bounded linear functional defined by

$$\langle \rho_\varepsilon(t,x,\cdot), f\rangle := \int_{B_\varepsilon(x)} \frac{d\mu(y)}{\mu(B_\varepsilon(x))}\; f(\theta(t,y)) \tag{1.16}$$

for $f \in \mathcal{C}_{\mathrm{b}}(S^1, \mathbb{R})$. Its operator norm is given by $\|\rho_\varepsilon(t,x,\cdot)\| = \langle \rho_\varepsilon(t,x,\cdot), 1\rangle = 1$. Furthermore, for $f \in \mathcal{C}^\infty(S^1,\mathbb{R})$ one has

$$\begin{aligned}
\langle \partial_t \rho_\varepsilon(t,x,\cdot), f\rangle &\overset{\text{def.}}{=} \partial_t \langle \rho_\varepsilon(t,x,\cdot), f\rangle = \int_{B_\varepsilon(x)} \frac{d\mu(y)}{\mu(B_\varepsilon(x))} \partial_t f(\theta(t,y)) \\
&= \int_{B_\varepsilon(x)} \frac{d\mu(y)}{\mu(B_\varepsilon(x))} f'(\theta(t,y)) \cdot \partial_t \theta(t,y) \\
&= \int_{B_\varepsilon(x)} \frac{d\mu(y)}{\mu(B_\varepsilon(x))} f'(\theta(t,y)) \cdot \mathrm{v}(y, \theta(t,y), \theta(t)) \\
&= o(\varepsilon^0) + \int_{B_\varepsilon(x)} \frac{d\mu(y)}{\mu(B_\varepsilon(x))} f'(\theta(t,y)) \cdot \mathrm{v}(x, \theta(t,y), \theta(t)) \\
&= o(\varepsilon^0) + \left\langle \rho_\varepsilon(t,x,\cdot),\ f' \cdot \mathrm{v}(x,\cdot,\theta(t))\right\rangle \\
&\overset{\text{def}}{=} o(\varepsilon^0) - \left\langle \partial_\vartheta \left[\rho_\varepsilon(t,x,\cdot) \cdot \mathrm{v}(x,\cdot,\theta(t))\right],\ f\right\rangle,
\end{aligned} \tag{1.17}$$

while $\rho_\varepsilon(t,x,\cdot)$ is to be interpreted as a distribution on $\mathcal{C}^\infty(S^1,\mathbb{R})$. This translates to

$$\partial_t \rho_\varepsilon(t,x,\cdot) = o(\varepsilon^0) - \partial_\vartheta \left[\rho_\varepsilon(t,x,\cdot) \cdot \mathrm{v}(x,\cdot,\theta(t))\right] \tag{1.18}$$

in the distributional sense. The error $o(\varepsilon^0)$ scales down with $\varepsilon \to 0$ uniformly in (t,x,θ), but pointwise in the distribution's argument $f \in \mathcal{C}^\infty(S^1,\mathbb{R})$. Note that the mappings $X \to \mathbb{R}$, $y \mapsto \mu(B_\varepsilon(y))$ and $y \mapsto \langle \rho_\varepsilon(t,y,\cdot), f\rangle$ (with $f \in \mathcal{C}_{\mathrm{b}}(S^1,\mathbb{R})$) are both measurable. This follows from the measurability of $(X\times X, \mathscr{B}(X\times X)) \to (\mathbb{R}, \mathscr{B}(\mathbb{R}))$, $(y,z) \mapsto 1_{B_\varepsilon(y)}(z)$ and the fact that $\mathscr{B}(X)\times\mathscr{B}(X) = \mathscr{B}(X\times X)$, the latter holding since X is separable. Furthermore, one has

$$\begin{aligned}
&\int_X d\mu(y)\ G(x,y) \cdot \langle \rho_\varepsilon(t,y,\cdot),\ I\rangle \\
=&\int_X d\mu(y)\ G(x,y) \cdot \int_{B_\varepsilon(y)} \frac{d\mu(z)}{\mu(B_\varepsilon(y))} I(\theta(t,z)) \\
=&o(\varepsilon^0) + \int_X d\mu(y)\ \int_{B_\varepsilon(y)} \frac{d\mu(z)}{\mu(B_\varepsilon(z))} \cdot \frac{\mu(B_\varepsilon(z))}{\mu(B_\varepsilon(y))} \cdot G(x,z) \cdot I(\theta(t,z)) \\
=&o(\varepsilon^0) + \int_X d\mu(y)\ \int_{B_\varepsilon(y)} \frac{d\mu(z)}{\mu(B_\varepsilon(z))} \cdot G(x,z) \cdot I(\theta(t,z)) \\
=&o(\varepsilon^0) + \int_X \frac{d\mu(z)}{\mu(B_\varepsilon(z))} \cdot G(x,z) \cdot I(\theta(t,z)) \int_X d\mu(y)\ 1_{B_\varepsilon(y)}(z) \\
=&o(\varepsilon^0) + \int_X d\mu(z)\ G(x,z) \cdot I(\theta(t,z)),
\end{aligned} \tag{1.19}$$

the error $o(\varepsilon^0)$ scaling down as $\varepsilon \to 0$ uniformly in (t,x,θ). Note that for the error estimate use has been made of the uniform continuity of G and $\mathscr{N}$ on X^2, the uniform convergence $\mu(B_\varepsilon(z))/\mu(B_\varepsilon(y)) \to \mathscr{N}(x,y)$ as $\varepsilon \to 0^+$, the fact that $\mathscr{N}(y,y) = 1$ and $\mu(X) < \infty$. Therefore $\mathrm{v}(x,\vartheta,\theta(t)) = o(\varepsilon^0) + \tilde{\mathrm{v}}(x,\vartheta,\rho_\varepsilon(t))$, with

$$\tilde{\mathrm{v}}(x,\vartheta,\rho_\varepsilon(t)) := \omega + \psi(\vartheta) \cdot \int_X d\mu(y)\ G(x,y) \cdot \langle \rho_\varepsilon(t,y,\cdot),\ I\rangle\,. \tag{1.20}$$

Together with (1.18) this implies

$$\partial_t \rho_\varepsilon(t,x,\cdot) = o(\varepsilon^0) - \partial_\vartheta \left[\rho_\varepsilon(t,x,\cdot) \cdot \tilde{\mathrm{v}}(x,\cdot,\rho_\varepsilon(t))\right] \tag{1.21}$$

in the distributional sense. The error $o(\varepsilon^0)$ scales down as $\varepsilon \to 0$ uniformly in (t,x,θ) but pointwise in the distribution's argument $f \in \mathcal{C}^\infty(S^1,\mathbb{R})$. The distribution $\rho_\varepsilon(t,x,\cdot)$ can be

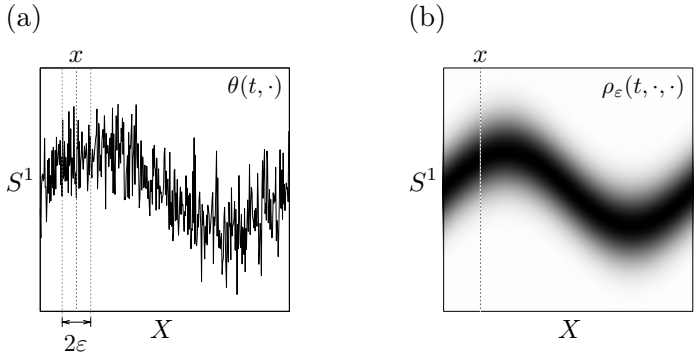

Figure 1.3: On the motivation of the fluid model as a statistical approximation to the field model, presented in section 1.3. On the left, an example field $\theta(t,\cdot) \in \mathcal{M}(X, S^1)$ is plotted over the one-dimensional space X. On the right, the corresponding density $\rho_\varepsilon(t,\cdot,\cdot)$ is for some $\varepsilon > 0$ illustrated as a colour map over $X \times S^1$. A darker colour represents a higher density. The density $\rho_\varepsilon(t,x,\cdot)$ at x results from a statistical evaluation of the field values within the disc $B_\varepsilon(x)$.

interpreted as a *probability density* for the random variable $\theta(t,\hat{Y})$ on S^1, where $\hat{Y}$ is a random variable distributed on $B_\varepsilon(x)$ by the law $\mu/\mu(B_\varepsilon(x))$. The continuity condition on G with respect to X ensure that oscillators in the ball $B_\varepsilon(x)$ are, for $\varepsilon > 0$ small enough, similarly coupled to the network. As $\varepsilon \to 0$, (1.21) formally takes the form of the continuity equation in the fluid model.

The advantage of the fluid model over the field model is the possibility to describe local patterns (other than synchronization) like statistically stationary states, in which current oscillator phases are even on a spatially local level, best described in a statistical way. In particular, the *local variation* of $\theta(t,\cdot)$ might tend to infinity, with $\rho_\varepsilon(t,x,\cdot)$ still continuous in $x \in X$.

1.4 Existence and uniqueness of solutions in the fluid model

In this section, existence and uniqueness results for solutions to initial value problems in the fluid model (1.10) are given, at least within a certain function class and for certain initial values. To the best of my knowledge, little has been published so far on this issue for continuity equations where the velocity field depends non-locally on the density itself. Also pointed out is the connection to the equivalent question for densities $\rho(t,x,\cdot)$ on $\mathbb{R}$, evolving within a velocity field $\mathrm{v}(t,x,\vartheta,\rho(t))$ which is periodic in ϑ. Throughout this section, X shall be a separable metric space and μ a finite Borel measure on it. For either $\Theta = \mathbb{R}$ or $\Theta = S^1$, let the function class

$$\Omega_{o,\Theta} := \left\{ \rho_o \in \mathcal{C}_{\mathrm{u,b}}(X \times \Theta, \mathbb{R}_+) : \|\rho_o(x,\cdot)\|_{L^1(\Theta)} = 1 \ \forall x \in X \right\} \tag{1.22}$$

be endowed with the supremum metric. The existence of maximal solutions to initial value problems for the continuity equation (1.10) will be examined in the function space

$$\begin{aligned} \Omega_\Theta := \{ \rho \in \mathcal{C}(J, \Omega_{o,\Theta}) : 0 \in J \subseteq \mathbb{R} \text{ interval } \wedge \ \exists \partial_\vartheta \rho, \partial_t \rho \\ \wedge \ (\partial_t \rho)(\cdot, x, \cdot) \in \mathcal{C}(J \times \Theta, \mathbb{R}) \ \forall x \in X \}. \end{aligned} \tag{1.23}$$

The main results are given by theorems 1.4.2 and 1.4.3 for quite abstract velocity fields. The velocity field (1.11) is only considered in theorem 1.4.5 as a special case. Most proofs are omitted, but will be published at a later time (Louca & Atay n.d.*a*).

Definition 1.4.1 (Wrapping, lift)**.** A function $\rho : S^1 \to \mathbb{R}$ shall be called a *wrapping* (Mardia & Jupp 2000) of $\tilde{\rho} : \mathbb{R} \to \mathbb{R}$ and $\tilde{\rho}$ an *unwrapping* of ρ if

$$\rho(\theta) = \sum_{n \in \mathbb{Z}} \tilde{\rho}(\theta + n) =: \Pi_\mathrm{w}(\tilde{\rho})(\theta) \tag{1.24}$$

for all $\theta \in S^1$, with the series converging absolutely. For any set R, a mapping $\rho : R \times S^1 \to \mathbb{R}$ shall be called a *wrapping* of $\tilde{\rho} : R \times \mathbb{R} \to \mathbb{R}$, denoted $\rho = \Pi_{\mathrm{w}}(\tilde{\rho})$, if $\rho(r, \cdot)$ is a wrapping of $\tilde{\rho}(r, \cdot)$ for every $r \in R$. Note that a similar notion to wrappings exists in the algebraic topology literature for maps $f \in \mathcal{C}(Q, S^1)$ defined on some topological space Q: A map $\tilde{f} \in \mathcal{C}(Q, \mathbb{R})$ is called a *lift* of f if $\Pi_{\mathrm{c}} \circ \tilde{f} = f$.

Note that for every $\rho : S^1 \to \mathbb{R}$ there exists an infinite number of unwrappings. In fact, each $\rho \in \mathcal{C}^k(S^1, \mathbb{R}_+)$ (with $k \in \mathbb{N}_0$) has at least one unwrapping $\tilde{\rho} \in \mathcal{C}^k(\mathbb{R}, \mathbb{R}_+)$ with support in $[-1, +1]$. Wrappings provide a natural link between solutions to the continuity equation in $\mathbb{R}$ and S^1, as will become clearer in the theorems below.

Theorem 1.4.2 (Existence and uniqueness of solutions to the continuity equation)
Let Ω_{o,S^1} and Ω_{S^1} be the function spaces defined in (1.22) and (1.23) respectively. Let the velocity field $\mathrm{v} : \mathbb{R} \times X \times S^1 \times \Omega_{o,S^1} \to \mathbb{R}$, $(t, x, \vartheta, \rho_1) \mapsto \mathrm{v}(t, x, \vartheta, \rho_1)$ satisfy:

V1. The mappings $\Omega_{o,S^1} \to \mathcal{C}_{\mathrm{u,b}}(\mathbb{R} \times X \times S^1, \mathbb{R})$ given by $\rho_1 \mapsto \mathrm{v}(\cdot, \cdot, \cdot, \rho_1)$, $\rho_1 \mapsto \partial_\vartheta \mathrm{v}(\cdot, \cdot, \cdot, \rho_1)$ and $\rho_1 \mapsto \partial_\vartheta^2 \mathrm{v}(\cdot, \cdot, \cdot, \rho_1)$ are well-defined, bounded and continuous.

V2. Both v and $\partial_\vartheta \mathrm{v}$ are Lipschitz continuous in Ω_{o,S^1} with Lipschitz constant L_{v}.

Let the initial state $\rho_o \in \Omega_{o,S^1}$ be such that $\partial_\vartheta \rho_o \in \mathcal{C}_{\mathrm{u,b}}(X \times S^1, \mathbb{R})$. Then in Ω_{S^1} there exists a maximal solution to the initial value problem

$$\rho(0, \cdot, \cdot) = \rho_o, \qquad \partial_t \rho(t, x, \vartheta) = -\partial_\vartheta \left[\rho(t, x, \vartheta) \cdot \mathrm{v}(t, x, \vartheta, \rho(t)) \right], \tag{1.25}$$

defined for all times $t \in \mathbb{R}$. That solution ρ is of class $\mathcal{C}^1\big(\mathbb{R}, \mathcal{C}_{\mathrm{u,b}}(X \times S^1, \mathbb{R})\big)$ and satisfies $\partial_\vartheta \rho \in \mathcal{C}(\mathbb{R} \times X \times S^1, \mathbb{R})$ as well as $(\partial_\vartheta \rho)(t, \cdot, \cdot) \in \mathcal{C}_{\mathrm{u,b}}(X \times S^1, \mathbb{R})$ for every $t \in \mathbb{R}$.

Outline of proof. The idea is to write the initial value problem as an integral fixed-point equation and apply Banach's fixed point theorem. Fix any compact time interval $J = [t_o, t_1] \subseteq \mathbb{R}$ ($t_1 > t_o$). For $\rho \in \mathcal{C}(J, \Omega_{o,S^1})$ define $\mathrm{v}[\rho] : J \times X \times S^1 \to \mathbb{R}$ by $\mathrm{v}[\rho](t, x, \vartheta) := \mathrm{v}(t, x, \vartheta, \rho(t))$. Let $\Phi[\rho] : J^2 \times X \times S^1 \to S^1$, $(s, t, x, \vartheta) \mapsto \Phi[\rho](s, t, x, \vartheta)$ be the flow generated on $X \times S^1$ by the velocity field $\mathrm{v}[\rho]$. Consider the function space

$$\Omega_J := \left\{ \rho \in \mathcal{C}_{\mathrm{b}}(J, \Omega_{o,S^1}) : \rho(t_o, \cdot, \cdot) = \rho_o \right\} \tag{1.26}$$

to be endowed with the supremum metric. Note that Ω_{o,S^1} is a closed subset of the complete metric space $\mathcal{C}_{\mathrm{u,b}}(X \times S^1, \mathbb{R})$, so that Ω_J is complete. Consider on Ω_J the functional $A : \Omega_J \to \Omega_J$, $\rho \mapsto A[\rho]$ defined by

$$A[\rho](t, x, \vartheta) := \rho_o \left(x, \Phi[\rho](t_o, t, x, \vartheta) \right) \cdot (\partial_\vartheta \Phi[\rho])(t_o, t, x, \vartheta), \tag{1.27}$$

for $(t, x, \vartheta) \in J \times X \times S^1$. It is not hard to see that A indeed maps Ω_J into Ω_J. Furthermore, one can show that for $|J|$ small enough, A is a contraction on Ω_J. By Banach's fixed point theorem, A has then in Ω_J a unique fixed point ρ_J. That fixed point solves the continuity equation $\partial_t \rho_J = -\partial_\vartheta(\rho_J \cdot \mathrm{v}[\rho_J])$ for times $t \in J$ and satisfies the initial value condition $\rho_J(t_o, \cdot, \cdot) = \rho_o$. Furthermore, it has the smoothness properties postulated in the theorem. Using an induction argument one can extend ρ_J to arbitrarily large J and in fact the whole real line, thus showing the existence of a global solution to (1.25). Its maximality (i.e. uniqueness) can be concluded using the uniqueness of the fixed point of A and a similar induction argument. □

The definition of the fixed point operator (1.27) reveals a profound connection between flows and densities satisfying the continuity equation. This relationship has its roots in the fact that the continuity equation is an ensemble description of orbits in S^1, generated by the underlying velocity field (which may itself depend on the ensemble distribution).

Theorem 1.4.3 (Evolution of unwrappings)
Let $\Omega_{o,S^1}, \Omega_{o,\mathbb{R}}$ and $\Omega_{S^1}, \Omega_{\mathbb{R}}$ be the function spaces defined in (1.22) and (1.23) respectively. Let the velocity field $\mathrm{v} : \mathbb{R} \times X \times S^1 \times \Omega_{o,S^1} \to \mathbb{R}$, $(t, x, \vartheta, \rho_o) \mapsto \mathrm{v}(t, x, \vartheta, \rho_o)$ satisfy the following:

V1. The mappings $\Omega_{o,S^1} \to \mathcal{C}_{\mathrm{u,b}}(\mathbb{R} \times X \times S^1, \mathbb{R})$ given by $\rho_1 \mapsto \mathrm{v}(\cdot, \cdot, \cdot, \rho_1)$, $\rho_1 \mapsto \partial_\vartheta \mathrm{v}(\cdot, \cdot, \cdot, \rho_1)$ and $\rho_1 \mapsto \partial_\vartheta^2 \mathrm{v}(\cdot, \cdot, \cdot, \rho_1)$ are well-defined, bounded and continuous.

V2. Both v and $\partial_\vartheta \mathrm{v}$ are Lipschitz continuous in Ω_{o,S^1} with Lipschitz constant L_v.

Let $\nu : \mathbb{R} \times X \times \mathbb{R} \times \Omega_{o,\mathbb{R}} \to \mathbb{R}$, $(t, x, \vartheta, \zeta_o) \mapsto \nu(t, x, \vartheta, \zeta_o)$ satisfy the following:

N1. ν is bounded.

N2. $\nu(\cdot, x, \cdot, \cdot), \partial_\vartheta \nu(\cdot, x, \cdot, \cdot) \in \mathcal{C}_\mathrm{b}(\mathbb{R} \times \mathbb{R} \times \Omega_{o,\mathbb{R}}, \mathbb{R})$ for every $x \in X$.

N3. ν is Lipschitz continuous in ϑ with Lipschitz constant L_ν.

N4. For all $\rho_1 \in \Omega_{o,\mathbb{R}}$ with $\operatorname{diam} \rho_1 < \infty$ one has $\nu(t, x, \vartheta, \rho_1) = \mathrm{v}(t, x, \vartheta, \Pi_\mathrm{w}(\rho_1))$.

Let the initial state *$\rho_o \in \Omega_{o,S^1}$ be such that $\partial_\vartheta \rho_o \in \mathcal{C}_{\mathrm{u,b}}(X \times S^1, \mathbb{R})$. Let $\rho \in \mathcal{C}^1(\mathbb{R}, \mathcal{C}_{\mathrm{u,b}}(X \times S^1, \mathbb{R}))$ be the maximal solution to the initial value problem*

$$\rho(0, \cdot, \cdot) = \rho_o, \qquad \partial_t \rho(t, x, \vartheta) = -\partial_\vartheta \left[\rho(t, x, \vartheta) \cdot \mathrm{v}(t, x, \vartheta, \rho(t))\right] \tag{1.28}$$

within Ω_{S^1}, as predicted by theorem 1.4.2. Let $\zeta_o \in \Omega_{o,\mathbb{R}}$ be a an unwrapping of ρ_o with $\operatorname{diam} \zeta_o < \infty$ and such that $\partial_\vartheta \zeta_o \in \mathcal{C}_{\mathrm{u,b}}(X \times \mathbb{R}, \mathbb{R})$.

Then there exists in $\Omega_\mathbb{R}$ a maximal solution ζ to the continuity equation $\partial_t \zeta(t, x, \vartheta) = -\partial_\vartheta \left[\zeta(t, x, \vartheta) \cdot \nu(t, x, \vartheta, \zeta(t))\right]$ with initial value $\zeta(0, \cdot, \cdot) = \zeta_o$. That solution $\zeta(t, \cdot, \cdot)$ is at all times $t \in \mathbb{R}$ a unwrapping of $\rho(t, \cdot, \cdot)$. It satisfies $\zeta \in \mathcal{C}^1(\mathbb{R}, \mathcal{C}_{\mathrm{u,b}}(X \times \mathbb{R}, \mathbb{R}))$ and $\partial_\vartheta \zeta \in \mathcal{C}(\mathbb{R} \times X \times \mathbb{R}, \mathbb{R})$. Furthermore, $\partial_\vartheta \zeta(t, \cdot, \cdot) \in \mathcal{C}_{\mathrm{u,b}}(X \times \mathbb{R}, \mathbb{R})$ and $\operatorname{supp}_\mathbb{R} \zeta(t, \cdot, \cdot) \subseteq \{\vartheta \in \mathbb{R} : d(\vartheta, \operatorname{supp}_\mathbb{R} \zeta_o) \leq \|\nu\|_\infty \cdot |t|\}$ for every $t \in \mathbb{R}$.

The theorem connects the evolution of densities on the circle to the evolution of densities on the real line. It shows what should be intuitively clear: For velocity fields $\mathrm{v}(t, x, \vartheta, \rho)$ depending only on the projection of ϑ and the wrapping of ρ on S^1, the wrapping and evolution of densities should be commuting operations. In the theorem below, the above results are applied to a slightly more general version of the fluid model than the one defined by the velocity field (1.11).

Lemma 1.4.4. *Let $(K, \mathcal{K}, \kappa)$ be a σ-finite measure space. Consider the function class*

$$\Omega_o := \left\{\rho \in \mathcal{M}_\mathrm{b}(X \times K, \mathbb{K}) : \|\rho(x, \cdot)\|_{L^1(\kappa)} = 1 \ \forall x \in X\right\} \tag{1.29}$$

endowed with the supremum metric. Let $I \in \mathcal{M}_\mathrm{b}(X \times K, \mathbb{K})$. Let $G : X \times X \to \mathbb{K}$ be measurable, such that the mapping $X \to L^1(\mu)$, $x \mapsto G(x, \cdot)$ is uniformly continuous and bounded. Then the stimulus

$$S(x, \rho) := \int_X d\mu(y)\ G(x, y) \cdot \int_K d\kappa(\varphi)\ \rho(y, \varphi) \cdot I(y, \varphi), \tag{1.30}$$

is well-defined for any $x \in X$ and $\rho \in \Omega_o$ and satisfies:

1. *For every $\rho \in \Omega_o$ one has $S(\cdot, \rho) \in \mathcal{C}_{\mathrm{u,b}}(X, \mathbb{K})$ and for every $x \in X$ one has $S(x, \cdot) \in \mathcal{C}_{\mathrm{b}}(\Omega_o, \mathbb{K})$. Furthermore, S is bounded on $X \times \Omega_o$.*

2. *Suppose $\kappa(K)$ is finite: Then $S \in \mathcal{C}_{\mathrm{u,b}}(X \times \Omega_o, \mathbb{K})$ and S is Lipschitz continuous in Ω_o with a Lipschitz constant uniform in X.*

For a proof see appendix A.2.1.

Theorem 1.4.5 (Existence and uniqueness of solutions for oscillator networks)
Let $G : X \times X \to \mathbb{R}$ be measurable and such that the mapping $X \to L^1(\mu)$, $x \mapsto G(x, \cdot)$ is bounded and uniformly continuous. Let $I : X \times S^1 \to \mathbb{R}$ be measurable and bounded. Let $u, \psi : \mathbb{R} \times X \times S^1 \to \mathbb{R}$, $(t, x, \vartheta) \mapsto u(t, x, \vartheta)$, $(t, x, \vartheta) \mapsto \psi(t, x, \vartheta)$ be such that $\psi, \partial_\vartheta \psi, \partial_\vartheta^2 \psi, u, \partial_\vartheta u, \partial_\vartheta^2 u \in \mathcal{C}_{\mathrm{u,b}}(\mathbb{R} \times X \times S^1, \mathbb{R})$. Let Ω_{o,S^1}, $\Omega_{o,\mathbb{R}}$ and $\Omega_{S^1}, \Omega_{\mathbb{R}}$ be the function spaces defined in (1.22) and (1.23), respectively. Define the velocity field $\mathrm{v} : \mathbb{R} \times X \times S^1 \times \Omega_{o,S^1} \to \mathbb{R}$ as

$$\mathrm{v}(t, x, \vartheta, \rho_o) := u(t, x, \vartheta) + \psi(t, x, \vartheta) \cdot \int_X d\mu(y)\ G(x, y) \cdot \int_{S^1} d\varphi\ \rho_o(y, \varphi) \cdot I(y, \varphi). \tag{1.31}$$

Identify u, ψ and I with their pullbacks on $\mathbb{R}$ (with respect to ϑ) and define the velocity field $\nu : \mathbb{R} \times X \times \mathbb{R} \times \Omega_{o,\mathbb{R}} \to \mathbb{R}$ as

$$\nu(t, x, \vartheta, \zeta_o) := u(t, x, \vartheta) + \psi(t, x, \vartheta) \cdot \int_X d\mu(y)\ G(x, y) \cdot \int_{\mathbb{R}} d\varphi\ \zeta_o(y, \varphi) \cdot I(y, \varphi). \tag{1.32}$$

Let the initial state $\rho_o \in \Omega_{o,S^1}$ be such that $\partial_\vartheta \rho_o \in \mathcal{C}_{\mathrm{u,b}}(X \times S^1, \mathbb{R})$. Let $\zeta_o \in \Omega_{o,\mathbb{R}}$ be an unwrapping of ρ_o such that $\partial_\vartheta \zeta_o \in \mathcal{C}_{\mathrm{u,b}}(X \times \mathbb{R}, \mathbb{R})$ and $\operatorname{diam} \zeta_o < \infty$. Then there exists in Ω_{S^1} a maximal, global solution to the initial value problem

$$\rho(0, \cdot, \cdot) = \rho_o, \qquad \partial_t \rho(t, x, \vartheta) = -\partial_\vartheta \left[\rho(t, x, \vartheta) \cdot \mathrm{v}(t, x, \vartheta, \rho(t))\right]. \tag{1.33}$$

That solution ρ is within $\mathcal{C}^1(\mathbb{R}, \mathcal{C}_{\mathrm{u,b}}(X \times S^1, \mathbb{R}))$ and satisfies $\partial_\vartheta \rho(t, \cdot, \cdot) \in \mathcal{C}_{\mathrm{u,b}}(X \times S^1, \mathbb{R})$ for every $t \in \mathbb{R}$ as well as $\partial_\vartheta \rho \in \mathcal{C}(\mathbb{R} \times X \times S^1, \mathbb{R})$. Similarly, there exists in $\Omega_{\mathbb{R}}$ a maximal, global solution to the initial value problem

$$\zeta(0, \cdot, \cdot) = \zeta_o, \qquad \partial_t \zeta(t, x, \vartheta) = -\partial_\vartheta \left[\zeta(t, x, \vartheta) \cdot \nu(t, x, \vartheta, \zeta(t))\right]. \tag{1.34}$$

That solution ζ is within $\mathcal{C}^1(\mathbb{R}, \mathcal{C}_{\mathrm{u,b}}(X \times \mathbb{R}, \mathbb{R}))$ and satisfies $\partial_\vartheta \zeta(t, \cdot, \cdot) \in \mathcal{C}_{\mathrm{u,b}}(X \times \mathbb{R}, \mathbb{R})$ for every $t \in \mathbb{R}$ as well as $\partial_\vartheta \zeta \in \mathcal{C}(\mathbb{R} \times X \times \mathbb{R}, \mathbb{R})$. Furthermore, at all times $t \in \mathbb{R}$ one has $\operatorname{supp}_{\mathbb{R}} \zeta(t, \cdot, \cdot) \subseteq \{\vartheta \in \mathbb{R} : d(\vartheta,\ \operatorname{supp}_{\mathbb{R}} \zeta_o) \leq \|\nu\|_\infty \cdot |t|\}$. Finally, $\rho(t, \cdot, \cdot)$ is at all times $t \in \mathbb{R}$ a wrapping of $\zeta(t, \cdot, \cdot)$.

Note that choosing $u(t, x, \vartheta) := \omega$, $\psi(t, x, \vartheta) \equiv \psi(\vartheta)$ and $I(y, \varphi) \equiv I(\varphi)$, reproduces the original fluid model with the velocity field (1.11).

Proof. I shall show that the velocity fields v and ν satisfy the assumptions of theorem 1.4.3. For $\rho_1 \in \Omega_{o,S^1}, \zeta_1 \in \Omega_{o,\mathbb{R}}$ and $x \in X$ denote

$$\begin{aligned} S_{S^1}(x, \rho_1) &:= \int_X d\mu(y)\ G(x, y) \cdot \int_{S^1} d\varphi\ \rho_1(y, \varphi) \cdot I(y, \varphi), \\ S_{\mathbb{R}}(x, \zeta_1) &:= \int_X d\mu(y)\ G(x, y) \cdot \int_{\mathbb{R}} d\varphi\ \zeta_1(y, \varphi) \cdot I(y, \varphi). \end{aligned} \tag{1.35}$$

By lemma 1.4.4(2) $S_{S^1} \in \mathcal{C}_{\mathrm{u,b}}(X \times \Omega_{o,S^1}, \mathbb{R})$ and S_{S^1} is Lipschitz continuous in Ω_{o,S^1}, uniformly in X. By the assumptions on u and v, the velocity field $\mathrm{v} = u + \psi \cdot S_{S^1}$ as well as its derivatives $\partial_\vartheta \mathrm{v}$, $\partial_\vartheta^2 \mathrm{v}$ are thus in $\mathcal{C}_{\mathrm{u,b}}(\mathbb{R} \times X \times S^1 \times \Omega_{o,S^1}, \mathbb{R})$. Similarly, v and $\partial_\vartheta \mathrm{v}$ are Lipschitz continuous in Ω_{o,S^1} uniformly in $\mathbb{R} \times X \times S^1$. Consequently v and ρ_o satisfy the assumptions of theorem 1.4.3.

Furthermore, by lemma 1.4.4(1) $S_{\mathbb{R}}$ is bounded and one has $S_{\mathbb{R}}(x, \cdot) \in \mathcal{C}_{\mathrm{b}}(\Omega_{o,\mathbb{R}}, \mathbb{R})$ for every $x \in X$. Consequently, ν satisfies conditions (N1) and (N2) of theorem 1.4.3. Since $\partial_\vartheta \nu$ is bounded, ν is Lipschitz continuous in ϑ, uniformly in $\mathbb{R} \times X \times \Omega_{o,\mathbb{R}}$. Condition 1.4.3(N4) is also clearly satisfied. Applying theorems 1.4.2 and 1.4.3 finishes the proof. □

Chapter 2

Synchrony in the field and fluid models

2.1 Introduction

This chapter examines the existence and local stability of synchrony in the field model (1.9) and fluid model (1.10). In the former, synchrony takes the form $\theta(t,x) = \phi(t)$ for some function $\phi : \mathbb{R} \to S^1$. In the latter, it takes the formal form of a Dirac distribution $\rho(t,x,\vartheta) = \delta(\vartheta - \phi(t))$ with time-dependent support $\phi(t)$. Throughout this chapter, X will be a separable metric space and μ a finite, strictly positive Borel measure on it. Note that the assumption of strict positivity is not a real restriction of generality, since X always contains a (closed) subset of full measure (i.e. with a complement of zero measure) on which the restricted measure is strictly positive (see appendix A.3.1).

It has been widely observed, that the connection topology of oscillator and neural networks plays a central role in the emergence of collective behaviour and synchronization in particular (Watts & Strogatz 1998, Lago-Fernández et al. 2001, Wu 2005, Arenas et al. 2008). My results on the stability of synchrony extend these findings to the models presented in this thesis. Section 2.2 introduces the property of *strong connectivity* to integral kernels, as a generalization of strong finite-graph connectivity. This property will allow the application of the generalized Jentzsch-Perron theorem, a generalization of the Perron-Frobenius theorem on irreducible matrices (Perron 1907, Frobenius 1912) to operators on Banach lattices. Applying it to the coupling kernel G, will give in section 2.3 the necessary insight to the point spectrum of the linearized dynamics around the limit cycle of synchrony. This insight is used in particular in theorem 2.3.3, which gives sufficient conditions on the coupling kernel, iPRC and oscillator pulse for the local stability of synchrony in the field model. The latter generalizes the results of Goel & Ermentrout (2002), who considered the special case of finitely many oscillators. In section 2.4 and in particular theorem 2.4.4, the stability of synchrony for the fluid model against distortions with an adequately narrow bandwidth is examined. More precisely, it is shown that under certain assumptions on the coupling kernel, the iPRC and oscillator pulse, the diameter $\operatorname{diam}\rho(t,\cdot,\cdot)$ decreases exponentially with time, provided it was initially below a certain threshold.

2.2 Connectivity of coupling kernels

As already indicated, one should expect the connectivity of the oscillator network to play a crucial role in the emergence and stability of synchronization. For finite networks of a structure similar to the Winfree model (1.4), it has been shown that the irreducibility of the coupling matrix $(G_{ij})_{i,j=1}^n$ is key to the stability of synchronization (Goel & Ermentrout 2002, Katriel 2005). In both of the cited articles, the Perron-Frobenius theorem was used to show the existence of a maximal positive eigenvalue of the coupling matrix with simple algebraic multiplicity. Note that the irreducibility of (G_{ij}) is equivalent to the following property: For every non-zero vector

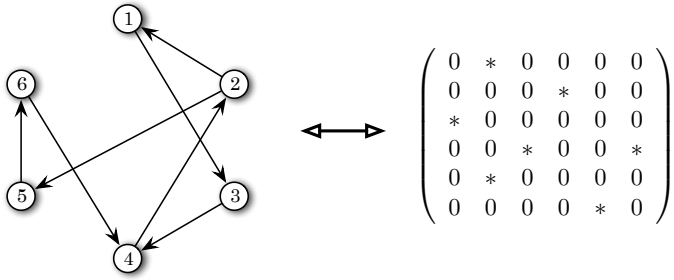

$$\begin{pmatrix} 0 & * & 0 & 0 & 0 & 0 \\ 0 & 0 & 0 & * & 0 & 0 \\ * & 0 & 0 & 0 & 0 & 0 \\ 0 & 0 & * & 0 & 0 & * \\ 0 & * & 0 & 0 & 0 & 0 \\ 0 & 0 & 0 & 0 & * & 0 \end{pmatrix}$$

Figure 2.1: Illustration of a strongly connected directed graph, consisting of 6 edges and corresponding to the irreducible 6×6 coupling matrix on the right. Node j connects to node i if and only if the matrix entry at column j and row i is strictly positive (marked with a star).

$\mathbf{x} \in \mathbb{R}_+^n$ with non-negative entries, the sum $\sum_{k=0}^m G^k \mathbf{x}$ has exclusively strictly positive entries, provided that $m \in \mathbb{N}_0$ is chosen large enough. The irreducibility of the coupling matrix is also equivalent to the strong connectivity of the directed graph it defines (node j connects to node i if and only if $G_{ij} > 0$). As a reminder, a directed graph is called *strongly connected* if from every node in the graph there exists a directed path to every other node (Berge 1976). For an example, see figure 2.1. Here, the notion of strong graph connectivity is generalized to so-called strong connectivity of coupling kernels on σ-finite measure spaces. The idea is to generalize the characterizing property of irreducible matrices mentioned above, by replacing the vector $\mathbf{x}$ with a non-negative, non-trivial function and the coupling matrix with the integral operator corresponding to the coupling kernel. In that sense, a strongly connecting kernel should *spread* any arbitrarily small *bump* to the whole space by means of iterated convolutions. It turns out, that this definition of strong kernel connectivity implies the *band irreducibility* (a generalization of matrix irreducibility) of the corresponding convolution operator.

The reader is referred to Schaefer (1974) and Zaanen (1997) for more information on Banach lattices and the terminology used in this section. As an overview, a real *lattice vector space* V_o is a real, partially ordered vector space in which any two elements $u, v \in V_o$ have a unique supremum $u \vee v$ and a unique infimum $u \wedge v$. The *supremum* of a subset $S \subseteq V_o$ refers to the least upper bound of S in V_o, while the *infimum* of S refers to its greatest lower bound. Every element $v \in V_o$ can be decomposed into its *positive part* $v^+ := v \vee 0$ and *negative part* $v^- := (-v) \vee 0$, so that $v = v^+ - v^-$. The *modulus* of v is defined as $|v| := v^+ + v^-$. A sub-lattice vector space $\mathcal{B}_o$ of V_o is called a *band* in V_o if:

B1. For each $v \in V_o$ and $b \in \mathcal{B}_o$ with $|v| \leq |b|$, also $v \in \mathcal{B}_o$.

B2. For each $\emptyset \neq A \subseteq \mathcal{B}_o$ for which the supremum $\sup A$ exists in V_o, one has $\sup A \in \mathcal{B}_o$.

If V is the $\mathbb{C}$-vector space given by complexification of V_o, then a *band* $\mathcal{B}$ in V is the complexification $\mathcal{B}_o + i\mathcal{B}_o$ of a band $\mathcal{B}_o$ in V_o. It still satisfies axiom (1) with respect to the *complex modulus* $|x + iy| := \sup_{\vartheta \in S^1} |x \cos\vartheta + y \sin\vartheta|$ $(x, y \in V_o)$. A band $\mathcal{B}$ is called *trivial* if either $\mathcal{B} = \{0\}$ or $\mathcal{B} = V$. For any sequence $(h_n)_{n\in\mathbb{N}} \subseteq V_o$ and $h \in V_o$, one writes $h_n \downarrow h$ if the sequence $(h_n)_n$ is decreasing and h is its infimum. One says that a linear operator K on V is *band irreducible* if there exists in V no non-trivial, K-invariant band. One calls K *σ-order continuous* if from $V_o \ni h_n \downarrow 0$ follows $Kh_n \downarrow 0$.

Definition 2.2.1 (Strongly connecting coupling kernel)**.** Let $(K, \mathcal{K}, \kappa)$ be a σ-finite measure space and $G : K \times K \to \mathbb{R}_+$ measurable. Let $\mathcal{F}$ be the set of measurable functions $h : K \to \mathbb{R}_+ \cup \{\infty\}$ and $\hat{G} : \mathcal{F} \to \mathcal{F}$ be the *integral operator corresponding to* G, defined as

$$(\hat{G}h)(x) := \int_K d\kappa(y)\; G(x, y) \cdot h(y), \qquad h \in \mathcal{F},\ x \in K. \tag{2.1}$$

Note that $\hat{G}h : K \to \mathbb{R}_+$ is by Tonelli's theorem (see for example Ambrosio et al. 2011, Theorem 6.4) indeed measurable. Then G shall be said to be *strongly connecting* K if for every $h \in \mathcal{F}$ with $\|h\|_{L^1(\kappa)} > 0$, the set

$$\bigcup_{n\in\mathbb{N}_0} \left(\hat{G}^n h\right)^{-1}((0,\infty]) \tag{2.2}$$

has full measure, that is, has a complement of measure zero. Note that for the definition it suffices to consider only indicator functions $h = 1_A$ of sets $A \in \mathcal{K}$ of non-zero measure.

Examples 2.2.2

(i) Let $G \in \mathbb{R}_+^{N\times N}$ be an N-dimensional square matrix with non-negative entries and let $K := \{1, .., N\}$ be endowed with the counting measure. Interpret $G : K \times K \to \mathbb{R}_+$ as integral kernel. Then G strongly connects K if and only if the matrix G is irreducible and if and only if the weighted, directed graph defined by G (edge $(m \to n)$ exists whenever $G_{nm} > 0$) is strongly connected.

(ii) If there exists a set $A \in \mathcal{K}$ such that $\kappa(A) > 0, \kappa(K \setminus A) > 0$ and $G(x, y) = 0$ for all $x \in A$, $y \in K \setminus A$, then G does not strongly connect K. See figure 2.2 for an example.

(iii) If the convolution $G * \cdots * G$ is strictly positive everywhere for some convolution order high enough, then G strongly connects K.

(iv) Let K be a path connected, separable metric space and κ a strictly positive, σ-finite Borel measure on K. Let G satisfy the following *blurring* property: For every $x \in K$ there exists an open neighbourhood U_x of x such that whenever $\kappa(U_x \cap A) > 0$ for some $A \in \mathscr{B}(K)$, one has $(\hat{G}1_A)|_{U_x} > 0$. Then G strongly connects K.

Proof: Note that the blurring property is in fact equivalent to the following: For every $x \in K$ there exists an open neighbourhood U_x of x such that whenever $\|h \cdot 1_{U_x}\|_{L^1(\kappa)} > 0$ for some $h \in \mathcal{F}$ one has $(\hat{G}h)|_{U_x} > 0$.

Now let $h \in \mathcal{F}$ be arbitrary with $\|h\|_{L^1(\kappa)} > 0$. For each $x \in K$ let U_x be a neighbourhood as described above. Since K is Lindelöf, it is the union of countably many of those neighbourhoods $\{U_x\}_{x\in K}$. Thus $\|h \cdot 1_{U_x}\|_{L^1(\kappa)} > 0$ for at least one $x \in K$ and by the blurring property $(\hat{G}h)|_{U_x} > 0$. Now let $y \in K$ be any other point. I shall show that $(\hat{G}^n h)(y) > 0$ for some $n \in \mathbb{N}$.

Since K is path connected, there exists a finite sequence of points $x_1 = x, x_2, .., x_n = y$ in K such that $U_{x_i} \cap U_{x_{i+1}} \neq \emptyset$ for every $i \in \{1, .., n-1\}$. We have seen that $(\hat{G}h)|_{U_{x_1}} > 0$. Since κ is strictly positive one knows that $\kappa(U_{x_1} \cap U_{x_2}) > 0$, so that $\|(\hat{G}h) \cdot 1_{U_{x_2}}\|_{L^1(\kappa)} > 0$ and thus by the blurring property $((\hat{G})^2 h)|_{U_{x_2}} > 0$. By induction one concludes that $((\hat{G})^n h)|_{U_{x_n}} > 0$. □

(v) Let K be a separable metric space and κ a σ-finite Borel measure on it. Let $G : K\times K \to \mathbb{R}_+$ be continuous and satisfy $G(x, x) > 0$ for every $x \in K$. Then G satisfies the blurring property from example (iv). See figure 2.2 for an example.

Proof: For $x \in K$ choose the open neighbourhood U_x so that $G|_{U_x\times U_x} > 0$. Let $A \in \mathscr{B}(K)$ be such that $\kappa(U_x \cap A) > 0$. Then for any $z \in U_x$ one can estimate

$$(\hat{G}1_A)(z) = \int_A d\kappa(y)\ G(z, y) \geq \int_{U_x\cap A} d\kappa(y)\ G(z, y) > 0. \quad \square \tag{2.3}$$

(vi) Let $\mathbb{T}^m := \mathbb{R}^m/\mathbb{Z}^m$ be the m-dimensional torus with the metric inherited from $\mathbb{R}^m$ and κ on it the normalized Haar measure. Let $G : \mathbb{T}^m \times \mathbb{T}^m \to \mathbb{R}_+$ be of the form $G(x, y) = g(x - y)$ for some continuous $g : \mathbb{T}^m \to \mathbb{R}_+$. If $g \neq 0$, then G strongly connects $\mathbb{T}^m$.

Proof: By continuity of g there exists a ball $B_{2r}(z) \subseteq \mathbb{T}^m$ of radius $2r > 0$ and centre $z \in \mathbb{T}^m$ such that $g|_{B_{2r}(z)} > 0$. Let $A \subseteq \mathbb{T}^m$ be of strictly positive measure, then there exists some point $x_o \in \mathbb{T}^m$ such that $\kappa(A \cap B_r(x_o)) > 0$. Let $x_1 := x_o + z$, then for any $x \in B_r(x_1)$ one has

$$(\hat{G}1_A)(x) = \int_A dy\ g(x - y) \geq \int_{A\cap B_r(x_o)} dy\ g(x - y) > 0, \tag{2.4}$$

that is $(\hat{G}1_A)|_{B_r(x_1)} > 0$. Note that in the last step, use has been made of the fact that the difference $(x - y)$ appearing in the integral is in $B_{2r}(z)$. Now suppose $h \in \mathcal{F}$ is strictly positive on some ball $B_{nr}(x_n)$. Set $x_{n+1} := x_n + z$, then for any $x := (x_{n+1} + \delta) \in B_{nr+r}(x_{n+1})$ one has

$$\begin{aligned} &\{y \in K : g(x - y) \cdot h(y) > 0\} \supseteq \{y \in K : y \in B_{nr}(x_n) \wedge (x - y) \in B_{2r}(z)\} \\ =&B_{nr}(x_n) \cap B_{2r}(x - z) = B_{nr}(x_n) \cap B_{2r}(x_n + \delta)\,. \end{aligned} \tag{2.5}$$

As the intersection $B_{nr}(x_n) \cap B_{2r}(x_n + \delta)$ is non-empty, one has $(\hat{G}h)(x) > 0$ for all $x \in B_{nr+r}(x_{n+1})$. By induction one concludes that $((\hat{G})^n 1_A)|_{B_{nr}(x_n)} > 0\ \forall n \in \mathbb{N}$ for appropriate centres $x_n \in \mathbb{T}^m$. Since $\mathbb{T}^m$ has finite diameter, $((\hat{G})^n h)|_{\mathbb{T}^m} > 0$ for $n \in \mathbb{N}$ large enough. Thus G strongly connects $\mathbb{T}^m$. □

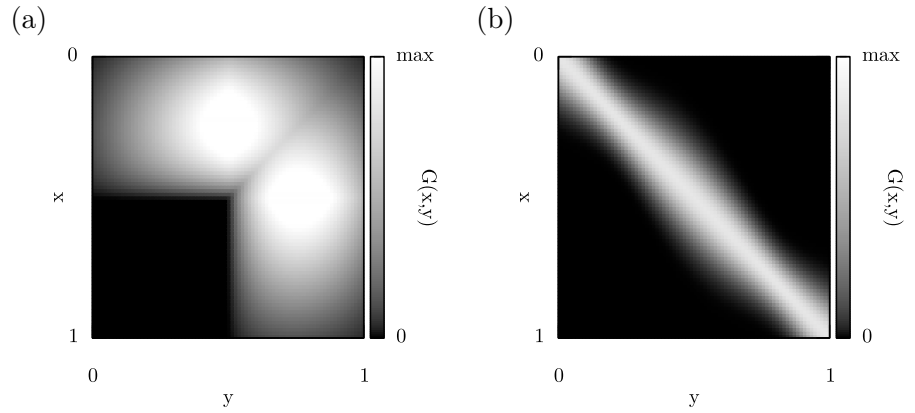

Figure 2.2: Illustration of two non-negative integral kernels on the interval $K := [0, 1]$, the latter endowed with the Lebesgue measure. A brighter colour corresponds to a greater value. The kernel on the left does not strongly connect K, due to the invariance of the subset $\{h \in \mathcal{F} : \operatorname{supp} h \subseteq [0, 0.5]\}$ under the action of $\hat{G}$. The kernel on the right strongly connects K. Note the apparent similarity to the concept of matrix irreducibility.

As the examples verify, the definition of strong connectivity of coupling kernels on measure spaces is a true generalization of strong finite-graph connectivity, with the implicitly assumed counting measure replaced by an arbitrary measure κ. The following lemma reinforces this interpretation, by linking the strong connectivity of coupling kernels to the band irreducibility of the corresponding integral operator.

Lemma 2.2.3 (Irreducibility of strongly connecting kernels)**.** *Let $G : X \times X \to \mathbb{R}_+$ be measurable, strongly connecting the space and such that the mapping $X \to L^1(\mu)$, $x \mapsto G(x, \cdot)$ is continuous, non-trivial and bounded. Consider the $\mathbb{C}$-linear space $V_{\mathbb{C}} := \mathcal{C}_{\mathrm{b}}(X, \mathbb{C})$ as the complexification of the $\mathbb{R}$-linear Banach lattice space $V := \mathcal{C}_{\mathrm{b}}(X, \mathbb{R})$ endowed with the pointwise partial order. Let $\hat{G} : V_{\mathbb{C}} \to V_{\mathbb{C}}$ be the integral operator corresponding to G. Then:*

1. $\hat{G} > 0$ *is a bounded, linear, positive operator, that is* $\hat{G}h \geq 0$ *whenever* $0 \leq h \in V$ *and* $\hat{G} \neq 0$.

2. $\hat{G}$ *is* σ*-order continuous.*

3. $\hat{G}$ *is band irreducible.*

Proof. The continuity of the operator $\hat{G} : V_{\mathbb{C}} \to V_{\mathbb{C}}$ follows from the fact that $\sup_{x \in X} \|G(x, \cdot)\|_{L^1(\mu)} < \infty$. Non-negativity is clear since G is real and non-negative. Non-triviality of $\hat{G}$ follows from the non-triviality of the mapping $x \mapsto G(x, \cdot) \in L^1(\mu)$. Its σ-order continuity follows from Lebesgue's dominated convergence theorem. Left to show is thus its band irreducibility.

Let $\{0\} \subsetneq \mathcal{B}_{\mathbb{C}} \subseteq V_{\mathbb{C}}$ be a $\hat{G}$-invariant band in $V_{\mathbb{C}} = V + iV$. I show that $\mathcal{B}_{\mathbb{C}} = V_{\mathbb{C}}$. For that it suffices to consider its real part $\mathcal{B} \supsetneq \{0\}$, a $\hat{G}$-invariant band in V, and show that $\mathcal{B} = V$. Claim: There exists a function $0 \leq f \in \mathcal{B}$, strictly positive on a dense subset of X.

> **Proof.** By assumption, there exists some $0 \neq h \in \mathcal{B}$. Since $\mathcal{B}$ is a band, one may without loss of generality assume $h \geq 0$. Then by continuity h is strictly positive on some non-empty, open subset of X. Since μ is strictly positive, this means $\|h\|_{L^1(\mu)} > 0$. Define the family of functions $0 \leq f_n := \hat{G}^n h \in \mathcal{B}$ for $n \in \mathbb{N}$. By strong connectivity of G the union $\bigcup_{n \in \mathbb{N}_0} f_n^{-1}((0, \infty])$ has full measure. By strict positivity of the measure that union is dense in X. Rescale $\tilde{f}_n := \frac{1}{(n+1)^2} \cdot f_n / (1 + \|f_n\|_\infty)$ and consider the pointwise sum $f := \sum_{k=0}^{\infty} \tilde{f}_k$. Then f is the uniform limit of the sequence of partial sums $\sum_{k=0}^{n} \tilde{f}_k$, so that $f \in \mathcal{C}_{\mathrm{b}}(X, \mathbb{R})$. It is also the supremum of the family $\{\tilde{f}_k\}_{k \in \mathbb{N}_0}$ in V, so that by band property (B2) (see page 17) in fact $f \in \mathcal{B}$. Furthermore, $f \geq 0$ is strictly positive on a dense subset of X.

The proof finishes by showing that every $h \in V$ is in $\mathcal{B}$. Since $\mathcal{B}$ is a sub-lattice vector space, it suffices to show that the positive part of h is within $\mathcal{B}$, so that one may assume $h \geq 0$. For each $x \in X$ define $h_x := \frac{h(x)}{f(x)} \cdot f$ if $f(x) > 0$ and $h_x := 0$ if $f(x) = 0$. Then $0 \leq h_x \in \mathcal{B}$. Furthermore $h_x(x) = h(x)$ whenever $f(x) > 0$. For each $x \in X$ define $\tilde{h}_x := \min(h_x, h)$, then $\tilde{h}_x \in \mathcal{B}$ by band property (B1), since dominated by h_x. By construction $\tilde{h}_x \leq h$ for all $x \in X$ and $\tilde{h}_x(x) = h(x)$ whenever $f(x) > 0$. Consequently, h is an upper bound for all $\{\tilde{h}_y\}_{y \in X}$ and $h(x)$ is the supremum of the values $\{\tilde{h}_y(x)\}_{y \in X}$ whenever $f(x) > 0$. Since h is continuous and f is strictly positive on a dense subset, h is the smallest upper bound for $\{\tilde{h}_y\}_{y \in X}$ in V, which by band property (B2) implies $h \in \mathcal{B}$. □

Corollary 2.2.4. *Let* $G : X \times X \to \mathbb{R}_+$ *be measurable, strongly connecting* X *and such that the mapping* $X \to L^1(\mu)$, $x \mapsto G(x, \cdot)$ *is continuous, non-trivial and bounded. Define* $V := \mathcal{C}_{\mathrm{b}}(X, \mathbb{C})$ *and consider the integral operator* $\hat{G} \in \mathcal{L}(V)$ *corresponding to* G. *Assume* $\hat{G}^n$ *is compact for some* $n \in \mathbb{N}$. *Then* $r(\hat{G}) > 0$ *and* $r(\hat{G})$ *is an eigenvalue of* $\hat{G}$ *of algebraic multiplicity one.*

Proof. Apply the generalized Jentzsch-Perron theorem for positive, σ-order continuous, band irreducible operators on Banach lattices (Grobler 1987, Theorem 6), which holds by lemma 2.2.3. □

Corollary 2.2.5. *Define* $V := \mathcal{C}_{\mathrm{b}}(X, \mathbb{C})$ *and let* $G : X \times X \to \mathbb{R}_+$ *be measurable, satisfying the following:*

G1. G *strongly connects* X.

G2. $\|G(x, \cdot)\|_{L^1(\mu)} = G_o$ *for some constant* $G_o > 0$ *and all* $x \in X$.

G3. The mapping $X \to L^1(\mu)$, $x \mapsto G(x, \cdot)$ *is continuous.*

G4. $\hat{G}^n$ *is compact for some* $n \in \mathbb{N}$*, with* $\hat{G} : V \to V$ *being the integral operator corresponding to* G*.*

Then $\hat{G} \in \mathcal{L}(V)$ *satisfies:*

1. *Both the spectral radius* $r(\hat{G})$ *and the operator norm* $\|\hat{G}\|$ *equal* G_o*.*
2. G_o *is an eigenvalue of* $\hat{G}$ *and* $\mathrm{kernel}(G_o - \hat{G}) = \mathrm{span}_{\mathbb{C}}\{1\}$*.*
3. $\sup\left\{\Re(\lambda) : \lambda \in \sigma(\hat{G}) \setminus \{G_o\}\right\} < G_o$*.*

Proof. Note that by assumptions (G2) and (G3), the integral operator $\hat{G} : V \to V$ is well-defined and continuous. In fact, it satisfies the assumptions of corollary 2.2.4, so that $r(\hat{G})$ is an eigenvalue of algebraic multiplicity one. For any $h \in \mathcal{C}_{\mathrm{b}}(X, \mathbb{C})$ one can by Hölder estimate $\|\hat{G}h\|_\infty \leq G_o \cdot \|h\|_\infty$, so that $r(\hat{G}) \leq \|G\| \leq G_o$. On the other hand, the constant function $1 \in V$ is an eigenvector of $\hat{G}$ for the eigenvalue G_o, so that the first and second claim are verified. Since $\hat{G}$ is power-compact, one has $\sigma(\hat{G}) = \sigma_{\mathrm{p}}(\hat{G}) \cup \{0\}$ and the only point of adherence of $\sigma_{\mathrm{p}}(\hat{G})$ is the origin. Thus $G_o > 0$ is isolated from $\sigma(\hat{G}) \setminus \{G_o\}$. Since $|\lambda| \leq G_o$ for any $\lambda \in \sigma(\hat{G})$, this implies the last claim. □

Example 2.2.6 Let $X := \mathbb{T}^m = \mathbb{R}^m/\mathbb{Z}^m$ be the m-dimensional torus and μ the normalized Haar measure on it. Let $G : \mathbb{T}^m \times \mathbb{T}^m \to \mathbb{R}_+$ be of the form $G(x, y) = g(x - y)$ for some continuous $0 \neq g : \mathbb{T}^m \to \mathbb{R}_+$. Then G satisfies all assumptions of corollary 2.2.5 (see example 2.2.2(vi) on its strong connectivity). The point spectrum of the integral operator $\hat{G} : \mathcal{C}_{\mathrm{b}}(\mathbb{T}^m, \mathbb{C}) \to \mathcal{C}_{\mathrm{b}}(\mathbb{T}^m, \mathbb{C})$ is given by the set $\sigma_{\mathrm{p}}(\hat{G}) = \{\tilde{g}(k) : k \in \mathbb{Z}^n\}$, with $\tilde{g}(k) := \int_{\mathbb{T}^m} dx\ g(x) \cdot e^{-i2\pi kx}$ being the k-th Fourier component of g and corresponding to the eigenfunction $e_k(x) := e^{i2\pi kx}$. Note that $\tilde{g}(0) = G_o$ and that for any $k \neq 0$ one has $|\tilde{g}(k)| < G_o$ since $g \geq 0$ and $g \neq 0$.

2.3 Synchrony in the field model

With a view on the strong connectivity of coupling kernels, this section gives sufficient conditions for the existence and stability of synchrony in the field model (1.9). Note that any synchronized solution, that is of the form $\theta(t, x) = \phi(t)$, must satisfy the EOM $\dot{\phi}(t) = \omega + \psi(\phi(t)) \cdot I(\phi(t)) \cdot \|G(x, \cdot)\|_{L^1(\mu)}$ for every $x \in X$. Thus, one of the necessary conditions for the existence of synchrony, is that the *total coupling strength* $\|G(x, \cdot)\|_{L^1(\mu)}$ be equal at all points $x \in X$ (provided $\psi \cdot I$ is non-trivial). Note that this was already an assumption in corollary 2.2.5.

Lemma 2.3.1 gives an auxiliary spectral result for the linearized dynamics around the limit cycle of synchrony, though the actual connection to the field model will become apparent later on. Lemma 2.3.2 provides sufficient conditions for the stability of sub-manifolds in a special class of abstract dynamical systems. In theorem 2.3.3 these two lemmas are applied to the field model and give sufficient conditions for the existence and stability of synchrony in oscillator networks.

Lemma 2.3.1. *Let* $G : X \times X \to \mathbb{R}_+$ *satisfy all assumptions of corollary 2.2.5 as well as* $\|G(\cdot, y)\|_{L^1(\mu)} = G_1\ \forall y \in X$ *for some constant* $G_1 \in \mathbb{R}$*. Let* $\psi, I \in \mathcal{C}^1(S^1, \mathbb{R})$ *and* $\omega > 0$*. Let* $\phi \in \mathcal{C}^1(\mathbb{R}, S^1)$ *be* T*-periodic for some minimal* $T > 0$ *and satisfy the ODE* $\dot{\phi}(t) = \omega + G_o \cdot \psi(\phi(t)) \cdot I(\phi(t)) > 0$*. Consider the time-dependent, bounded linear operator*

$$\hat{\mathcal{H}}(t) := G_o \cdot \psi'(\phi(t)) \cdot I(\phi(t)) \cdot \mathrm{Id} + \psi(\phi(t)) \cdot I'(\phi(t)) \cdot \hat{G} \tag{2.6}$$

on the Banach-space $V := \mathcal{C}_{\mathrm{b}}(X, \mathbb{C})$*, with* $\hat{G} \in \mathcal{L}(V)$ *being the integral operator corresponding to* G*. Then the following hold:*

1. *The differential equation* $\dot{h}(t) = \mathcal{H}(t)h(t)$ *admits for each initial value* $h(t_o) \in V$ *a global, maximal solution* $h \in \mathcal{C}^1(\mathbb{R}, V)$*, given by*

$$h(t) = U(t, t_o)h(t_o) := \exp\left[A(t, t_o) \cdot G_o - B(t, t_o) \cdot \hat{G}\right] h(t_o), \tag{2.7}$$

where

$$\begin{aligned} A(t, t_o) &:= \int_{t_o}^{t} ds\ \psi'(\phi(s)) \cdot I(\phi(s)), \\ B(t, t_o) &:= -\int_{t_o}^{t} ds\ \psi(\phi(s)) \cdot I'(\phi(s)). \end{aligned} \tag{2.8}$$

2. *The operator* $K := U(t_o + T, t_o) : V \to V$ *is independent of* t_o *and given by* $K = \exp[B \cdot (G_o - \hat{G})]$*, where*

$$B := B(t_o + T, t_o) = \int_{S^1} d\varphi\ \frac{\psi'(\varphi) \cdot I(\varphi)}{\omega + G_o \cdot \psi(\varphi) \cdot I(\varphi)}. \tag{2.9}$$

3. *The linear sub-Banach space* $V_2 := \{h \in V : \mu(h) = 0\}$ *is* $\hat{G}$*- and flow-invariant, that is* $\hat{G}(V_2) \subseteq V_2$ *and* $U(t, t_o)(V_2) \subseteq V_2$ *for all* $t, t_o \in \mathbb{R}$*.*

4. *If* $B < 0$ *then* $r(K|_{V_2}) < 1$*.*

Proof. As a preliminary, let us note that by Tonelli's theorem and the assumptions on G one has

$$\begin{aligned} \mu(X) \cdot G_o &= \int_X d\mu(x) \int_X d\mu(y)\ G(x, y) \\ &= \int_X d\mu(y) \int_X d\mu(x)\ G(x, y) = \mu(X) \cdot G_1, \end{aligned} \tag{2.10}$$

so that $G_1 = G_o$.

1. Existence and uniqueness follow from the continuity of the mapping $t \mapsto \mathcal{H}(t) \in \mathcal{L}(V)$. The correctness of (2.7) can be directly verified by differentiation.

2. Substituting $d\varphi = \frac{d\phi(s)}{ds} ds$ in (2.8) yields

$$\begin{aligned} B(t_o + T, t_o) &= -\int_{S^1} d\varphi\ \frac{\psi(\varphi) \cdot I'(\varphi)}{\omega + G_o \cdot \psi(\varphi) \cdot I(\varphi)} \\ &= -\frac{1}{G_o} \int_{S^1} d\varphi\ \frac{d}{d\varphi} \ln\left[\omega + G_o \cdot \psi(\varphi) \cdot I(\varphi)\right] \\ &\quad + \int_{S^1} d\varphi\ \frac{\psi'(\varphi) \cdot I(\varphi)}{\omega + G_o \cdot \psi(\varphi) \cdot I(\varphi)} \\ &= \int_{S^1} d\varphi\ \frac{\psi'(\varphi) \cdot I(\varphi)}{\omega + G_o \cdot \psi(\varphi) \cdot I(\varphi)} = A(t_o + T, t_o). \end{aligned} \tag{2.11}$$

   Independence of $B(t_o + T, t_o)$ and $U(t_o + T, t_o)$ from t_o is apparent from (2.11).

3. Since the linear functional $\mu : V \to V$ is continuous, V_2 is indeed a Banach space. The rest follows from the easily verifiable fact that $\mu(\hat{G}h) = G_o \cdot \mu(h)$ thus

$$\mu\left[U(t, t_o)h\right] = \exp\left[G_o \cdot (A(t, t_o) - B(t, t_o))\right] \cdot \mu(h) \tag{2.12}$$

   for all $h \in V$.

4. Since $B \cdot (G_o - \hat{G}|_{V_2}) : V_2 \to V_2$ is a bounded operator, one knows that

$$\begin{aligned} \sigma(K|_{V_2}) &= \exp\left[\sigma\left(B \cdot (G_o - \hat{G}|_{V_2})\right)\right] = \exp\left[B \cdot (G_o - \sigma(\hat{G}|_{V_2}))\right] \\ &= \exp\left[B \cdot (G_o - \{0\} \cup \sigma_{\mathrm{p}}(\hat{G}|_{V_2}))\right]. \end{aligned} \tag{2.13}$$

In the last step the fact that $\hat{G}$ is power-compact was used. By corollary 2.2.5 one has $r(\hat{G}) = G_o$ and the only eigenvectors of $\hat{G}$ in V corresponding to the eigenvalue G_o are the constant non-trivial functions, which are not in V_2. By corollary 2.2.5(3) it follows that $r(K|_{V_2}) < 1$. □

Lemma 2.3.2. *Let V_1, V_2 be Banach spaces and $(\mathcal{H}_1, \mathcal{H}_2), (\mathcal{H}_{1,o}, \mathcal{H}_{2,o}) : V_1 \times V_2 \to V_1 \times V_2$ functionals satisfying:*

1. *$\mathcal{H} := (\mathcal{H}_1, \mathcal{H}_2) : V_1 \times V_2 \to V_1 \times V_2$ is Lipschitz continuous.*
2. *$\mathcal{H}_{2,o}(v_1, v_2) = \mathcal{H}_{2,o}(v_1)v_2$ with $\mathcal{H}_{2,o}(v_1) : V_2 \to V_2$ being a bounded, linear operator for each $v_1 \in V_1$.*
3. *The mapping $V_1 \to \mathcal{L}(V_2)$, $v_1 \mapsto \mathcal{H}_{2,o}(v_1)$ is Lipschitz continuous and bounded.*
4. *$[(\mathcal{H}_1, \mathcal{H}_2)(v_1, v_2) - (\mathcal{H}_{1,o}, \mathcal{H}_{2,o})(v_1, v_2)] \in o(v_2)$ as $v_2 \to 0$, uniformly in $v_1 \in V_1$.*
5. *$\mathcal{H}_{1,o}(v_1, v_2) = \mathcal{H}_{1,o}(v_1)$ only depends on v_1.*

Let $U := ((U_1, U_2)(t, t_o))_{t \geq t_o}$ be the autonomous flow generated by $\mathcal{H} := (\mathcal{H}_1, \mathcal{H}_2)$ on $V_1 \times V_2$. Suppose that there exists some period $T > 0$ such that the propagator $K : V_2 \to V_2$ from time t_o to $t_o + T$ induced on V_2 by the non-autonomous ODE $\dot{v}_2(t) = \mathcal{H}_{2,o}(U_1(t, t_o)(v_1, 0))v_2(t)$ does not depend on the fixed $v_1 \in V_1$. Furthermore, suppose that there exists an $n_o \in \mathbb{N}$ such that $\|K^{n_o}\| < 1$.

Then the U-invariant sub-space $V_1 \times \{0\} \subseteq V_1 \times V_2$ is locally exponentially stable. That is to say, there exist constants $A, \beta, \delta > 0$ such that $\|U_2(t, t_o)(v_1, v_2)\| \leq Ae^{-\beta \cdot (t - t_o)} \cdot \|v_2\|$ for all $t \geq t_o$, $v_1 \in V_1$ and $v_2 \in V_2$, provided that $\|v_2\| \leq \delta$.

The rather technical proof of this lemma is given in appendix A.3.2.

Theorem 2.3.3 (Local exponential stability of synchrony)
Let $G : X \times X \to \mathbb{R}_+$ satisfy all assumptions of corollary 2.2.5 as well as $\|G(\cdot, y)\|_{L^1(\mu)} = G_1$ $\forall y \in X$ for some constant $G_1 \in \mathbb{R}$. Let $\psi, I \in \mathcal{C}^2(S^1, \mathbb{R})$ and assume that $\omega + \psi(\varphi) \cdot G_o \cdot I(\varphi) > 0$ for all $\varphi \in S^1$. Consider the field equation (1.9) in the phase field $\theta \in \mathcal{C}_{\mathrm{b}}(X, S^1)$. Then synchrony $\theta(t, x) := \phi(t)$ is a solution to (1.9), provided that the function $\phi \in \mathcal{C}^1(\mathbb{R}, S^1)$ satisfies the autonomous ODE

$$\frac{d\phi}{dt}(t) = \omega + \psi(\phi(t)) \cdot I(\phi(t)) \cdot G_o. \tag{2.14}$$

Note that in that case, ϕ is T-periodic for some minimal $T > 0$. Assume furthermore that the value

$$B := \int_{S^1} d\varphi \, \frac{\psi'(\varphi) \cdot I(\varphi)}{\omega + G_o \cdot \psi(\varphi) \cdot I(\varphi)} \tag{2.15}$$

is strictly negative. For the following stability statement let us regard the field equation as an ODE on the Banach-space $\mathcal{C}_{\mathrm{b}}(X, \mathbb{R})$ by identifying ψ and I with their pullbacks on $\mathbb{R}$ (see also remark 2.3.4 below). For $\theta \in \mathcal{C}_{\mathrm{b}}(X, \mathbb{R})$ write $\overline{\theta} := \mu(\theta)/\mu(X)$ for the mean phase and $\theta_{\mathrm{v}} := \theta - \overline{\theta}$ for the variation about it.

Then synchrony is locally exponentially stable, that is, there exist constants $A, \beta > 0$ *and* $0 < \delta < 1/2$ *such that* $\|\theta_{\mathrm{v}}(t)\|_\infty \leq A \cdot e^{-\beta t} \cdot \|\theta_{\mathrm{v}}(0)\|_\infty$ *for all* $t \geq 0$*, provided that* $\|\theta_{\mathrm{v}}(0)\|_\infty \leq \delta$ *and* $\theta \in \mathcal{C}^1(\mathbb{R}, \mathcal{C}_{\mathrm{b}}(X, \mathbb{R}))$ *solves the field equation.*

Proof. The proof makes use of the stability lemma 2.3.2. Note that similarly to lemma 2.3.1, one has $G_1 = G_o$. Also note the approximation

$$\psi(\theta(x)) = \psi(\overline{\theta}) + \psi'(\overline{\theta}) \cdot (\theta(x) - \overline{\theta}) + o(\|\theta(\cdot) - \overline{\theta}\|_\infty), \tag{2.16}$$

valid for any $\theta \in \mathcal{C}_{\mathrm{b}}(X, \mathbb{R})$. The uniformity of the error on the right hand side of (2.16) follows from the uniform continuity of ψ'. A similar approximation holds for $I(\theta(t))$. One may thus write the field equation as

$$\begin{aligned} \frac{d\theta}{dt}(t,x) = \omega &+ \psi(\overline{\theta}(t))I(\overline{\theta}(t))G_o + \psi'(\overline{\theta}(t))I(\overline{\theta}(t))G_o \cdot (\theta(t,x) - \overline{\theta}(t)) \\ &+ \psi(\overline{\theta}(t))I'(\overline{\theta}(t)) \cdot \int_X d\mu(y)\ G(x,y) \cdot (\theta(t,y) - \overline{\theta}(t)) \\ &+ o(\|\theta(t,\cdot) - \overline{\theta}(t)\|_\infty), \end{aligned} \tag{2.17}$$

while use was made of the fact that $\|G(x,\cdot)\|_{L^1(\mu)} = G_o$ for all $x \in X$. Using (2.17), one finds that

$$\begin{aligned} \frac{d\overline{\theta}}{dt}(t) =& \frac{1}{\mu(X)} \int_X d\mu(x)\ \frac{d\theta}{dt}(t,x) \\ =& \omega + \psi(\overline{\theta}(t))I(\overline{\theta}(t))G_o + o(\|\theta(t,\cdot) - \overline{\theta}(t)\|_\infty), \end{aligned} \tag{2.18}$$

while use was made of the fact that $\|G(\cdot,y)\|_{L^1(\mu)} = G_o$ for all $y \in X$. Note that integration and differentiation were swapped, an action that is allowed since the time-derivative $\frac{d}{dt}\theta(t)$ is a derivative in $\mathcal{C}_{\mathrm{b}}(X, \mathbb{R})$. Combining (2.17) with (2.18), leads to the coupled system of ODEs

$$\begin{aligned} \frac{d\overline{\theta}}{dt}(t) =& \omega + \psi(\overline{\theta}(t)) \cdot I(\overline{\theta}(t)) \cdot G_o + o(\|\theta_{\mathrm{v}}\|_\infty), \\ \frac{d\theta_{\mathrm{v}}}{dt}(t) =& \left[\psi'(\overline{\theta}(t)) \cdot I(\overline{\theta}(t)) \cdot G_o + \psi(\overline{\theta}(t)) \cdot I'(\overline{\theta}(t)) \cdot \hat{G}\right] \theta_{\mathrm{v}}(t) + o(\|\theta_{\mathrm{v}}\|_\infty), \end{aligned} \tag{2.19}$$

in the variables

$$\begin{aligned} \overline{\theta} \in V_1 &:= \{f : X \to \mathbb{R} : \text{const}\} \cong \mathbb{R}, \\ \theta_{\mathrm{v}} \in V_2 &:= \{f \in \mathcal{C}_{\mathrm{b}}(X, \mathbb{R}) : \mu(f) = 0\}. \end{aligned} \tag{2.20}$$

Note that the error in (2.19) depends on both $\overline{\theta}$ and θ_{v} but scales down as $\|\theta_{\mathrm{v}}\|_\infty \to 0$, uniformly in $\overline{\theta}$. Observe the similarity of the first part of (2.19) to the ODE (2.14) for the common phase in case of synchrony. It reveals that up to first order in the variation θ_{v} the mean phase $\overline{\theta}$ advances as if the network was in total synchrony. Note that the mapping

$$V_1 \to \mathcal{L}(V_2), \qquad \overline{\theta} \mapsto \mathcal{H}_{2,o}(\overline{\theta}) := \psi'(\overline{\theta}) \cdot I(\overline{\theta}) \cdot G_o + \psi(\overline{\theta}) \cdot I'(\overline{\theta}) \cdot \hat{G} \tag{2.21}$$

is Lipschitz continuous and bounded. Any solution $\phi \in \mathcal{C}^1(\mathbb{R}, V_1)$ of the ODE

$$\frac{d\phi}{dt}(t) = \mathcal{H}_{1,o}(\phi(t)) := \omega + \psi(\phi(t)) \cdot I(\phi(t)) \cdot G_o \tag{2.22}$$

is T-periodic if projected to S^1. Let $K|_{V_2} : V_2 \to V_2$ be the propagator induced by the non-autonomous ODE $\dot{\theta}_{\mathrm{v}}(t) = \mathcal{H}_{2,o}(\phi(t))\theta_{\mathrm{v}}(t)$ from time t_o to time $t_o + T$, as described in lemma

2.3.1. By lemma 2.3.1(2), $K|_{V_2}$ is independent of the initial value $\phi(t_o)$ and initial time t_o. By lemma 2.3.1(4), $K|_{V_2}$ has a spectral radius smaller than 1, so that $\|(K|_{V_2})^{n_o}\| < 1$ for some $n_o \in \mathbb{N}_o$ large enough. Identify $\mathcal{C}_\mathrm{b}(X,\mathbb{R}) \cong V_1 \oplus V_2$ by means of the decomposition $\theta = \overline{\theta} + \theta_\mathrm{v}$. Identify $(\mathcal{H}_1, \mathcal{H}_2) : V_1 \times V_2 \to V_1 \times V_2$ as the Lipschitz-continuous functional appearing on the right hand side of (1.9), that is with $\mathcal{H}_i : V_1 \times V_2 \to V_i$ $(i \in \{1,2\})$ so that $\frac{d\overline{\theta}}{dt} = \mathcal{H}_1(\theta)$ and $\frac{d\theta_\mathrm{v}}{dt} = \mathcal{H}_2(\theta)$. Then the dynamics (2.19) satisfy the assumptions of lemma 2.3.2. By that lemma, the flow-invariant sub-space $V_1 \times \{0_{V_2}\}$ is indeed stable in the way postulated above. □

Remark 2.3.4 The stability result of theorem 2.3.3 holds at first instance for solutions of the field equation in $\mathcal{C}_\mathrm{b}(X,\mathbb{R})$. But in fact it remains valid in an equivalent form for solutions in $\mathcal{C}_\mathrm{b}(X,S^1)$ if one replaces $\|\theta_\mathrm{v}(t)\|_\infty$ by $\operatorname{diam}\theta(t,X)$: There exist constants $A, \beta > 0$ and $0 < \delta < 1/2$ such that $\operatorname{diam}\theta(t,X) \leq A \cdot e^{-\beta t} \cdot \operatorname{diam}\theta(0,X)$ for all $t \geq 0$, provided that $\operatorname{diam}\theta(0,X) \leq \delta$ and $\theta \in \mathcal{C}^1(\mathbb{R}, \mathcal{C}_\mathrm{b}(X,S^1))$ solves the field equation (1.9).

To see this note that for any $\theta_o \in \mathcal{C}(X,S^1)$ with $\operatorname{diam}\theta_o(X) < 1/2$, there exists a lift $\tilde{\theta}_o \in \mathcal{C}_\mathrm{b}(X,\mathbb{R})$ with respect to the covering map $\Pi_\mathrm{c} : \mathbb{R} \to S^1$, such that $\|(\tilde{\theta}_o)_\mathrm{v}\|_\infty \leq \operatorname{diam}\theta_o(X)$. If $\theta \in \mathcal{C}^1(\mathbb{R}, \mathcal{C}_\mathrm{b}(X,S^1))$ has initial value $\theta(0) = \theta_o$, then by the homotopy lifting property of covering maps (see for example Nicolaescu 2007, §6.2.3) there exists a unique lift $\tilde{\theta} \in \mathcal{C}(\mathbb{R}\times X, \mathbb{R})$ of θ with $\tilde{\theta}(0,\cdot) = \tilde{\theta}_o$. Since the covering map Π_c is a local diffeomorphism and a local isometry, one has $\partial_t\tilde{\theta}(t,x) = \partial_t\theta(t,x)$ and $\tilde{\theta} \in \mathcal{C}^1(\mathbb{R}, \mathcal{C}_\mathrm{b}(X,\mathbb{R}))$ satisfies the field equation. Finally, the exponential decay of $\|\tilde{\theta}_\mathrm{v}(t)\|_\infty$ as $t \to \infty$ implies the exponential decay of $\operatorname{diam}\theta(t,X)$.

Remark 2.3.5 Key to the proof of the theorem is the exponential stability of the iterated dynamical system $(V_2, ((K|_{V_2})^n)_{n\in\mathbb{N}_0})$, given by the fact that the spectrum $\sigma(K|_{V_2}) = \exp[B \cdot (G_o - \{0\} \cup \sigma_\mathrm{p}(\hat{G}|_{V_2}))]$ lies in the open, complex unit disc (see lemma 2.3.1). The subspace $V_2 \subseteq V$ corresponds to the stable subspace of the linear propagator $K : V \to V$, mapping phase fields $\theta(t_o)$ at time t_o to phase fields $\theta(t_o+T)$ at time t_o+T. It is a complement to the one-dimensional neutral subspace $V_1 := \{f \in V : f \equiv \text{const}\}$ of constant functions. The latter corresponds to uniform phase shifts across the oscillator population, to which the limit cycle of synchrony is invariant.

Example 2.2.6 gives a hint on how the *strength* of stability might depend on the detailed shape of G. For that example, where $X = \mathbb{T}^m$ and $G(x,y) = g(x-y)$ for some $g \in \mathcal{C}(\mathbb{T}^m, \mathbb{R}_+)$, one knows in connection with the proof of lemma 2.3.1(4) that the point spectrum of $\hat{G}|_{V_2} : V_2 \to V_2$ is the Fourier spectrum of g, the value G_o excluded. The stronger any non-trivial modes are represented in the latter (more precisely, the greater the real part of their eigenvalues), the closer the eigenvalues of $K|_{V_2}$ will be to the boundary of the unit disc. If on the other hand g is constant on $\mathbb{T}^m$, then all eigenvalues of $\hat{G}|_{V_2}$ are zero and the spectral radius of $K|_{V_2}$ takes the value $e^{B\cdot G_o}$ (B being strictly negative).

Remark 2.3.6 Compare theorem 2.3.3 to the asymptotic stability result by Goel & Ermentrout (2002, §2.5) for the special case of finitely many oscillators, that is for X finite with μ as counting measure. Their condition (ii) corresponds to our condition $\|G(x,\cdot)\|_{L^1(\mu)} = \|G(\cdot,y)\|_{L^1(\mu)} = G_o > 0$ $\forall x,y \in X$ with G strongly connecting X, their condition (iii) to our condition $\omega + \psi(\varphi)\cdot G_o \cdot I(\varphi) > 0$ $\forall \varphi \in S^1$, their condition (iv) to our condition $G(x,y) \geq 0$ $\forall x,y \in X$ and their condition (v) to our condition $B < 0$. Apart from the greater generality achieved in theorem 2.3.3, the latter allows the study of the local stability of synchrony in the fluid model. This will be the subject of the following section.

2.4 Synchrony in the fluid model

I now proceed with similar statements on the existence and stability of synchrony in the fluid model, that is, of solutions formally of the form $\rho(t,x,\vartheta) = \delta(\vartheta - \phi(t))$. Since Dirac distributions

are somewhat pathological when it comes to stability analysis, the methods used and the results obtained are of a special character, the measure of deviation from synchrony being the bandwidth (i.e. diameter of the support) of the phase density $\rho(t)$.

This section is built around theorem 2.4.4. In the following lemma, a rather technical stability statement is given for abstract dynamical systems. The lemma is applied in the theorem, which gives sufficient conditions on the coupling kernel, iPRC and oscillator pulse for the local stability of synchrony. The proof of the theorem will underline the relationship between the field and fluid models, supplementing the interpretation provided in section 1.3.

Lemma 2.4.1. *Let $\Gamma_o \neq \emptyset$ be some set and Γ a collection of mappings $\gamma : [0,\infty) \to \Gamma_o$, henceforth referred to as orbits. Let $\{D_\alpha\}_{\alpha\in A}$ be a family of functions $D_\alpha : \Gamma_o \to \mathbb{R}_+$ such that for any orbit $(\gamma(t))_{t\geq 0} \in \Gamma$, the mappings $[0,\infty) \to \mathbb{R}_+$, $t \mapsto D_\alpha(\gamma(t))$ are differentiable and the family $\{D_\alpha(\gamma(\cdot))\}_{\alpha\in A}$ is equicontinuous. Let $D_{\mathrm{loc}} := \sup_{\alpha\in A} D_\alpha$ be defined pointwise. Let V_1, V_2 be Banach spaces, $V := V_1 \times V_2$ and $\mathcal{H}_o : V \to V$ a Lipschitz-continuous functional. Let $\Theta_1 : \Gamma_o \to V_1$, $\Theta_2 : \Gamma_o \to V_2$, $\mathcal{E} : \Gamma_o \to V$ be such that for any orbit $(\gamma(t))_{t\geq 0} \in \Gamma$, the mappings $t \mapsto \Theta_1(\gamma(t))$, $t \mapsto \Theta_2(\gamma(t))$ are differentiable, the mapping $t \mapsto \mathcal{E}(\gamma(t))$ is continuous and all three of them satisfy*

$$\frac{d}{dt}\left(\Theta_1(\gamma(t)), \Theta_2(\gamma(t))\right) = \mathcal{H}_o\left[\Theta_1(\gamma(t)), \Theta_2(\gamma(t))\right] + \mathcal{E}\left(\gamma(t)\right). \tag{2.23}$$

Assume that $\mathcal{E}(\gamma_o) \in O\left(D_{\mathrm{loc}}(\gamma_o)\right)$ as $D_{\mathrm{loc}}(\gamma_o) \to 0$, $\gamma_o \in \Gamma_o$. Define $D_{\mathrm{gl}} := 2\left\|\Theta_2\right\| + 2D_{\mathrm{loc}}$ and assume the following stability conditions:

C1. There exists an $\varepsilon > 0$ such that whenever $D_{\mathrm{gl}}(\gamma(t)) \leq \varepsilon$, one has $\frac{d}{dt}D_\alpha(\gamma(t)) \leq 0$ for all $\alpha \in A$ and any orbit $(\gamma(t))_{t\geq 0} \in \Gamma$.

C2. There exists a period $T > 0$ and a constant $r < 1$ such that: Whenever $(\gamma(t))_{t\geq 0} \in \Gamma$ and $t_o \geq 0$ are such that $D_{\mathrm{gl}}(\gamma(t)) \leq \varepsilon$ for all $t \in [t_o, t_o{+}T]$, one has $D_\alpha(\gamma(t_o{+}T)) \leq r \cdot D_\alpha(\gamma(t_o))$ for all $\alpha \in A$.

C3. The dynamical system induced by $\mathcal{H}_o$ on $V = V_1 \times V_2$ is locally exponentially stable in the second coordinate. That is to say that, there exist constants $A_o, \beta_o, \delta_o > 0$ such that whenever $(\Theta_{o1}(t), \Theta_{o2}(t))$ satisfies the ODE $\frac{d}{dt}(\Theta_{o1}(t), \Theta_{o2}(t)) = \mathcal{H}_o\left[\Theta_{o1}(t), \Theta_{o2}(t)\right]$ in V and the initial smallness condition $\|\Theta_{o2}(0)\| \leq \delta_o$, one has $\|\Theta_{o2}(t)\| \leq A_o e^{-\beta_o \cdot t} \cdot \|\Theta_{o2}(0)\|$ for all $t \geq 0$.

Then there exist constants $A, \beta, \delta > 0$ such that for any orbit $(\gamma(t))_{t\geq 0} \in \Gamma$ satisfying $D_{\mathrm{gl}}(\gamma(0)) \leq \delta$, one has $D_{\mathrm{gl}}(\gamma(t)) \leq Ae^{-\beta t} \cdot D_{\mathrm{gl}}(\gamma(0))$ for all $t \geq 0$ and every $D_\alpha(\gamma(t))$ ($\alpha \in A$) is decreasing in t.

For a proof of this rather abstract statement see A.3.3. The reasons of its apparent complexity should become clear later on in the proof of theorem 2.4.4, which is preceded by the following two remarks.

Remark 2.4.2 As already seen in the proof of theorem 1.4.2, phase densities are closely related to the flow generated by the underlying velocity field. In fact, the latter allows for a representation of the former in a way that shall be given here for future reference. Specifically, let $J \subseteq \mathbb{R}$ be some time interval (finite or infinite) and $\Theta \in \{\mathbb{R}, S^1\}$. Let $\mathrm{v} : J \times \Theta \to \mathbb{R}$, $(t,\vartheta) \mapsto \mathrm{v}(t,\vartheta)$ be such that both v and $\partial_\vartheta \mathrm{v}$ are continuous and bounded on $J \times \Theta$. Suppose that $\rho : J \times \Theta \to \mathbb{R}$, $(t,\vartheta) \mapsto \rho(t,\vartheta)$ is partially differentiable in t and ϑ, with $\partial_t\rho$ being continuous on $J \times \Theta$. Let $\Phi : J^2 \times \Theta \to \Theta$ be the flow induced on Θ by the velocity field v. If ρ satisfies the continuity equation

$$\partial_t\rho(t,\vartheta) = -\partial_\vartheta\left[\rho(t,\vartheta) \cdot \mathrm{v}(t,\vartheta)\right], \tag{2.24}$$

then ρ is of the form

$$\rho(t,\vartheta) = \rho(t_o, \Phi(t_o,t,\vartheta)) \cdot \exp\left[-\int_{t_o}^{t} d\tau\ (\partial_\vartheta \mathrm{v})\,(\tau, \Phi(\tau,t,\vartheta))\right] \tag{2.25}$$

for $(t,\vartheta) \in J \times \Theta$ and any $t_o \in J$ (note the reversed role of t_o and t in the flow). To see this, fix some $(t_o, s, \vartheta) \in J^2 \times \Theta$ and let $\varphi := \Phi(t_o, s, \vartheta)$. For $t \in J$ define $\eta(t) := \rho(t, \Phi(t, t_o, \varphi))$. Since $\partial_\varphi \rho(t,\varphi)$ exists and $\partial_t \rho(t,\varphi)$ is continuous in (t,φ), $\rho(t,\varphi)$ is differentiable in (t,φ) and by the chain rule

$$\begin{aligned}\frac{d\eta}{dt}(t) =&(\partial_t\rho)(t,\Phi(t,t_o,\varphi)) + (\partial_\vartheta\rho)(t,\Phi(t,t_o,\varphi)) \cdot \partial_t\Phi(t,t_o,\varphi)\\ =&-\partial_\vartheta(\rho\cdot \mathrm{v})(t,\Phi(t,t_o,\varphi)) + (\partial_\vartheta\rho)(t,\Phi(t,t_o,\varphi)) \cdot \mathrm{v}(t,\Phi(t,t_o,\varphi))\\ =&-(\partial_\vartheta \mathrm{v})(t,\Phi(t,t_o,\varphi)) \cdot \eta(t).\end{aligned} \tag{2.26}$$

Note that the mapping $J \to \mathbb{R}$, $t \mapsto (\partial_\vartheta \mathrm{v})(t, \Phi(t,t_o,\varphi))$ is continuous. Thus $\eta(t)$ is given by

$$\eta(t) = \eta(t_o) \cdot \exp\left[-\int_{t_o}^{t} d\tau\ (\partial_\vartheta \mathrm{v})(\tau, \Phi(\tau,t_o,\varphi))\right]. \tag{2.27}$$

Setting $t = s$ and using $\Phi(\tau, t_o, \varphi) = \Phi(\tau, s, \vartheta)$ leads to

$$\rho(s,\vartheta) = \rho(t_o, \Phi(t_o,s,\vartheta)) \cdot \exp\left[-\int_{t_o}^{s} d\tau\ (\partial_\vartheta \mathrm{v})(\tau, \Phi(\tau,s,\vartheta))\right], \tag{2.28}$$

as claimed.

Remark 2.4.3 In the proof of the theorem below, use will be made of the following fact: Let $\rho : [t_o,\infty) \times \mathbb{R} \to \mathbb{R}$, $(t,\vartheta) \mapsto \rho(t,\vartheta)$ be continuous, such that $\rho(t,\cdot) \in \mathcal{C}^1(\mathbb{R},\mathbb{R})$ for every $t \geq t_o$ and such that the partial derivative $\partial_t\rho$ exists and is continuous on $[t_o,\infty)\times\mathbb{R}$. Let $\mathrm{v} : [t_o,\infty)\times\mathbb{R} \to \mathbb{R}$ be such that $\mathrm{v}(\cdot,\vartheta) \in \mathcal{C}([t_o,\infty),\mathbb{R})$ for every $\vartheta \in \mathbb{R}$ and $\mathrm{v}(t,\cdot) \in \mathcal{C}^1(\mathbb{R},\mathbb{R})$ for every $t \geq t_o$. Suppose ρ satisfies the continuity equation

$$\partial_t\rho(t,\vartheta) = -\partial_\vartheta\left[\rho(t,\vartheta)\cdot \mathrm{v}(t,\vartheta)\right]. \tag{2.29}$$

Let $t_1 \geq t_o$ and let $\theta : [t_o,t_1] \to \mathbb{R}$ be a continuously differentiable solution to the EOM $\dot\theta(t) = \mathrm{v}(t,\theta(t))$. Then

$$\int_{t_o}^{t_1} dt\ (\rho\cdot\mathrm{v})(t,\theta(t_o)) = \int_{\theta(t_o)}^{\theta(t_1)} d\vartheta\ \rho(t_1,\vartheta). \tag{2.30}$$

To see why this is true, note that

$$\begin{aligned}&\int_{\theta(t_o)}^{\theta(t_1)} d\vartheta\ \rho(t_1,\vartheta)\\ =&\int_{t_o}^{t_1} dt\ \frac{d}{dt}\int_{\theta(t_o)}^{\theta(t)} d\vartheta\ \rho(t,\vartheta)\\ =&\int_{t_o}^{t_1} dt\ \left[\dot\theta(t)\cdot\rho(t,\theta(t)) + \int_{\theta(t_o)}^{\theta(t)} d\vartheta\ (\partial_t\rho)(t,\vartheta)\right]\\ =&\int_{t_o}^{t_1} dt\ \left[\dot\theta(t)\cdot\rho(t,\theta(t)) - \int_{\theta(t_o)}^{\theta(t)} d\vartheta\ \partial_\vartheta\left[\rho(t,\vartheta)\cdot\mathrm{v}(t,\vartheta)\right]\right]\\ =&\int_{t_o}^{t_1} dt\ \left[\dot\theta(t)\cdot\rho(t,\theta(t)) - \rho(t,\theta(t))\cdot\mathrm{v}(t,\theta(t)) + \rho(t,\theta(t_o))\cdot\mathrm{v}(t,\theta(t_o))\right]\\ =&\int_{t_o}^{t_1} dt\ \rho(t,\theta(t_o))\cdot\mathrm{v}(t,\theta(t_o)).\end{aligned} \tag{2.31}$$

An interpretation of (2.30) is that the time-integrated probability flux through $\theta(t_o)$ from time t_o to t_1 equals the mass between $\theta(t_o)$ and $\theta(t_1)$ at time t_1.

Theorem 2.4.4 (Stability of synchrony against perturbations with small support)
Let $G : X \times X \to \mathbb{R}_+$ be measurable, $\omega > 0$ and $\psi \in \mathcal{C}^2(S^1, \mathbb{R})$, $I \in \mathcal{C}^2(S^1, \mathbb{R}_+)$ satisfying the following conditions:

C1. The derivative ψ' is strictly negative on some circular arc containing $\operatorname{supp} I$.

C2. The mapping $X \to L^1(\mu)$, $x \mapsto G(x, \cdot)$ is uniformly continuous and bounded.

Let Ω_{o,S^1} and Ω_{S^1} be the function spaces defined in (1.22) and (1.23). Consider the continuity equation

$$\partial_t \rho(t, x, \vartheta) = -\partial_\vartheta \Big[\rho(t, x, \vartheta) \cdot [\omega + \psi(\vartheta) \cdot S_{S^1}(x, \rho(t))] \Big] \tag{2.32}$$

with the stimulus

$$S_{S^1}(x, \rho_o) := \int_X d\mu(y)\ G(x, y) \cdot \int_{S^1} d\varphi\ \rho_o(y, \varphi) \cdot I(\varphi) \tag{2.33}$$

defined for any $x \in X$ and $\rho_o \in \Omega_{o,S^1}$. Consider the collection of orbits

$$\Omega_{\mathrm{CE},S^1} := \big\{ \rho = (\rho(t))_{t \geq 0} \in \Omega_{S^1} : \partial_\vartheta \rho(0, \cdot, \cdot) \in \mathcal{C}_{\mathrm{u,b}}(X \times S^1, \mathbb{R}) \ \wedge\ \rho \text{ solves (2.32)} \big\}. \tag{2.34}$$

Identify I and ψ with their pullbacks on $\mathbb{R}$. Consider the dynamical system on the Banach space $V := \mathcal{C}_\mathrm{b}(X, \mathbb{R})$ induced by the ODE $\dot\theta(t) = \mathcal{H}_o(\theta(t))$ (field model), with $\mathcal{H}_o : V \to V$ being the Lipschitz-continuous functional defined as

$$\mathcal{H}_o(\theta)(x) := \omega + \psi(\theta(x)) \cdot \int_X d\mu(y)\ G(x, y) \cdot I(\theta(y)), \qquad \theta \in \mathcal{C}_\mathrm{b}(X, \mathbb{R}). \tag{2.35}$$

For $\theta \in V$ denote $\overline{\theta} := \mu(\theta)/\mu(X)$ and $\theta_\mathrm{v} := \theta - \overline{\theta}$. Assume the following stability condition: Synchrony is locally exponentially stable in the dynamical system $(V, \mathcal{H}_o)$, that is, there exist constants $A_o, \beta_o > 0$ and $0 < \delta_o < 1/2$ such that

$$\|\theta_\mathrm{v}(t)\|_\infty \leq A_o \cdot e^{-\beta_o \cdot t} \cdot \|\theta_\mathrm{v}(0)\|_\infty \tag{2.36}$$

for all $t \geq 0$, provided that $\|\theta_\mathrm{v}(0)\|_\infty \leq \delta_o$ and $(\theta(t))_{t \geq 0} \subseteq V$ solves the ODE $\dot\theta(t) = \mathcal{H}_o(\theta(t))$ (see theorem 2.3.3).

Then synchrony is locally exponentially stable in Ω_{CE,S^1} in the following sense: There exist constants $A, \beta > 0$ and $0 < \delta < 1/2$ such that for any orbit $(\rho(t))_{t \geq 0} \in \Omega_{\mathrm{CE},S^1}$ with $\operatorname{diam} \rho(0) \leq \delta$, one has $\operatorname{diam} \rho(t) \leq A e^{-\beta t} \cdot \operatorname{diam} \rho(0)$ for all $t \geq 0$.

Remark 2.4.5 By the stability assumption on the field model, the pulse I can not be trivial and in particular $\|I\|_{L^1(S^1)} > 0$. By condition (C1), $I \cdot \psi$ is also non-trivial. Furthermore, by the stability condition on the field model there exists a solution of the type $\theta(t, x) = \phi(t)$ (synchrony) for some appropriate $\phi \in \mathcal{C}^1(\mathbb{R}, \mathbb{R})$. This implies that $\|G(x, \cdot)\|_{L^1(\mu)}$ is independent of $x \in X$ and in fact equal to some constant $G_o > 0$.

Proof of the theorem. The proof consists of preparations necessary for an application of lemma 2.4.1. Consider the continuity equation

$$\partial_t \rho(t, x, \vartheta) = -\partial_\vartheta \Big[\rho(t, x, \vartheta) \cdot [\omega + \psi(\vartheta) \cdot S_{\mathbb{R}}(x, \rho(t))] \Big] \tag{2.37}$$

for densities $\rho : \mathbb{R} \times X \times \mathbb{R} \to \mathbb{R}_+$ instead of $\mathbb{R} \times X \times S^1 \to \mathbb{R}_+$, with $S_{\mathbb{R}}$ defined as (2.33) with the integration domain S^1 replaced by $\mathbb{R}$. Recall that by theorem 1.4.5 every orbit in Ω_{CE,S^1} is a wrapping of an orbit of class

$$\begin{aligned}\Omega_{\mathrm{CE},\mathbb{R}} := \{(\rho(t))_{t\geq 0} \in \Omega_{\mathbb{R}} : \partial_\vartheta \rho(0,\cdot,\cdot) \in \mathcal{C}_{\mathrm{u,b}}(X \times \mathbb{R}, \mathbb{R}) \\ \wedge \ \operatorname{diam} \rho(0) < \infty \ \wedge \ \rho \text{ solves } (2.37)\},\end{aligned} \tag{2.38}$$

with $\Omega_{\mathbb{R}}$ defined in (1.23). For technical convenience, the theorem is proven for orbits in $\Omega_{\mathrm{CE},\mathbb{R}}$ instead. Recall that by theorem 1.4.5, every orbit $(\rho(t))_{t\geq 0} \in \Omega_{\mathrm{CE},\mathbb{R}}$ is in fact in $\mathcal{C}^1([0,\infty), \mathcal{C}_{\mathrm{u,b}}(X \times \mathbb{R}, \mathbb{R}))$ and satisfies $\partial_\vartheta \rho(t,\cdot,\cdot) \in \mathcal{C}_{\mathrm{u,b}}(X \times \mathbb{R}, \mathbb{R})$ for all $t \geq 0$. Furthermore $\operatorname{supp}_{\mathbb{R}} \rho(t,\cdot,\cdot) \subseteq \{\vartheta \in \mathbb{R} : d(\vartheta, \operatorname{supp}_{\mathbb{R}} \rho(0,\cdot,\cdot)) \leq Ct\}$ for all $t \geq 0$ and some constant $C > 0$.

For any fixed orbit $(\rho(t))_{t\geq 0} \in \Omega_{\mathrm{CE},\mathbb{R}}$ and $x \in X$ consider the non-autonomous EOM

$$\frac{d\theta_x^p(t)}{dt} = \mathrm{v}(t, x, \theta_x^p(t)) := \omega + \psi(\theta_x^p(t)) \cdot S_{\mathbb{R}}(x, \rho(t)) \tag{2.39}$$

in the real variable θ_x^p, whose solutions shall be referred to as *point orbits*. Beforehand some regularity statements:

R.1. Every $\rho_o \in \Omega_{o,\mathbb{R}}$ is also in $\mathcal{C}_{\mathrm{b}}(X, L^1(\mathbb{R},\mathbb{R}))$. To see this note that $\rho_o \in \mathcal{C}_{\mathrm{b}}(X, \mathcal{C}_{\mathrm{b}}(\mathbb{R},\mathbb{R}))$. Furthermore, by Brézis & Lieb (1983) every sequence $(f_n)_n \in \mathcal{C}_{\mathrm{b}}(\mathbb{R},\mathbb{R})$ with $\|f_n\|_{L^1(\mathbb{R})} = 1 \ \forall n$, converging uniformly to some $f \in \mathcal{C}_{\mathrm{b}}(\mathbb{R},\mathbb{R})$ with $\|f\|_{L^1(\mathbb{R})} = 1$, also converges to f in $L^1(\mathbb{R},\mathbb{R})$.

R.2. By condition (C2) and lemma 1.4.4(1), for any $\rho_o \in \Omega_{o,\mathbb{R}}$ the mapping $X \to \mathbb{R}$, $x \mapsto S_{\mathbb{R}}(x, \rho_o)$ is well-defined and continuous. Furthermore, for any orbit $(\rho(t))_{t\geq 0} \in \Omega_{\mathbb{R}}$ and fixed $x \in X$, the mapping $[0,\infty) \to \mathbb{R}$, $t \mapsto S_{\mathbb{R}}(x, \rho(t))$ is continuous. Finally, $S_{\mathbb{R}}$ is bounded on $X \times \Omega_{o,\mathbb{R}}$.

R.3. The velocity field $\mathrm{v} : [0,\infty) \times X \times \mathbb{R} \to \mathbb{R}$, $(t, x, \vartheta) \mapsto \mathrm{v}(t, x, \vartheta)$ defined in (2.39) is bounded by $\mathrm{v}_{\max} := \omega + \|\psi\|_\infty \cdot G_o \cdot \|I\|_\infty$, continuous in (t, ϑ) and Lipschitz-continuous in ϑ, while the Lipschitz constant can be chosen to be independent of $t \in [0,\infty)$, $x \in X$ and in fact the orbit $(\rho(t))_{t\geq 0}$ itself. A similar statement holds for $\partial_\vartheta \mathrm{v}$. Thus the initial value problem for the EOM (2.39) has for any intermediate value at some time $t_1 \geq 0$ one maximal corresponding point orbit $[0,\infty) \to \mathbb{R}$.

For any orbit $(\rho(t))_{t\geq 0} \in \Omega_{\mathrm{CE},\mathbb{R}}$ and any corresponding point orbit $(\theta_x^p(t))_{t\geq 0}$, one has by remark 2.4.2 the representation

$$\rho(t, x, \theta_x^p(t)) = \exp\left[-\int_0^t d\tau \ \psi'(\theta_x^p(\tau)) \cdot S_{\mathbb{R}}(x, \rho(\tau))\right] \cdot \rho(0, x, \theta_x^p(0)). \tag{2.40}$$

This shows that $\rho(t, x, \theta_x^p(t))$ is either for all $t \geq 0$ zero or for all $t \geq 0$ non-zero, depending on the initial position $\theta_x^p(0)$. One thus concludes that any two point orbits $\theta_x^f(\cdot), \theta_x^b(\cdot)$ initially *enclosing* $\rho(0, x, \cdot)$, that is $\operatorname{supp} \rho(0, x, \cdot) \subseteq [\theta_x^b(0), \theta_x^f(0)]$, do so for all $t \geq 0$. For any $\rho_o \in \Omega_{o,\mathbb{R}}$ with $\operatorname{diam} \rho_o < \infty$ and $x \in X$ define

$$\Theta(\rho_o)(x) := \int_{\mathbb{R}} d\vartheta \ \rho_o(x, \vartheta) \cdot \vartheta. \tag{2.41}$$

Then the mapping $X \to \mathbb{R}$, $x \mapsto \Theta(\rho_o)(x)$ is well-defined and by (R.1) continuous and bounded. Furthermore, for any orbit $(\rho(t))_{t\geq 0} \in \Omega_{\mathrm{CE},\mathbb{R}}$ the mapping $[0,\infty) \to \mathcal{C}_{\mathrm{b}}(X,\mathbb{R})$, $t \mapsto \Theta(\rho(t))$ is continuous. This follows from the definition of $\Omega_{\mathrm{CE},\mathbb{R}}$ and the fact that the boundaries of

$\mathrm{supp}_{\mathbb{R}}\,\rho(t,\cdot,\cdot)$ grow at most linearly with time. In fact, the mapping is for similar reasons differentiable with derivative

$$\frac{d}{dt}\Theta(\rho(t))(x) = \int_{\mathbb{R}} d\vartheta\ (\mathrm{d}_t\rho)(t,x,\vartheta)\cdot\vartheta, \tag{2.42}$$

with $\mathrm{d}_t\rho$ being the time-derivative of ρ in $\mathcal{C}^1([0,\infty),\mathcal{C}_{\mathrm{u,b}}(X\times\mathbb{R},\mathbb{R}))$. By continuity of the map $t\mapsto(\mathrm{d}_t\rho)(t)\in\mathcal{C}_{\mathrm{u,b}}(X\times\mathbb{R},\mathbb{R})$ one finds that $t\mapsto\frac{d}{dt}\Theta(\rho(t))\in\mathcal{C}_{\mathrm{b}}(X,\mathbb{R})$ is continuous. One thus concludes that $\Theta(\rho(\cdot))\in\mathcal{C}^1([0,\infty),\mathcal{C}_{\mathrm{b}}(X,\mathbb{R}))$ for any orbit $(\rho(t))_{t\geq0}\in\Omega_{\mathrm{CE},\mathbb{R}}$. Using (2.37) and (2.42) one finds that $\Theta(\rho(t))$ satisfies the ODE

$$\begin{aligned}\frac{d}{dt}\Theta(\rho(t))(x) =& -\int_{\mathbb{R}} d\vartheta\ \vartheta\cdot\partial_\vartheta(\rho\cdot\mathrm{v})(t,x,\vartheta) \overset{(2)}{=} \int_{\mathbb{R}} d\vartheta\ (\rho\cdot\mathrm{v})(t,x,\vartheta)\\ =&\omega + S_{\mathbb{R}}(x,\rho(t))\cdot\int_{\mathbb{R}} d\vartheta\ \rho(t,x,\vartheta)\cdot\psi(\vartheta).\end{aligned} \tag{2.43}$$

In step (2) partial integration was used. Take any $\rho_o\in\Omega_{o,\mathbb{R}}$ with $\mathrm{diam}\,\rho_o(y,\cdot)<\infty$ for some $y\in X$. Then since I' is uniformly continuous, one can approximate

$$\int_{\mathbb{R}} d\vartheta\ \rho_o(y,\vartheta)\cdot I(\vartheta) = I(\Theta(\rho_o)(y)) + o([\mathrm{diam}\,\rho_o(y,\cdot)]), \tag{2.44}$$

with the error term on the right hand side of (2.44) depending on $\rho_o(y,\cdot)$, but scaling down as $\mathrm{diam}\,\rho_o(y,\cdot)\to0$. A similar estimate holds for $\int_{\mathbb{R}} d\vartheta\ \rho_o(y,\vartheta)\cdot\psi(\vartheta)$. Using (2.44) and the fact that $\sup_x\|G(x,\cdot)\|_\infty<\infty$, for any $\rho_o\in\Omega_{o,\mathbb{R}}$ and $x\in X$ one finds

$$S_{\mathbb{R}}(x,\rho_o) = \int_X d\mu(y)\ G(x,y)\cdot I(\Theta(\rho_o)(y)) + o\Big(\sup_{y\in Y}\mathrm{diam}\,\rho_o(y,\cdot)\Big), \tag{2.45}$$

with the error term on the right hand side of (2.45) depending on ρ_o and x but scaling down as $\sup_y\mathrm{diam}\,\rho_o(y,\cdot)\to0$ uniformly in x. Since $S_{\mathbb{R}}$ is bounded on $X\times\Omega_{o,\mathbb{R}}$, using (2.43) and (2.45) one concludes that for any orbit $(\rho(t))_{t\geq0}\in\Omega_{\mathrm{CE},\mathbb{R}}$, $\Theta(\rho(t))$ satisfies the ODE

$$\frac{d}{dt}\Theta(\rho(t)) = \mathcal{H}_o(\Theta(\rho(t))) + \mathcal{E}_o(\rho(t)), \tag{2.46}$$

with $\mathcal{H}_o:\mathcal{C}_{\mathrm{b}}(X,\mathbb{R})\to\mathcal{C}_{\mathrm{b}}(X,\mathbb{R})$ given by (2.35) and the term $\mathcal{E}_o(\rho(t))$ being of order $o(\sup_y\mathrm{diam}\,\rho(t,y,\cdot))$. The following auxiliary statement about the growth of density diameters will be of use later on.

Statement: *There exist constants $\varepsilon>0$, $0<r<1$ and a period $T>0$ such that: For any orbit $(\rho(t))_{t\geq0}\in\Omega_{\mathrm{CE},\mathbb{R}}$ and any corresponding family $\{\theta^b_x(t),\theta^f_x(t)\}_{x\in X}$ of point orbits enclosing $\rho(t)$, that is $\mathrm{supp}\,\rho(t,x,\cdot)\subseteq[\theta^b_x(t),\theta^f_x(t)]$ for all $t\geq0$ and $x\in X$, one has (1), $\frac{d}{dt}\big(\theta^f_x(t)-\theta^b_x(t)\big)\leq0$ for all $x\in X$ whenever*

$$2\left\|\Theta(\rho(t))-\overline{\Theta}(\rho(t))\right\|_\infty + 2\sup_{x\in X}\left|\theta^f_x(t)-\theta^b_x(t)\right|\leq\varepsilon \tag{2.47}$$

and (2),

$$\big(\theta^f_x(t_o+T)-\theta^b_x(t_o+T)\big)\leq r\cdot\big(\theta^f_x(t_o)-\theta^b_x(t_o)\big) \tag{2.48}$$

for all $x\in X$ provided that (2.47) holds for all $t\in[t_o,t_o+T]$ and some $t_o\geq0$.

> **Proof of statement.** By condition (C1) there exist $0<\varepsilon_I<\varepsilon_\psi<1/2$ and $\vartheta_o\in S^1$ such that $\mathrm{supp}\,I\subseteq B_{\varepsilon_I}(\vartheta_o)$ and ψ' is strictly negative on $B_{\varepsilon_\psi}(\vartheta_o)$. Without loss of generality one may assume $\vartheta_o=0$. Furthermore, there exists a constant $\alpha>0$

such that $\psi(\vartheta_1) - \psi(\vartheta_2) \leq -\alpha \cdot (\vartheta_1 - \vartheta_2)$ for any $-\varepsilon_\psi \leq \vartheta_2 \leq \vartheta_1 \leq +\varepsilon_\psi$. Choose $\varepsilon := (\varepsilon_\psi - \varepsilon_I)/2 > 0$ and denote $\theta^b(t) := \inf_{x\in X} \theta^b_x(t)$. Then whenever condition (2.47) is met one has $\theta^b(t) \leq \theta^b_x(t) \leq \theta^f_x(t) \leq \theta^b(t) + \varepsilon$ and $\operatorname{supp} \rho(t, x, \cdot) \subseteq [\theta^b(t), \theta^b(t) + \varepsilon]$ for all $x \in X$. The former stems from the fact that $\Theta(\rho(t))(x)$ is always between $\theta^b_x(t)$ and $\theta^f_x(t)$. Denote $L_x(t) := \theta^f_x(t) - \theta^b_x(t)$ and suppose that (2.47) is satisfied at some time $t \geq 0$. Then

$$\begin{aligned} \frac{d}{dt} L_x(t) =& S_{\mathbb{R}}(x, \rho(t)) \cdot \Big[\psi(\theta^f_x(t)) - \psi(\theta^b_x(t))\Big] \\ \leq& -\alpha \cdot L_x(t) \cdot S_{\mathbb{R}}(x, \rho(t)) \end{aligned} \tag{2.49}$$

for all $x \in X$. The equality in (2.49) follows from (2.39). To see the inequality, consider the following complementary cases:

- $B_{\varepsilon_I}(n) \cap \big[\theta^b(t), \theta^b(t) + \varepsilon\big] = \emptyset$ for all $n \in \mathbb{Z}$, then $S_{\mathbb{R}}(x, \rho(t)) = 0$ for all $x \in X$.
- $B_{\varepsilon_I}(n) \cap \big[\theta^b(t), \theta^b(t) + \varepsilon\big] \neq \emptyset$ for some $n \in \mathbb{Z}$, then $\big[\theta^b_x(t), \theta^f_x(t)\big] \subseteq n + [-\varepsilon_\psi, +\varepsilon_\psi]$ for all $x \in X$, so that indeed $\psi(\theta^f_x(t)) - \psi(\theta^b_x(t)) \leq -\alpha \cdot L_x(t)$.

In both cases the inequality in (2.49) and thus the first part of the claim are verified. One also sees that whenever (2.47) is satisfied for all $t \in [t_o, t_o + T]$ and some $t_o \geq 0$, the estimate

$$L_x(t_o + T) \leq \exp\left[-\alpha \int_{t_o}^{t_o+T} dt\ S_{\mathbb{R}}(x, \rho(t))\right] \cdot L_x(t_o) \tag{2.50}$$

holds. Now choose $T := 4 \cdot 1/\omega$. Then one may estimate

$$\int_{t_o}^{t_o+T} dt\ S_{\mathbb{R}}(x, \rho(t)) \geq \min\left\{\frac{1}{\|\psi\|_\infty},\ \frac{G_o}{\mathrm{v}_{\max}} \cdot \|I\|_{L^1(S^1)}\right\} > 0. \tag{2.51}$$

To see this, consider the two complementary cases:

- During $[t_o, t_o + T]$, every point orbit $\theta^b_x(t)$ ($x \in X$) has advanced by at least 2. By 1-periodicity in ϑ of the corresponding velocity field $\mathrm{v} : (t, x, \vartheta) \mapsto \mathrm{v}(t, x, \vartheta)$ defined in (2.39), this implies that any point orbit $\theta^p_x(t)$ (with arbitrary initial value) has during $[t_o, t_o + T]$ advanced by at least 1. Consequently, by remark 2.4.3 one may estimate

$$\int_{t_o}^{t_o+T} dt\ \left[\rho(t, y, \vartheta) \cdot \mathrm{v}(t, y, \vartheta)\right] \geq \int_{\vartheta}^{\vartheta+1} d\varphi\ \rho(t_o + T, y, \varphi) \tag{2.52}$$

  for all $\vartheta \in \mathbb{R}$. This implies

$$\begin{aligned} &\int_{\mathbb{R}} d\vartheta\ I(\vartheta) \int_{t_o}^{t_o+T} dt\ \rho(t, y, \vartheta) \\ \geq& \frac{1}{\mathrm{v}_{\max}} \int_{\mathbb{R}} d\vartheta\ I(\vartheta) \int_{t_o}^{t_o+T} dt\ \rho(t, y, \vartheta) \cdot \mathrm{v}(t, y, \vartheta) \\ \geq& \frac{1}{\mathrm{v}_{\max}} \int_{\mathbb{R}} d\vartheta\ I(\vartheta) \int_{\vartheta}^{\vartheta+1} d\varphi\ \rho(t_o + T, y, \varphi) \\ =& \frac{1}{\mathrm{v}_{\max}} \int_{\mathbb{R}} d\varphi\ \rho(t_o + T, y, \varphi) \int_{\varphi-1}^{\varphi} d\vartheta\ I(\vartheta) \\ =& \frac{\|I\|_{L^1(S^1)}}{\mathrm{v}_{\max}} \cdot \int_{\mathbb{R}} d\varphi\ \rho(t_o + T, y, \varphi) = \frac{\|I\|_{L^1}}{\mathrm{v}_{\max}} \end{aligned} \tag{2.53}$$

for any $y \in X$. This allows for the estimate

$$\begin{aligned}\int_{t_o}^{t_o+T} dt\ S_{\mathbb{R}}(x,\rho(t)) &= \int_X d\mu(y)\ G(x,y) \int_{\mathbb{R}} d\vartheta\ I(\vartheta) \int_{t_o}^{t_o+T} dt\ \rho(t,y,\vartheta) \\ &\geq \|G(x,\cdot)\|_{L^1(S^1)} \cdot \frac{\|I\|_{L^1}}{\mathrm{v}_{\max}} = \frac{G_o}{\mathrm{v}_{\max}} \cdot \|I\|_{L^1(S^1)}\,,\end{aligned} \tag{2.54}$$

which verifies (2.51).

- There exists an $x \in X$ so that the point orbit $\theta^b_x(t)$ has during $[t_o, t_o+T]$ advanced by less than 2. Since $|\theta^b_y(t) - \theta^b_x(t)| \leq \varepsilon < 1/2$ for all $y \in X$ at all times $t \in [t_o, t_o+T]$, this implies that all point orbits $\theta^b_y(t)$ have during $[t_o, t_o+T]$ advanced by less than 3. In particular

$$\begin{aligned}3 \geq& \int_{t_o}^{t_o+T} dt\ \left[\omega - \|\psi\|_\infty \cdot S_{\mathbb{R}}(y,\rho(t))\right] \\ =& 4 - \|\psi\|_\infty \cdot \int_{t_o}^{t_o+T} dt\ S_{\mathbb{R}}(y,\rho(t)),\end{aligned} \tag{2.55}$$

so that $\int_{t_o}^{t_o+T} S_{\mathbb{R}}(y,\rho(t))\ dt \geq 1/\|\psi\|_\infty$ for all $y \in X$. This also verifies (2.51).

Choosing $r := \exp\left[-\alpha \cdot \min\left\{1/\|\psi\|_\infty, G_o \|I\|_{L^1(S^1)}/\mathrm{v}_{\max}\right\}\right]$ verifies by (2.50) the second part of the claim.

The proof finishes by putting the above into the context of lemma 2.4.1. Define the set

$$\begin{aligned}\Gamma_o := \{&(\rho_o, (\theta^b_x)_{x\in X}, (\theta^f_x)_{x\in X}) \in \Omega_{o,\mathbb{R}} \times \mathbb{R}^X \times \mathbb{R}^X \\ &: \mathrm{diam}_{\mathbb{R}}\, \rho_o < \infty\ \wedge\ \mathrm{supp}\, \rho_o(x,\cdot) \subseteq [\theta^b_x, \theta^f_x]\ \forall x \in X\}\end{aligned} \tag{2.56}$$

and Γ as the collection of orbits $(\gamma(t))_{t\geq 0} = (\rho(t), (\theta^b_x(t))_x, (\theta^f_x(t))_x)_{t\geq 0} \subseteq \Gamma_o$ satisfying:

- $(\rho(t))_{t\geq 0}$ is of class $\Omega_{\mathrm{CE},\mathbb{R}}$.
- $(\theta^b_x(t))_{t\geq 0}$ and $(\theta^f_x(t))_{t\geq 0}$ are point orbits corresponding to and enclosing $(\rho(t))_{t\geq 0}$.

For each $x \in X$ define the function

$$D_x : \Gamma_o \to \mathbb{R}\ \ ,\ \ D_x\big(\rho_o, (\theta^b_y)_{y\in X}, (\theta^f_y)_{y\in X}\big) := \theta^f_x - \theta^b_x. \tag{2.57}$$

Then for any orbit $(\gamma(t))_{t\geq 0} \in \Gamma$, the mappings $t \mapsto D_x(\gamma(t))$ are differentiable with a derivative bounded by $2\mathrm{v}_{\max}$, so that the family $\{D_x(\gamma(\cdot))\}_{x\in X}$ is equicontinuous. Define the functions

$$\begin{aligned}&\Theta_1 : \Gamma_o \to V_1 := \mathbb{R}\ \ ,\ \ \Theta_1\big(\rho_o, (\theta^b_x)_x, (\theta^f_x)_x\big) := \overline{\Theta}(\rho_o) = \mu(\Theta(\rho_o))/\mu(X), \\ &\Theta_2 : \Gamma_o \to V_2 := \{f \in \mathcal{C}_{\mathrm{b}}(X,\mathbb{R}) : \mu(f) = 0\}\ \ ,\ \ \Theta_2\big(\rho_o, (\theta^b_x)_x, (\theta^f_x)_x\big) := \Theta(\rho_o) - \Theta_1(\rho_o), \\ &\mathcal{E} : \Gamma_o \to V_1 \times V_2 \cong \mathcal{C}_{\mathrm{b}}(X,\mathbb{R})\ \ ,\ \ \mathcal{E}\big(\rho_o, (\theta^b_x)_x, (\theta^f_x)_x\big) := \mathcal{E}_o(\rho_o).\end{aligned} \tag{2.58}$$

Note the identification $\mathcal{C}_{\mathrm{b}}(X,\mathbb{R}) \cong V_1 \times V_2$ by means of the decomposition $\theta = \overline{\theta} + \theta_{\mathrm{v}}$ for $\theta \in \mathcal{C}_{\mathrm{b}}(X,\mathbb{R})$. As seen above, for any orbit $(\gamma(t))_{t\geq 0} \in \Gamma$ the mapping $t \mapsto (\Theta_1(\gamma(t)), \Theta_2(\gamma(t)))$ is continuously differentiable and satisfies by (2.46) the ODE

$$\frac{d}{dt}\left(\Theta_1(\gamma(t)), \Theta_2(\gamma(t))\right) = \mathcal{H}_o\left(\Theta_1(\gamma(t)), \Theta_2(\gamma(t))\right) + \mathcal{E}(\gamma(t)), \tag{2.59}$$

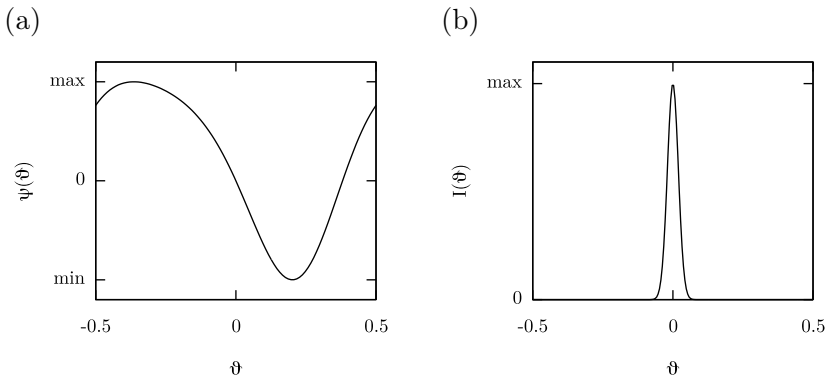

Figure 2.3: On theorem 2.4.4. (a) Example iPRC $\psi : S^1 \to \mathbb{R}$ and (b), example pulse $I : S^1 \to \mathbb{R}_+$ satisfying condition (C1) of theorem 2.4.4. The localization of the pulse within the region $\{\psi' < 0\}$ results in the local stability of network synchrony.

with $\mathcal{H}_o : V \to V$ being the Lipschitz continuous functional defined in (2.35). This ensures the continuity of $t \mapsto \mathcal{E}(\gamma(t))$. Furthermore, $\mathcal{E}(\gamma_o)$ has been shown to be of order $o(\sup_{x\in X} d_x(\gamma_o))$, uniformly in $\gamma_o \in \Gamma_o$. Conditions (C1) and (C2) of lemma 2.4.1 are satisfied by the auxiliary statement above. Condition 2.4.1(C3) is satisfied by the stability assumptions of this theorem on the field model. Therefore, lemma 2.4.1 can be readily applied. Observe that $\operatorname{diam}_{\mathbb{R}} \rho_o \leq 2\,\|\Theta_2(\gamma_o)\| + 2\sup_{x\in X} D_x(\gamma_o)$ for any $\gamma_o = \big(\rho_o, (\theta^b_x)_x, (\theta^f_x)_x\big) \in \Gamma_o$ and that for any $\rho_o \in \Omega_{o,\mathbb{R}}$ with $\operatorname{diam} \rho_o < \infty$ there exists a $\gamma_o = \big(\rho_o, (\theta^b_x)_x, (\theta^f_x)_x\big) \in \Gamma_o$ such that $2\,\|\Theta_2(\gamma_o)\| + 2\sup_{x\in X} D_x(\gamma_o) \leq 4 \operatorname{diam}_{\mathbb{R}} \rho_o$. This translates the results of lemma 2.4.1 to the claim of this theorem. □

By theorem 1.4.5 any initial state $\rho_o \in \Omega_{o,S^1}$ satisfying $\rho_o, \partial_\vartheta \rho_o \in \mathcal{C}_{\mathrm{u,b}}(X \times S^1, \mathbb{R})$ corresponds to a global, maximal solution of the continuity equation (2.32) within Ω_{CE,S^1}. The theorem ensures the asymptotic synchronization of the network, provided initial states are smooth enough and have an adequately small bandwidth ($\operatorname{diam} \rho_o < \delta$). Condition (C1) is related to findings in finite networks of spiking oscillators (Goel & Ermentrout 2002, Achuthan & Canavier 2009), that suggest a special role of the iPRC derivative ψ' at the spiking point. Also compare it to the condition in the stability theorem 2.3.3 for the field model, demanding that the scalar product (2.15) defining the constant B be strictly negative. If condition (C1) of theorem 2.4.4 is satisfied, B will indeed be strictly negative. Figure 2.3 gives an example of an iPRC ψ and pulse I satisfying the two conditions.

The condition of a bounded initial density bandwidth can be translated to a condition on the upper bound in the inter-network variation of external perturbations, that keep the network within the basin of attraction of synchrony. Let the oscillator phase density be satisfying the continuity equation (2.32), and suppose that at time 0 each oscillator is subject to a random, short-pulsed external stimulus, independent of other oscillators. Specifically, let the network be in the state $\rho(0^-, \cdot, \cdot) \in \mathcal{C}_{\mathrm{u,b}}(X \times S^1, \mathbb{R}_+)$ at time 0^-. At each point $x \in X$ let $\hat{F}(x)$ be a real random variable representing an external random stimulus acting on oscillators at x. One could model the perturbative effects of the stimulus $\hat{F}$ on the network, by setting $\rho(0^+, x, \cdot)$ to be the probability density on S^1 of the random variable $\hat{\theta} + \psi(\hat{\theta}) \cdot \hat{F}(x)$, with $\hat{\theta}$ being some random variable on S^1, distributed with probability density $\rho(0^-, x, \cdot)$ and independent of $\hat{F}(x)$. If the network was at time 0^- synchronized, that is $\rho(0^-, x, \vartheta) = \delta(\vartheta - \varphi_o)$ for some common phase $\varphi_o \in S^1$ and all $x \in X$, the new density $\rho(0^+, x, \cdot)$ will correspond to the distribution of the random variable $\varphi_o + \psi(\varphi_o) \cdot \hat{F}(x)$. If furthermore there exist an $\varepsilon_F > 0$ and $F_o \in \mathbb{R}$ such that for every $x \in X$ one has $|\hat{F}(x) - F_o| \leq \varepsilon_F$ almost surely, then $\operatorname{diam} \rho(0^+, \cdot, \cdot)$ will be at most $2 \cdot |\psi(\varphi_o)| \cdot \varepsilon_F$. Let $f(x, \cdot)$ be the probability density for $\hat{F}(x)$ and assume $f, \partial_\vartheta f \in \mathcal{C}_{\mathrm{u,b}}(X \times \mathbb{R}, \mathbb{R})$. If $\delta > 0$ is as postulated by theorem 2.4.4, then condition $\varepsilon_F \leq \delta/(2\,\|\psi\|_\infty)$ ensures the asymptotic recovery of synchrony after any such external perturbation.

Chapter 3

All-to-all spike-coupled networks with noise

3.1 Introduction

In this chapter I study infinite, all-to-all spike-coupled networks of identical phase oscillators with additive white noise. This will be done by examining the Fokker-Planck equation (1.12) in the time-dependent, oscillator-phase probability density $\rho(t, \vartheta)$. The advantage of the Dirac pulse limit is the apparent simplicity against the original model (1.6). Its validity should be tested experimentally or by numerical simulations on a case by case basis. A further difference of this model to the ones examined in the previous chapter, is the introduction of additive white noise, represented by a diffusion term in (1.12). The effects of noise can be compared to the effects of non-zero temperature in mechanical many-particle systems. Special interest is given to stationary network states, corresponding to time independent phase densities $\rho(t, \vartheta) = \rho_s(\vartheta)$. In such states, oscillators keep firing but the macroscopic network activity (e.g. the network stimulus $\rho(t, 0)$) seems to have settled on a fixed value. Stationary states, sometimes also called *incoherent states*, have already been studied within the Kuramoto model (Strogatz & Mirollo 1991, Bonilla et al. 1992) as well as the Winfree model (1.6) for pulses of the shape $I(\vartheta) \propto 1 + \cos(2\pi\vartheta)$ and iPRCs of the form $\psi(\vartheta) = -\psi_o \cdot \sin(2\pi\vartheta)$ (Ariaratnam 2002). In this chapter, general iPRCs $\psi \in \mathcal{C}^2(S^1, \mathbb{R})$ with $\psi(0) = 0$ are considered. It is always assumed that the density $\rho(t, \vartheta)$ is continuously differentiable (or twice continuously differentiable if $D > 0$) in ϑ.

Section 3.2 gives existence and uniqueness results for stationary states. In particular, it is shown that determining stationary states is equivalent to solving certain one-dimensional, fixed point equations. These so-called *stationary state equations*, are integral equations in the stationary stimulus $\rho(t, 0)$ and are derived using a self-consistency argument. The main parameters of interest are the *coupling strength* $\|\psi\|_\infty / \omega$ and *noise strength* D/ω. In particular, the transition of stationary states in the limits $D \to 0^+$ and $D \to \infty$ is examined.

Section 3.3 examines the local stability of stationary states using a spectral stability analysis of the linearized dynamics of small perturbations. For noise-free networks, the corresponding eigenvalue equation is reduced to a one-dimensional, integral equation. For noisy networks (i.e. with $D > 0$), an alternative approach is introduced for the linear stability analysis, based on a trigonometric approximation of eigenperturbations.

Section 3.4 suggests numerical methods for the evaluation of the stationary state equations and the spectral stability analysis of stationary states in noise-free as well as noisy networks. Furthermore, an explicit numerical integration scheme is presented for the Fokker-Planck equation (1.12), based on the so-called *spectral* method introduced by Perez & Ritort (1997) for the Kuramoto model.

Analytical results and numerical methods are applied to two concrete iPRC families: (1),

type I iPRCs of the form $\psi(\vartheta) = \frac{\psi_o}{2}\left[1 - \cos\left(2\pi\xi(\vartheta;\vartheta_o)\right)\right]$ and (2), *type II* iPRCs of the form $\psi(\vartheta) = -\psi_o \cdot \sin(2\pi\xi(\vartheta;\vartheta_o))$, with $\xi(\cdot\,;\vartheta_o) : S^1 \to S^1$ being for $\vartheta_o \in (0,1)$ the smooth mapping defined by

$$\xi(\vartheta;\vartheta_o) := \vartheta + \frac{1}{2}\left(1 - 2\vartheta_o\right) \cdot \frac{1 - \cos\left(2\pi\vartheta\right)}{1 - \cos\left(2\pi\vartheta_o\right)}. \tag{3.1}$$

Note that $\xi(\vartheta_o;\vartheta_o) = 0.5$. Therefore, for type I iPRCs with $\vartheta_o \approx 0.5$, ϑ_o corresponds to the local extremum other than the origin (see figure 3.1(a)). For type II iPRCs with $\vartheta_o \approx 0.5$, ϑ_o corresponds to the point of sign change other than the origin (see figure 3.1(b)). In view of this, the parameter ϑ_o shall be referred to as the iPRC's *turning point*. The deviation of the turning point ϑ_o from 0.5, can be seen as a measure for the deviation of the iPRC from its *symmetric* version ($\vartheta_o = 0.5$). The two-type classification of iPRCs follows the ideas of Hansel et al. (1995) and Ermentrout (1996), who linked two large classes of PRCs to the bifurcation types of excitable neuron membranes. In this thesis, type I iPRCs shall be called *accelerating* or *delaying* if $\psi_o > 0$ or $\psi_o < 0$, respectively. Type II iPRCs shall be called *attracting* or *repulsing* if $\psi_o > 0$ or $\psi_o < 0$, respectively, due to the way oscillators near the spiking point react to incoming stimuli from other, spiking oscillators. These iPRC classes have been chosen because they generalize their symmetric versions, which have already seen attention in the literature (Ermentrout 1996, Ariaratnam 2002). Furthermore, they qualitatively resemble several iPRCs measured on real neurons (Netoff et al. 2005, Preyer & Butera 2005, Ota et al. 2011). Finally, their amplitude $\|\psi\|_\infty = |\psi_o|$ and turning point can be treated as independent parameters.

Type I and type II iPRCs are considered in sections 3.5 and 3.6 respectively. It is shown how stationary states and their stability vary with the iPRC parameters $\vartheta_o, \psi_o/\omega$ and noise strength D/ω. Attention is restricted to the ranges $\vartheta_o \in [0.3, 0.7]$, $|\psi_o|/\omega \in [0, 0.5]$ and $D/\omega \in [0, 1]$. The linear stability analysis reveals that for all non-symmetric type I iPRCs, all non-symmetric repulsing type II iPRCs and all attracting type II iPRCs, stationarity is unstable in noise-free networks. In fact, for type I iPRCs and repulsing type II iPRCs, stationary states undergo a bifurcation at $\vartheta_o \approx 0.5$, with the unstable eigenperturbations being qualitatively different for $\vartheta_o \gtrsim 0.5$ and $\vartheta_o \lesssim 0.5$. Numerical integration of the Fokker-Planck equation (1.12) reveals (in the linearly unstable case) the existence of a locally stable limit cycle, on which the network splits into multiple groups of synchronized oscillators. The number of groups equals, in most of the cases at least, the order (i.e. the number of maxima in the real part) of the leading eigenperturbation. The basin of attraction of this limit cycle, which persists for low non-zero noise in a modified form, includes at least a neighbourhood of the stationary state (excluding the latter itself). Above a certain noise threshold the limit cycle merges with the stationary state, which then becomes locally stable and apparently, globally stable as well. Furthermore, simulations reveal the coexistence of a second locally stable limit cycle for sufficiently low noise, at least for certain type II iPRCs.

The chapter finishes with section 3.7, which compares the predictions of the Fokker-Planck equation (1.12) to the finite Winfree model (1.4) for identical, all-to-all pulse-coupled oscillators with continuous pulses $I \in \mathcal{C}(S^1, \mathbb{R}_+)$ and additive white noise. For that purpose, the Langevin equation (1.7) is numerically integrated in the stochastic processes $\theta_1, .., \theta_N$ on S^1. Both type I and type II iPRCs are considered. Particular interest is devoted to a comparison of the long term network behaviour in the two models, for large N and narrow Gaussian pulses. The results indicate a good agreement of the two models for large oscillator counts and small pulse widths.

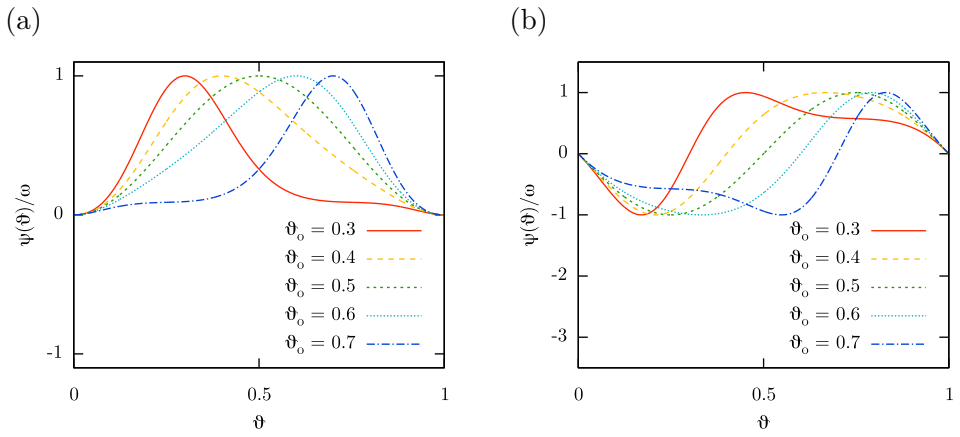

Figure 3.1: Illustration of (a), accelerating type I and (b), attracting type II iPRCs for $\psi_o/\omega = 1$ and $\vartheta_o \in \{0.3, 0.4, 0.5, 0.6, 0.7\}$.

3.2 Existence and uniqueness of stationary states

In noise-free networks, stationary states correspond to phase probability densities $\rho_s \in \mathcal{C}^1(S^1, \mathbb{R}_+)$ satisfying the differential equation

$$\frac{d}{d\vartheta}\Big[\rho_s(\vartheta) \cdot [\omega + \psi(\vartheta) \cdot \rho_s(0)]\Big] = 0. \tag{3.2}$$

Condition (3.2) can be interpreted as the constance of the *probability flux* $\rho_s(\vartheta) \cdot [\omega + \psi(\vartheta) \cdot \rho_s(0)]$ on S^1. Since $\psi(0) = 0$, the flux must be strictly positive. This yields the form

$$\rho_s(\vartheta) = \frac{\omega \rho_s(0)}{\omega + \psi(\vartheta) \cdot \rho_s(0)} \tag{3.3}$$

for all stationary densities ρ_s. The condition that ρ_s be a probability density translates to the fixed-point equation

$$\rho_s(0) = \frac{1}{\omega} \cdot \left[\int_{S^1} \frac{d\vartheta}{\omega + \psi(\vartheta) \cdot \rho_s(0)}\right]^{-1} \tag{3.4}$$

in the stationary stimulus $\rho_s(0) > 0$. Inversely, solving it (under the condition $\omega + \psi(\vartheta) \cdot \rho_s(0) > 0$, $\forall \vartheta \in S^1$) yields through (3.3) a stationary probability density. Eq. (3.4) shall be referred to as the *stationary state equation* for noise-free networks. The following assertion ensures the existence and uniqueness of its solutions, provided that oscillator coupling is weak enough.

Lemma 3.2.1. *Suppose the coupling strength* $\mathcal{E} := \|\psi\|_\infty / \omega$ *is strictly smaller than* $\frac{1}{2}$ *and let* $D = 0$. *Then there exists a unique stationary probability density* $\rho_s \in \mathcal{C}^1(S^1, \mathbb{R})$. *The stationary stimulus* $\rho_s(0)$ *is within* $(2/3, 2)$. *Moreover,* $\rho_s \to 1$ *uniformly as* $\mathcal{E} \to 0$.

Proof. Abbreviate the right hand side of the stationary state equation (3.4) by $A_0(\rho_s(0))$. Then for any stationary probability density ρ_s one can easily estimate

$$A_0(\rho_s(0)) \leq 1 + \mathcal{E} \cdot \rho_s(0), \tag{3.5}$$

which by (3.4) and $\mathcal{E} < \frac{1}{2}$ implies $\rho_s(0) < 2$. On the other hand, $A_0(r)$ is for all $r \in [0, 2]$ well-defined since $\|\psi\|_\infty \cdot r < \omega$. In fact, by (3.5) one has $A_0(r) \leq 2$. The compact interval

$J := [0,2]$ is thus A_0-invariant. The function $A_0 : J \to J$ is continuous and differentiable on $J^o := (0,2)$, with derivative

$$A_0'(r) = \frac{A_0^2(r)}{\omega} \cdot \int_{S^1} \frac{\psi(\vartheta)\, d\vartheta}{\left[1 + \frac{r}{\omega} \cdot \psi(\vartheta)\right]^2}. \tag{3.6}$$

Since the mapping $x \mapsto \frac{x}{1+\alpha x}$ (where $\alpha \geq 0$) is increasing in x for $x > -1/\alpha$, one has

$$\frac{\psi(\vartheta)}{[1+\alpha\cdot\psi(\vartheta)]^2} \leq \frac{\psi(\vartheta)}{1+\alpha\cdot\psi(\vartheta)} \leq \frac{\|\psi\|_\infty}{1+\alpha\cdot\|\psi\|_\infty} \tag{3.7}$$

whenever $\psi(\vartheta) > -1/\alpha$. Letting $\alpha := r/\omega$ for any $r \in (0,2)$, leads by (3.6) and (3.7) to the estimate

$$A_0'(r) \leq \frac{\mathcal{E}}{1+\mathcal{E}r} \cdot A_0^2(r) \leq \frac{\mathcal{E}}{1+\mathcal{E}r} \cdot [1+\mathcal{E}r]^2 \leq \mathcal{E}\cdot[1+2\mathcal{E}] < 1 \tag{3.8}$$

for all $r \in (0,2)$. Therefore $A_0 : J \to J$ has a unique fixed point r_o. Since $\|\psi\|_\infty \cdot r_o < \omega$, that unique fixed point in fact corresponds to a stationary probability density ρ_s with $\rho_s(0) = r_o$, having the form (3.3). Furthermore, one can similarly to (3.5) estimate $A_0(\rho_s(0)) \geq 1 - \mathcal{E}\cdot\rho_s(0)$, which implies $\rho_s(0) > 2/3$. In fact, together with (3.5) this implies

$$\frac{1}{1+\mathcal{E}} \leq \rho_s(0) \leq \frac{1}{1-\mathcal{E}}. \tag{3.9}$$

This shows that $\rho_s(0) \to 1$ as $\mathcal{E} \to 0$ and by (3.4), that $\rho_s \to 1$ uniformly as $\mathcal{E} \to 0$. □

In noisy networks ($D > 0$), stationary states correspond to phase probability densities $\rho_s \in \mathcal{C}^2(S^1, \mathbb{R}_+)$ solving the differential equation

$$\frac{d}{d\vartheta}\Big[\rho_s(\vartheta)\cdot[\omega + \psi(\vartheta)\cdot\rho_s(0)] - D\cdot\frac{d}{d\vartheta}\rho_s(\vartheta)\Big] = 0. \tag{3.10}$$

This is equivalent to

$$\frac{d}{d\vartheta}\rho_s(\vartheta) = \frac{1}{D}\left[\omega + \psi(\vartheta)\cdot\rho_s(0)\right]\cdot\rho_s(\vartheta) + C \tag{3.11}$$

for some appropriate constant $C \in \mathbb{R}$. When regarding the stimulus $\rho_s(0)$ as given, (3.11) is a first order ordinary differential equation, admitting on $[0,1]$ the unique solution

$$\begin{aligned}\rho_s(\vartheta) = &\exp\left[\frac{1}{D}\left[\omega\vartheta + \Psi(0,\vartheta)\cdot\rho_s(0)\right]\right] \\ &\cdot\left[C\int_0^\vartheta d\varphi\ \exp\left[-\frac{1}{D}\left[\omega\varphi + \Psi(0,\varphi)\cdot\rho_s(0)\right]\right] + \rho_s(0)\right],\end{aligned} \tag{3.12}$$

where $\Psi(\vartheta_1,\vartheta_2) := \int_{\vartheta_1}^{\vartheta_2} d\varphi\ \psi(\varphi)$ for $\vartheta_1, \vartheta_2 \in \mathbb{R}$. The periodicity condition $\rho_s(0) = \rho_s(1)$ determines the constant C as

$$\begin{aligned}C = &\rho_s(0)\cdot\left\{\exp\left[-\frac{1}{D}\left[\omega + \Psi(0,1)\cdot\rho_s(0)\right]\right] - 1\right\} \\ &\cdot\left\{\int_0^1 d\varphi\ \exp\left[-\frac{1}{D}\left[\omega\varphi + \Psi(0,\varphi)\cdot\rho_s(0)\right]\right]\right\}^{-1}.\end{aligned} \tag{3.13}$$

Inserting (3.13) into (3.12) yields the representation

$$\begin{aligned}\rho_{\mathrm{s}}(\vartheta) = \rho_{\mathrm{s}}(0) \cdot \left\{ \int_0^1 d\varphi \ \exp\left[-\frac{1}{D} \left[\omega\varphi + \Psi(0,\varphi) \cdot \rho_{\mathrm{s}}(0) \right] \right] \right\}^{-1} \\ \cdot \int_0^1 d\varphi \ \exp\left[-\frac{1}{D} \left[\omega\varphi + \Psi(\vartheta, \vartheta+\varphi) \cdot \rho_{\mathrm{s}}(0) \right] \right].\end{aligned} \tag{3.14}$$

Note that for (3.14) use has been made of the fact that $\Psi(0,1) + \Psi(0,\varphi) = \Psi(0,1+\varphi)$. Finally, the normalization condition $\int_0^1 d\vartheta \ \rho_{\mathrm{s}}(\vartheta) = 1$ is equivalent to the fixed point equation

$$\begin{aligned}\rho_{\mathrm{s}}(0) = \left\{ \int_0^1 d\vartheta \ \int_0^1 d\varphi \ \exp\left[-\frac{1}{D} \left[\omega\varphi + \Psi(\vartheta, \vartheta+\varphi) \cdot \rho_{\mathrm{s}}(0) \right] \right] \right\}^{-1} \\ \cdot \int_0^1 d\varphi \ \exp\left[-\frac{1}{D} \left[\omega\varphi + \Psi(0,\varphi) \cdot \rho_{\mathrm{s}}(0) \right] \right]\end{aligned} \tag{3.15}$$

in the stationary stimulus $\rho_{\mathrm{s}}(0) > 0$. Inversely, the solutions to (3.15) correspond through (3.14) to stationary probability densities. To see this, note that the periodicity of ρ_{s} implies by (3.11) the periodicity of $\partial_\vartheta \rho_{\mathrm{s}}$. The latter in turn implies the periodicity of $\partial_\vartheta^2 \rho_{\mathrm{s}}(\vartheta)$, so that indeed $\rho_{\mathrm{s}} \in \mathcal{C}^2(S^1, \mathbb{R}_+)$. Similarly to (3.4), (3.15) shall be referred to as the *stationary state equation* for networks with noise. The following two propositions and two lemmas provide existence and local uniqueness statements for its solutions.

Proposition 3.2.2. *Denote the right hand side of the stationary state equation (3.15) by $A_D(\rho_{\mathrm{s}}(0))$. For any $\beta \geq 0$ define $J_\beta := [0, \beta]$. Then, provided that $\beta \geq 0$ and $\mathcal{E} := \|\psi\|_\infty / \omega \leq 1/(4\beta)$, one has $A_D(J_\beta) \subseteq J_{5/3}$ and the mapping $A_D : J_\beta \to J_{5/3}$ is a contraction with Lipschitz constant $25/27$.*

For a proof see appendix A.4.1.

Proposition 3.2.3. *For $D > 0$ let $A_D : \mathbb{R}_+ \to \mathbb{R}_+$ be the functional introduced in proposition 3.2.2 and let $A_0 : \mathbb{R}_+ \to \mathbb{R}_+$ be the functional introduced in lemma 3.2.1. Let $\mathcal{E} := \|\psi\|_\infty / \omega$ and $r \geq 0$ be such that $\mathcal{E} r < 1$. Then $A_D(r)$ tends to $A_0(r)$ as $D \to 0^+$.*

For a proof see appendix A.4.2.

Lemma 3.2.4. *Let $\beta \geq 2$ and $\mathcal{E} := \|\psi\|_\infty / \omega \leq 1/4\beta$. Then for each diffusion coefficient $D > 0$ there exists exactly one stationary probability density $\rho_{\mathrm{s}} \in \mathcal{C}^2(S^1, \mathbb{R})$ such that $\rho_{\mathrm{s}}(0) \in J_\beta := [0, \beta]$. That density in fact satisfies $\rho_{\mathrm{s}}(0) \in [0, 5/3]$. As $D \to 0^+$, ρ_{s} converges pointwise to the stationary probability density for noise-free networks (the existence and uniqueness of which is ensured by lemma 3.2.1). Furthermore, the density ρ_s depends continuously (in the supremum norm) on $D > 0$.*

Proof. By proposition 3.2.2, the functionals $A_D : J_\beta \to J_{5/3} \subseteq J_\beta$ ($D > 0$) are contractions with a Lipschitz constant $L_A < 1$ not depending on D. By Banach's fixed point theorem, each A_D has in J_β a unique fixed point r_D corresponding to the stationary state $\rho_{\mathrm{s}}(\cdot\,; D, r_D)$, where

$$\begin{aligned}\rho_{\mathrm{s}}(\vartheta; D, r) := r \cdot \left\{ \int_0^1 d\varphi \ \exp\left[-\frac{1}{D} \left[\omega\varphi + \Psi(0,\varphi) \cdot r \right] \right] \right\}^{-1} \\ \cdot \int_0^1 d\varphi \ \exp\left[-\frac{1}{D} \left[\omega\varphi + \Psi(\vartheta, \vartheta+\varphi) \cdot r \right] \right].\end{aligned} \tag{3.16}$$

By proposition 3.2.3 one knows that $A_D(r_0) \to A_0(r_0)$ as $D \to 0^+$, with $r_0 \in J_2$ being the fixed point of A_0. Together with the estimate

$$\begin{aligned}|r_D - r_0| &= |A_D(r_D) - A_0(r_0)| \leq |A_D(r_D) - A_D(r_0)| + |A_D(r_0) - A_0(r_0)| \\ &\leq L_A \cdot |r_D - r_0| + |A_D(r_0) - A_0(r_0)|\,,\end{aligned} \tag{3.17}$$

this implies $r_D \to r_0$ as $D \to 0^+$. Furthermore, in a way similar to the proof of proposition 3.2.2 (see appendix A.4.1) one finds that $\rho_s(\vartheta; D, r)$ is Lipschitz continuous in $r \in J_\beta$, with a Lipschitz constant L_r uniform in $D > 0$ and $\vartheta \in S^1$. Denote

$$\rho_s(\vartheta; 0, r) := \frac{r \cdot \omega}{\omega + \psi(\vartheta) \cdot r} \tag{3.18}$$

for $\vartheta \in S^1$ and $r \in J_\beta$. Then $\rho_s(\cdot\,; 0, r_0)$ is by (3.3) the stationary state in the noise-free case. Similar to proposition 3.2.3 one finds that $\rho_s(\vartheta; D, r) \to \rho_s(\vartheta; 0, r)$ as $D \to 0^+$, for every $r \in J_\beta$ and $\vartheta \in S^1$. Using the estimate

$$\begin{aligned} |\rho_s(\vartheta; D, r_D) - \rho_s(\vartheta; 0, r_0)| &\leq |\rho_s(\vartheta; D, r_D) - \rho_s(\vartheta; D, r_0)| + |\rho_s(\vartheta; D, r_0) - \rho_s(\vartheta; 0, r_0)| \\ &\leq L_r \cdot |r_D - r_0| + |\rho_s(\vartheta; D, r_0) - \rho_s(\vartheta; 0, r_0)|\,, \end{aligned} \tag{3.19}$$

one concludes that $\rho_s(\vartheta; D, r_D) \to \rho_s(\vartheta; 0, r_0)$ as $D \to 0^+$, for every $\vartheta \in S^1$. Left to show is the continuity of ρ_s on $D > 0$. For two $D, D' > 0$ and the corresponding stationary stimuli r_D, $r_{D'}$, one can similarly to (3.17) estimate

$$(1 - L_A) \cdot |r_D - r_{D'}| \leq |A_D(r_D) - A_{D'}(r_D)|\,. \tag{3.20}$$

From (3.15) it is clear that the right hand side of (3.20) vanishes as $D' \to D$. Since $L_A < 1$ this implies that $r_D \to r_{D'}$ as $D' \to D$. Consequently also $\rho_s(\vartheta; D, r_D) \to \rho_s(\vartheta; D', r_{D'})$ as $D' \to D$, uniformly in $\vartheta \in S^1$. □

Lemma 3.2.5. *For any $\mathcal{E}_m > 0$ and $r_m > 1$ there exists a constant $C > 0$ such that whenever $\mathcal{E} := \|\psi\|_\infty / \omega \leq \mathcal{E}_m$ and $D/\omega \geq C$, there exists exactly one stationary state $\rho_s \in \mathcal{C}^2(S^1, \mathbb{R})$ with $\rho_s(0) \in [0, r_m]$. Furthermore, $\rho_s(\vartheta)$ tends to 1 as $D/\omega \to \infty$ uniformly in $\vartheta \in S^1$ and $\mathcal{E} \leq \mathcal{E}_m$.*

Proof. From (3.15) it is easy to see that the derivative A_D' of the functional $A_D : \mathbb{R}_+ \to \mathbb{R}_+$ is given by

$$\begin{aligned} A_D'(r) = \frac{\omega}{D} \cdot \frac{1}{N^2(r)} \cdot \Bigg[\frac{M(r)}{\omega} \cdot \int_0^1 d\vartheta \int_0^1 d\varphi\; e^{-\frac{\omega}{D} \cdot V(\vartheta, \varphi, r)} \Psi(\vartheta, \vartheta + \varphi) \\ - \frac{N(r)}{\omega} \cdot \int_0^1 d\varphi\; e^{-\frac{\omega}{D} \cdot V(0, \varphi)} \Psi(0, \varphi) \Bigg], \end{aligned} \tag{3.21}$$

where

$$\begin{aligned} V(\vartheta, \varphi, r) &:= \varphi + \frac{1}{\omega} \Psi(\vartheta, \vartheta + \varphi) \cdot r, \\ M(r) &:= \int_0^1 d\varphi\; e^{-\frac{\omega}{D} \cdot V(0, \varphi, r)}, \\ N(r) &:= \int_0^1 d\vartheta \int_0^1 d\varphi\; e^{-\frac{\omega}{D} \cdot V(\vartheta, \varphi, r)}. \end{aligned} \tag{3.22}$$

Note that $|\Psi(\vartheta, \vartheta + \varphi)/\omega|$ and $|V(\vartheta, \varphi, r)|$ are uniformly bounded for $(\vartheta, \varphi, r) \in \mathbb{R} \times [0, 1] \times [0, r_m]$ and $\mathcal{E} \leq \mathcal{E}_m$. Thus $M(r) \to 1$ and $N(r) \to 1$ as $D/\omega \to \infty$, uniformly in $\mathcal{E} \leq \mathcal{E}_m$ and $r \in [0, r_m]$. Together with (3.21) this implies that $A_D'(r) \to 0$ as $D/\omega \to \infty$, uniformly in $\mathcal{E} \leq \mathcal{E}_m$ and $r \in [0, r_m]$.

Now choose $C > 0$ so large that $A_D'|_{[0, r_m]} < \min\{1, (r_m - 1)/r_m\}$ whenever $D/\omega \geq C$ and $\mathcal{E} \leq \mathcal{E}_m$. Since $A_D(0) = 1$, one finds that A_D has a unique fixed point in $[0, r_m]$ whenever $D/\omega \geq C$ and $\mathcal{E} \leq \mathcal{E}_m$, corresponding to the stimulus $\rho_s(0)$ of a stationary state $\rho_s \in \mathcal{C}^2(S^1)$. Furthermore, $\rho_s(0)$ tends to 1 as $D/\omega \to \infty$ uniformly in $\mathcal{E} \leq \mathcal{E}_m$. Recall that by (3.14) one has the representation

$$\rho_s(\vartheta) = \frac{\rho_s(0)}{M(\rho_s(0))} \cdot \int_0^1 d\varphi\; e^{-\frac{\omega}{D} \cdot V(\vartheta, \varphi, \rho_s(0))}. \tag{3.23}$$

Consequently, $\rho_s(\vartheta) \to 1$ as $D/\omega \to \infty$, uniformly in $\vartheta \in S^1$ and $\mathcal{E} \leq \mathcal{E}_m$. □

The last two lemmas describe the local bifurcation behaviour of stationary states in noisy networks as noise tends to zero or to infinity. They show that for weak coupling, the stationary state is preserved in a modified form as noise is increased from zero and tends to the uniform distribution as noise tends to infinity. Contrary to the noise-free case (lemma 3.2.1), this preserved stationary state is only locally unique and in fact little information is provided on the possible appearance of other stationary states. Nonetheless, the radius of uniqueness (in the supremum norm) can be chosen large enough, provided that coupling is weak enough or noise is adequately strong.

3.3 Linear stability of stationary states

The local stability analysis of stationary states ρ_{s} presented in this thesis, consists of a spectral analysis of the linearized dynamics of small perturbations $h(t) \in \mathcal{C}^1(S^1)$ ($h \in \mathcal{C}^2(S^1)$ if $D > 0$). This approach turns out to be much more fruitful in the noise-free case, where the corresponding eigenvalue equation reduces to a one-dimensional integral equation as shown below.

Let $\rho_{\mathrm{s}} + h$ satisfy the Fokker-Planck equation (1.12). It is straightforward to see that in the noise-free case h satisfies the evolution equation

$$\partial_t h(t,\vartheta) = (\mathcal{Q}h(t,\cdot))(\vartheta) - h(t,0)\cdot\left(h(t,\vartheta)\cdot\psi(\vartheta)\right)', \tag{3.24}$$

with the linear operator $\mathcal{Q}$ given by

$$\mathcal{Q}f = -\left[(\omega + \psi\cdot\rho_{\mathrm{s}}(0))\cdot f\right]' - (\psi\cdot\rho_{\mathrm{s}})'\cdot f(0), \qquad f \in \mathcal{C}^1(S^1). \tag{3.25}$$

The prime symbol " $'$ " will be used to denote the partial derivative with respect to the circular coordinate $\vartheta \in S^1$. Note that if one considers $\mathcal{C}^1(S^1)$ as a normed space with the supremum norm, then $\mathcal{Q}h$ is for $h \in \mathcal{C}^1(S^1)$ the Gâteaux differential of the non-linear operator $\mathcal{C}^1(S^1) \to \mathcal{C}(S^1)$ on the right hand side of the Fokker-Planck equation (1.12), at its fixed point ρ_{s} along h. Also note that $\mathcal{Q}$ maps $\mathcal{C}^1(S^1)$ into the space $\mathcal{C}_{\mathrm{zm}}(S^1)$ of continuous functions with zero mean. In fact, in view of the normalization condition $\int_{S^1}(\rho_{\mathrm{s}} + h) = 1$ imposed on all network states, only the restriction of $\mathcal{Q}$ to the domain $\mathcal{C}^1_{\mathrm{zm}}(S^1)$ shall be considered, the latter seen as a subspace of $\mathcal{C}_{\mathrm{zm}}(S^1)$. Determining those *eigenperturbations* $h \in \mathcal{C}^1_{\mathrm{zm}}(S^1)$ that evolve as $h(t) \approx e^{\lambda t}h(0)$ in the linear approximation of (3.24) corresponds to a point-spectral analysis of $\mathcal{Q}$ and will give insight to the local stability of ρ_{s}.

Lemma 3.3.1. *The linear operator $\mathcal{Q}$ defined in (3.25) has the following spectral properties:*

1. *The point spectrum $\sigma_{\mathrm{p}}(\mathcal{Q})$ is given by the complex solutions $\lambda \in \mathbb{C}$ to the eigenvalue equation*

$$\int_0^1 d\vartheta\ \frac{e^{\lambda T_{\mathrm{s}}(\vartheta)}}{\mathrm{v}_{\mathrm{s}}^2(\vartheta)} = 0, \tag{3.26}$$

   with the so-called stationary velocity $\mathrm{v}_{\mathrm{s}}(\vartheta) := \omega + \psi(\vartheta)\cdot\rho_{\mathrm{s}}(0)$ and the so-called stationary travel time $T_{\mathrm{s}}(\vartheta) := \int_0^\vartheta d\varphi\ 1/\mathrm{v}_{\mathrm{s}}(\varphi)$. All eigenvalues are of geometric multiplicity one.

2. *The eigenvalue equation (3.26) has a countably infinite number of solutions $\lambda_n \in \mathbb{C}$ ($n \in \mathbb{Z}$), which can be numbered so that $\lambda_n \sim n\cdot i2\pi/T_{\mathrm{s}}(1)$ as $|n| \to \infty$. Furthermore, all eigenvalues satisfy $|\Re(\lambda_n)| \le \rho_{\mathrm{s}}(0)\cdot\|\psi'\|_\infty$.*

Proof.

1. The eigenvalue equation in the eigenperturbation $h \in \mathcal{C}^1_{\mathrm{zm}}(S^1)$ with eigenvalue $\lambda \in \mathbb{C}$ reads

$$(\omega + \psi \cdot \rho_{\mathrm{s}}(0)) \cdot h' + \big(\lambda + \psi' \cdot \rho_{\mathrm{s}}(0)\big) \cdot h + (\psi \cdot \rho_{\mathrm{s}})' \cdot h(0) = 0. \tag{3.27}$$

When regarding the *perturbation stimulus* $h(0)$ as constant, the above is an inhomogeneous, linear differential equation for h of order one. Its solution on $[0,1]$ is given by

$$h(\vartheta) = h(0) \cdot e^{A_\lambda(\vartheta)} \cdot \left[1 + \int_0^\vartheta d\varphi \; B(\varphi) e^{-A_\lambda(\varphi)}\right], \tag{3.28}$$

with A_λ and B defined as

$$\begin{aligned} A_\lambda(\vartheta) &:= -\int_0^\vartheta \frac{d\varphi}{\mathrm{v_s}(\varphi)} \cdot \left[\psi'(\varphi) \cdot \rho_{\mathrm{s}}(0) + \lambda\right], \\ B(\vartheta) &:= -\frac{(\psi \cdot \rho_{\mathrm{s}})'(\vartheta)}{\mathrm{v_s}(\vartheta)} = \frac{\omega \cdot \rho_{\mathrm{s}}'(\vartheta)}{\mathrm{v_s}(\vartheta) \cdot \rho_{\mathrm{s}}(0)}. \end{aligned} \tag{3.29}$$

The periodicity condition $h(0) = h(1) \neq 0$ is equivalent to

$$\chi(\lambda) := 1 - e^{A_\lambda(1)} \left[1 + \int_0^1 d\varphi \; B(\varphi) e^{-A_\lambda(\varphi)}\right] = 0. \tag{3.30}$$

Note that by the stationary state equation (3.4) one has $T_{\mathrm{s}}(1) = 1/(\mathrm{v_s}(0)\rho_{\mathrm{s}}(0))$ and

$$A_\lambda(\vartheta) = \ln \frac{\mathrm{v_s}(0)}{\mathrm{v_s}(\vartheta)} - \lambda T_{\mathrm{s}}(\vartheta) \tag{3.31}$$

for $\vartheta \in [0,1]$. Every non-trivial solution λ to (3.30) corresponds through (3.28) to a function $h_\lambda \in \mathcal{C}(S^1) \cap \mathcal{C}^1([0,1])$ solving (3.27). The latter ensures that in fact $h_\lambda \in \mathcal{C}^1(S^1)$. Since $\lambda h_\lambda = \mathcal{Q} h_\lambda$ is in $\mathcal{C}_{\mathrm{zm}}(S^1)$ and $\lambda \neq 0$, one concludes that $h_\lambda \in \mathcal{C}^1_{\mathrm{zm}}(S^1)$, so that h_λ is an eigenperturbation with eigenvalue λ. The value $\lambda = 0$ always solves (3.30), but it corresponds by (3.3) and (3.28) to the perturbation

$$h_0(\vartheta) = h_0(0) \cdot \frac{\rho_{\mathrm{s}}(\vartheta)}{\rho_{\mathrm{s}}(0)} \cdot \left[1 + \omega T_{\mathrm{s}}(1) \cdot [\rho_{\mathrm{s}}(\vartheta) - \rho_{\mathrm{s}}(0)]\right] = h_0(0) \cdot \frac{\rho_{\mathrm{s}}^2(\vartheta)}{\rho_{\mathrm{s}}^2(0)}, \tag{3.32}$$

which, given $h_0(0) \neq 0$, has non-zero mean. One concludes that the eigenvalues of $\mathcal{Q}$ are exactly the non-trivial solutions λ to the *eigenvalue equation* (3.30). Using (3.31) one finds that

$$\begin{aligned} \chi(\lambda) =& 1 - e^{-\lambda T_{\mathrm{s}}(1)} \left[1 + \int_0^1 d\varphi \; \frac{\rho_{\mathrm{s}}'(\varphi)}{\rho_{\mathrm{s}}(0)} e^{\lambda T_{\mathrm{s}}(\varphi)}\right] \\ \overset{(1)}{=}& e^{-\lambda T_{\mathrm{s}}(1)} \frac{\lambda}{\rho_{\mathrm{s}}(0)} \int_0^1 d\varphi \; \frac{\rho_{\mathrm{s}}(\varphi)}{\mathrm{v_s}(\varphi)} e^{\lambda T_{\mathrm{s}}(\varphi)} \\ \overset{(2)}{=}& e^{-\lambda T_{\mathrm{s}}(1)} \lambda\omega \int_0^1 d\varphi \; \frac{e^{\lambda T_{\mathrm{s}}(\varphi)}}{\mathrm{v_s^2}(\varphi)}. \end{aligned} \tag{3.33}$$

In step (1) partial integration was used. In step (2) use has been made of the fact that $\rho_{\mathrm{s}}(\varphi) = \rho_{\mathrm{s}}(0)\omega/\mathrm{v_s}(\varphi)$. Therefore, the non-trivial roots of χ are exactly the solutions of

$$\int_0^1 d\varphi \; \frac{e^{\lambda T_{\mathrm{s}}(\varphi)}}{\mathrm{v_s^2}(\varphi)} = 0. \tag{3.34}$$

The single multiplicity of eigenvalues is evident from (3.28).

2. Note that the eigenvalue equation (3.26) can be brought into the form of a standard exponential integral

$$\int_0^{T_\mathrm{s}(1)} dt\ f(t)\cdot e^{\lambda t} = 0, \tag{3.35}$$

with $f(t) := 1/\mathrm{v_s}(\theta(t))$ and $\theta : \mathbb{R} \to S^1$ as the solution to the initial value problem $\theta(0) = 0$, $\dot\theta(t) = \mathrm{v_s}(\theta(t))$. Note that $\theta(T_\mathrm{s}(1)) = \theta(0)$. One has $-f'(t)/f(t) = \rho_\mathrm{s}(0)\cdot\psi'(\theta(t))$. By Pólya (1918, §4) any solution to (3.35) must therefore satisfy $|\Re(\lambda)| \leq \rho_\mathrm{s}(0)\cdot\|\psi'\|_\infty$. Furthermore, defining $g(\varphi) := f\left[T_\mathrm{s}(1)(\varphi+1)/2\right]/f(0)$ allows one to write (3.35) in the equivalent form

$$\int_{-1}^{1} d\varphi\ g(\varphi) e^{\frac{\lambda}{2}T_\mathrm{s}(1)\cdot\varphi} = 0, \tag{3.36}$$

with $g(-1) = g(1) = 1$. It is a known fact (Langer 1931, Theorem 13) that the zeros $(\lambda_n)_{n\in\mathbb{Z}}$ of (3.36) can be numbered in such a way that $\lambda_n T_\mathrm{s}(1)/2 \sim n\pi i$ as $|n| \to \infty$.

□

Note that $T_\mathrm{s}(\vartheta)$ is for $\vartheta \in [0,1]$ the time it takes for an oscillator to advance from phase 0 to ϑ, when the noise-free network is in the stationary state. Assertion 2 of lemma 3.3.1 can be interpreted in the following way: Eigenperturbations of high orders (i.e. high frequencies) oscillate at frequencies which are approximately integer multiples of the *stationary oscillator frequency* $1/T_\mathrm{s}(1)$. Furthermore, they tend to have slow dynamics, decaying or exploding at a rate approaching zero as their order tends to infinity. Lemma 3.3.2 below takes this finding to an extreme for iPRCs with certain symmetry properties. Note that spectra approximating the grid $i2\pi/T_\mathrm{s}(1)\cdot\mathbb{Z}$ have, in the limit of weak coupling, already been found in the stability analysis of stationary states for similar noise-free networks with smooth (as opposed to Dirac-like) pulses by Abbott & van Vreeswijk (1993).

Lemma 3.3.2. *Suppose the iPRC ψ to be satisfying the symmetry property $\psi(\vartheta) = \psi(-\vartheta)$ for $\vartheta \in S^1$. Then either all eigenvalues of $\mathcal{Q}$ are purely imaginary, or all but a finite number of eigenvalues are purely imaginary and some eigenvalues have strictly positive real part. In particular, stationary states are in noise-free networks either (linearly) neutrally stable or unstable.*

Proof. Let us begin with the following auxiliary statement: If $\lambda = x + iy \in \mathbb{C}$ (with $x, y \in \mathbb{R}$) solves the eigenvalue equation (3.26), then so does its *reflection* $\tilde\lambda := -x + iy$. To see why this is true, note that $\mathrm{v_s}(\vartheta) = \mathrm{v_s}(1-\vartheta)$ and thus $T_\mathrm{s}(\vartheta) = T_\mathrm{s}(1) - T_\mathrm{s}(1-\vartheta)$ for $\vartheta \in [0,1]$. Therefore

$$\begin{aligned}\int_0^1 d\vartheta\ \frac{e^{\tilde\lambda\cdot T_\mathrm{s}(\vartheta)}}{\mathrm{v_s}^2(\vartheta)} &= e^{\tilde\lambda\cdot T_\mathrm{s}(1)}\cdot\int_0^1 d\vartheta\ \frac{e^{\lambda^*\cdot T_\mathrm{s}(1-\vartheta)}}{\mathrm{v_s}^2(\vartheta)} = e^{\tilde\lambda\cdot T_\mathrm{s}(1)}\cdot\int_0^1 d\vartheta\ \frac{e^{\lambda^*\cdot T_\mathrm{s}(\vartheta)}}{\mathrm{v_s}^2(1-\vartheta)} \\ &= e^{\tilde\lambda\cdot T_\mathrm{s}(1)}\cdot\left[\int_0^1 d\vartheta\ \frac{e^{\lambda\cdot T_\mathrm{s}(\vartheta)}}{\mathrm{v_s}^2(\vartheta)}\right]^* = 0.\end{aligned} \tag{3.37}$$

Now suppose $\sigma_\mathrm{p}(\mathcal{Q})$ is not purely imaginary. Then by the above statement, at least one eigenvalue has strictly positive real part. Furthermore, due to the asymptotic distribution of eigenvalues for large orders predicted by lemma 3.3.1(2), only a finite number of eigenvalues λ_n admits a reflection $\tilde\lambda_n \neq \lambda_n$. □

In analogy to noise-free networks, a good starting point for a local stability analysis of stationarity in noisy networks, is the linearized dynamics of small perturbations $h(t) \in \mathcal{C}^2_\mathrm{zm}(S^1)$. Similarly to (3.24) one finds the dynamics

$$\partial_t h = \mathcal{Q}_D h - h(0)\cdot(h\cdot\psi)', \tag{3.38}$$

with the linear part

$$\mathcal{Q}_D h := -(\mathrm{v_s} \cdot h)' - (\psi \cdot \rho_\mathrm{s})' \cdot h(0) + D \cdot h'' \tag{3.39}$$

and provided that $\rho_\mathrm{s} + h$ satisfies the Fokker-Planck equation (1.12). Note that $\mathcal{Q}_D$ maps $\mathcal{C}^2(S^1)$ into $\mathcal{C}_\mathrm{zm}(S^1)$. Unlike in the noise-free case, the eigenvalue equation $\mathcal{Q}_D h = \lambda h$ is not easily reducible to a lower dimensional form.

An alternative approach would be a trigonometric approximation of eigenperturbations and an evaluation of the eigenvalue equation in the Fourier space. The condition $Dh'' = \lambda h + (\mathrm{v_s} \cdot h)' + (\psi \cdot \rho_\mathrm{s})' \cdot h(0)$ implies that any eigenperturbation $h \in \mathcal{C}^2_\mathrm{zm}(S^1)$ is in fact in $\mathcal{C}^3_\mathrm{zm}(S^1)$ (recall that by section 3.2 one has $\rho_\mathrm{s} \in \mathcal{C}^2(S^1)$). Thus, the Fourier series of h, h' and h'' converge uniformly. It is straightforward to see that the eigenvalue equation $\mathcal{Q}_D h = \lambda h$ is equivalent to

$$\begin{aligned} \lambda \cdot \mathcal{F}_n(h) = &- (2\pi n)^2 D \cdot \mathcal{F}_n(h) \\ &- i2\pi n \sum_{k=-\infty}^{\infty} \mathcal{F}_k(h) \cdot \mathcal{F}_{n-k}(\mathrm{v_s}) \\ &- i2\pi n \cdot \mathcal{F}_n(\psi \cdot \rho_\mathrm{s}) \cdot \sum_{k=-\infty}^{\infty} \mathcal{F}_k(h) \end{aligned} \tag{3.40}$$

for $n \in \mathbb{Z} \setminus \{0\}$, with $\mathcal{F}_0(h) = 0$. This algebraic system in the Fourier components $\mathcal{F}_n(h)$ is the starting point for the approximative method used in the numerical spectral stability analysis described in section 3.4.3 below.

3.4 Numerical methods

This section outlines the numerical methods I used to further investigate the behaviour of the model, in particular with respect to the shape and stability of stationary states. Specifically, section 3.4.1 describes the evaluation of the stationary state equations (3.4) and (3.15). Sections 3.4.2 and 3.4.3 elaborate on the numerical spectral stability analysis of stationary states for noise-free and noisy networks, respectively. Section 3.4.4 presents the scheme used for the integration of the Fokker-Planck equation (1.12).

The numerical analysis described below was applied exclusively to type I and type II iPRCs, defined in the introduction of this chapter. Attention was restricted to the parameter values $\vartheta_o \in [0.3, 0.7]$, $|\psi_o| / \omega \in [0, 0.5]$ and $D/\omega \in [0, 1]$. For the calculations ω was set to 1, though the dimensionless parameters ψ_o/ω and D/ω are used for the presentation of all results.

3.4.1 Solving the stationary state equations

Both stationary state equations (3.4) and (3.15) are generally difficult to solve analytically. In order to get a better feeling for the shapes of stationary states and their dependence on the iPRC and noise strength, numerical quadratures were implemented for the integral expressions involved. Using them, routines were constructed for the evaluation of the operators A_D ($D \geq 0$) introduced in lemma 3.2.1 and proposition 3.2.2. In view of proposition 3.2.2, a fixed-point iteration of A_D was used to search for stationary states (or better, their corresponding stimuli) for both type I and type II iPRCs. As starting point the stimulus value 1 was chosen, corresponding to the uniform density. The iteration process was considered complete whenever subsequent iterations only changed the stationary stimulus by a value of less than 1/1000. Within the considered parameter range, the above iteration always converged to a limit in $[0, 2]$, apparently

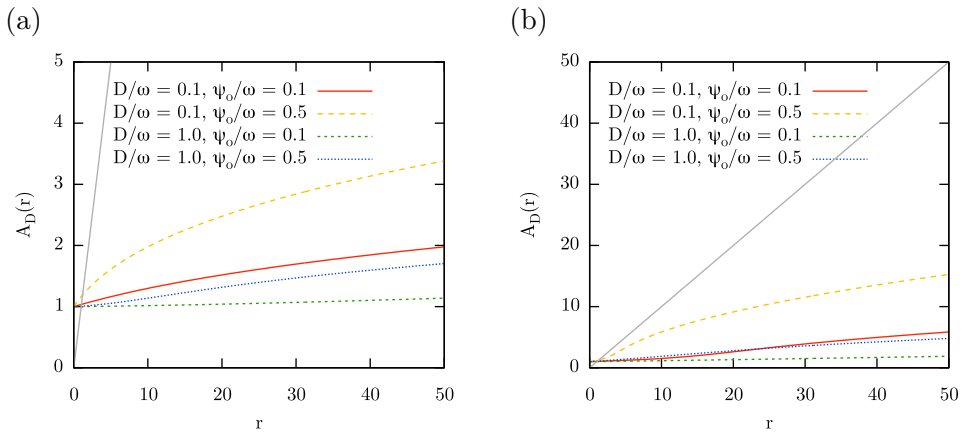

Figure 3.2: Graph of the functional $A_D : \mathbb{R}_+ \to \mathbb{R}_+$, $r \mapsto A_D(r)$ introduced in proposition 3.2.2, for (a), symmetric accelerating type I iPRCs and (b), symmetric attracting type II iPRCs and various coupling and noise strengths. The grey straight line represents the diagonal in $\mathbb{R}_+^2$. Fixed points of A_D correspond to stationary stimuli. Though the graphs only cover the domain $[0, 50]$, the functionals A_D follow a similar shape for larger values r as well (at least up to $r = 1000$). Note that all graphs intersect the diagonal exactly once and within the domain $[0, 2]$. This property is in fact shared by all symmetric and non-symmetric type I (accelerating and delaying) and type II (attracting and repulsing) iPRCs, at least for all tested $\vartheta_o \in [0.3, 0.7]$, $\psi_o/\omega \in [0, 0.5]$ and $D/\omega \in [0, 1]$.

independently on the start value, at least among start values within $[0, 1000]$. Figure 3.2 shows a numerical evaluation of the functional A_D for symmetric type I and type II iPRCs and typical combinations of D/ω and ψ_o/ω. As can be seen, the graph of the functional $A_D : \mathbb{R}_+ \to \mathbb{R}_+$ always intersects, at least within the illustrated domain, the diagonal exactly once. This suggests the uniqueness of the calculated stationary states.

3.4.2 Spectral stability analysis for noise-free networks

The eigenvalue equation (3.26) for the operator $\mathcal{Q}$ was solved numerically for both type I and type II iPRCs. For that, Newton's method with quadratic backtracking (Press et al. 1997) was used. Start values were taken on a grid considered fine enough for the purpose. Specifically, the distance of adjacent grid points was taken to be roughly one tenth of $2\pi/T_\mathrm{s}(1)$. The latter corresponds to the typical distance between successive eigenvalues as suggested by lemma 3.3.1(2). This length scale is verified analytically for symmetric type I and type II iPRCs in sections 3.5 and 3.6 below. As all eigenvalues appear in complex-conjugate pairs, only the upper half plane was considered. In order to limit the search to a finite domain, use has been made of the estimate $|\Im(\lambda)| \leq \tilde{M} \cdot \left(1 - e^{-|\Re(\lambda)| \cdot T_\mathrm{s}(1)}\right)^{-1}$, valid for any eigenvalue $\lambda \in \sigma_\mathrm{p}(\mathcal{Q})$ with $\Re(\lambda) \neq 0$. The constant $\tilde{M}$, given in (A.49), depends on ψ and ω and was calculated numerically. A proof of this estimate can be found in appendix A.4.3. In view of this estimate and lemma 3.3.1(2), the grid was a priori limited to the domain $[-M, M] + i\mathbb{R}_+$, where $M := \rho_\mathrm{s}(0) \cdot \|\psi'\|_\infty$. This domain was scanned in a real-part-first and increasing imaginary part direction. As soon as an eigenvalue $\lambda \in \mathbb{C}$ with non-trivial real part was found, the domain's imaginary part was reduced (if applicable) on the corresponding (left or right) half plane in a way that no eigenvalues with real parts of comparable or greater magnitude would be omitted. More precisely, if the search domain was $([-M, 0] + i \cdot [0, N_\mathrm{l})) \cup ([0, M] + i \cdot [0, N_\mathrm{r}))$, then finding a new eigenvalue λ with $\Re(\lambda) < 0$ would reduce it to $([-M, 0] + i \cdot [0, \tilde{N}_\mathrm{l})) \cup ([0, M] + i \cdot [0, N_\mathrm{r}))$, where

$$\tilde{N}_\mathrm{l} := \max\left\{N_\mathrm{min}, \min\left\{N_\mathrm{l}, \tilde{M} \cdot \left(1 - e^{-|\Re(\lambda)| \cdot T_\mathrm{s}(1)}\right)^{-1} + \omega\right\}\right\}. \tag{3.41}$$

Similar adjustments were made when $\Re(\lambda) > 0$. The lower limit $N_{\min} > 0$ was set sufficiently high to get an acceptable picture of the point spectrum at hand (recall that by lemma 3.3.1(2) the point spectrum approaches the grid $i2\pi/T_{\mathrm{s}}(1) \cdot \mathbb{Z}$ for larger imaginary parts). The number of iterations was limited to 500 per start value. During these iterations, an attained value $\lambda \in \mathbb{C}$ was considered to be an eigenvalue if it satisfied the eigenvalue equation (3.26) up to an error of less than $\omega^{-2}/1000$ and if subsequent iteration values only differed by less than $\omega/100$. Eigenvalues closer than $\omega/100$ to each other were considered identical. The shapes of eigenperturbations corresponding to the found eigenvalues were approximated using numerical quadratures for the representation (3.28). Their periodicity (equivalent to the eigenvalue equation) served as a verification of their correctness.

3.4.3 Spectral stability analysis for noisy networks

For determining the point spectrum of the linearized dynamics at stationary states in noisy networks, the starting point was the infinite system of equations (3.40) in the Fourier spectrum of eigenperturbations, introduced in section 3.3. For its numerical evaluation, only a finite subset of it was considered, by implicitly assuming $\mathcal{F}_n(h) = 0 \; \forall \, |n| > N$ for the sought eigenperturbations $h \in \mathcal{C}^2_{\mathrm{zm}}(S^1)$. The threshold N was chosen to be 100. More precisely, the low-order point spectrum of the linear operator $\mathcal{Q}_D : C^2_{\mathrm{zm}}(S^1) \subseteq \mathcal{C}_{\mathrm{zm}}(S^1) \to \mathcal{C}_{\mathrm{zm}}(S^1)$ was approximated by the spectrum of the finite matrix $Q^{(N)} \in \mathbb{C}^{2N \times 2N}$, defined as

$$\left(Q^{(N)}\right)_{nk} := -(2\pi n)^2 D \cdot \delta_{nk} - i2\pi n \cdot \mathcal{F}_{n-k}(\mathrm{v_s}) - i2\pi n \cdot \mathcal{F}_n(\psi \cdot \rho_{\mathrm{s}}), \tag{3.42}$$

with the indices n, k ranging within $I_N := \{-N, .., N\} \setminus \{0\}$. The eigenperturbations h were then approximated by the found eigenvectors $(h_n)_{n \in I_N} \in \mathbb{C}^{2N}$ as $h(\vartheta) \approx \sum_{n \in I_N} h_n \cdot e^{in2\pi\vartheta}$. The LAPACK library (Anderson et al. 1999) was used for the spectral analysis of $Q^{(N)}$. The Fourier components $\mathcal{F}_n(\mathrm{v_s})$ and $\mathcal{F}_n(\psi \cdot \rho_{\mathrm{s}})$ were calculated numerically. Further increasing N did not seem to have any noteworthy influence neither on the calculated leading eigenvalues, nor on the approximations of corresponding eigenperturbations. Furthermore, the results of this approach agree very well with those of the *exact* spectral analysis for the special case $D = 0$, described in section 3.4.2.

3.4.4 Integrating the Fokker-Planck equation

In order to better understand the behaviour of the network near stationary states and determine other possible attractors, the Fokker-Planck equation (1.12) was numerically integrated for both type I and type II iPRCs. Starting point was the so-called *spectral method* (see (Acebrón et al. 2005, §3.C) for a review on this approach to the Kuramoto model). The idea is to write the density $\rho(t, \vartheta)$ in the spectral form

$$\rho(t, \vartheta) = \sum_{n \in \mathbb{Z}} \rho_n(t) \cdot e^{in2\pi\vartheta}. \tag{3.43}$$

Inserting (3.43) into (1.12) yields the hierarchy of differential equations

$$\dot{\rho}_n(t) + \left[in2\pi\omega + (n2\pi)^2 D\right] \cdot \rho_n(t) + i \sum_{k \in \mathbb{Z}} \rho_k(t) \cdot n2\pi \sum_{m \in \mathbb{Z}} \mathcal{F}_{n-m}(\psi) \cdot \rho_m(t) = 0 \tag{3.44}$$

in the time-dependent Fourier components $(\rho_n)_{n \in \mathbb{Z}}$. A finite subset of the above hierarchy was numerically integrated, by ignoring any spectral components of order higher than a threshold $N \in \mathbb{N}$, that is, by assuming $\rho_n(t) = 0$ whenever $|n| > N$. The *spectral order* N was chosen large enough for $\sum_{|n| \le N/2} \rho_n(0) e^{in2\pi \cdot (\cdot)}$ and $\sum_{|n| \le N/2} \mathcal{F}_n(\psi) e^{in2\pi \cdot (\cdot)}$ to adequately represent the

initial density $\rho(0,\cdot)$ and iPRC $\psi(\cdot)$, respectively. Typical spectral orders were $N \gtrsim 100$. Further increasing N did not seem to have any notable effects on the observed density evolution. For the reduced hierarchy, an explicit integration scheme with fixed time step was used, based on a short-time propagator of second order in the time step, as described in appendix A.5. It should be mentioned that in the case $D > 0$, explicit fixed-time-step Runge–Kutta methods of order up to 4 turned out to be less efficient, requiring impractically small time steps to ensure a satisfactory accuracy. This stiffness of the system (Burden & Faires 2001, §5.11) can be traced back to the factor $n^2 D$, dominating the differential equation (3.44) for larger orders n. Typical time steps ranged between 2×10^{-4} and 2×10^{-5}. The integration was aborted as soon as the modulus of the marginal components $\rho_{\pm N}$ became larger than 10^{-4}. This was the case whenever narrow peaks appeared in the distribution $\rho(t,\cdot)$ and in fact only encountered for low noise strengths ($D/\omega \lesssim 10^{-5}$).

3.5 Type I iPRCs

3.5.1 Stationary states and stationary stimuli

For noise-free networks with symmetric type I iPRCs $\psi(\vartheta) = \frac{\psi_o}{2}[1 - \cos(2\pi\vartheta)]$, the stationary state equation (3.4) takes the form $\rho_s(0) = [1 + \psi_o \rho_s(0)/\omega]^{1/2}$ and yields the unique stationary stimulus

$$\rho_s(0) = \frac{\psi_o}{2\omega} + \sqrt{\left(\frac{\psi_o}{2\omega}\right)^2 + 1}. \tag{3.45}$$

Solving the stationary state equation for networks with noise or non-symmetric iPRCs turns out to be more difficult, which is why I resorted to numerical methods as described in section 3.4.1. Figure 3.3(a) shows typical stationary states in networks with symmetric, accelerating type I iPRCs and various noise strengths. For delaying, symmetric iPRCs, stationary states qualitatively follow a similar pattern, though with swapped minima and maxima. For non-symmetric iPRCs, stationary states change accordingly.

In view of the interpretation of the stimulus $\rho(t,0)$ as current *network activity*, special interest is devoted to the dependency of the stationary stimulus $\rho_s(0)$ on parameters like the coupling strength $|\psi_o|/\omega$ and noise strength D/ω. Figures 3.3(b) and 3.3(c) illustrate how $\rho_s(0)$ varies with these parameters for symmetric type I iPRCs. Figure 3.3(b) shows that for accelerating iPRCs, an increased oscillator coupling and a weaker noise lead to a higher stationary network activity. Figure 3.3(c) on the other hand shows that for delaying iPRCs, an increased coupling and a weaker noise lead to a lower stationary network activity. Similar relations were found to hold for non-symmetric type I iPRCs as well.

3.5.2 Stability of stationarity in noise-free networks

For noise-free networks with symmetric type I iPRCs, the eigenvalue equation (3.26) for the linearized dynamics at ρ_s can be treated analytically (see appendix A.4.4). As it turns out, the point spectrum is purely imaginary and given by

$$\sigma_p(\mathcal{Q}) = \left\{\lambda_n := \frac{i2\pi n}{T_s(1)} : n \in \mathbb{Z} \setminus \{0, \pm 1\}\right\} \cup \left\{\lambda_{\pm 1} := \pm i\omega 2\pi \cdot \sqrt{1 + \frac{\psi_o}{2\omega}\rho_s(0)}\right\}. \tag{3.46}$$

Compare this to the predictions of lemmas 3.3.1(2) and 3.3.2. Eigenperturbations h_n of *order* n corresponding to eigenvalues λ_n, are characterized by $|n|$ local maxima and $|n|$ local minima, in their real as well as imaginary parts. Each one can be interpreted as tending to split oscillators

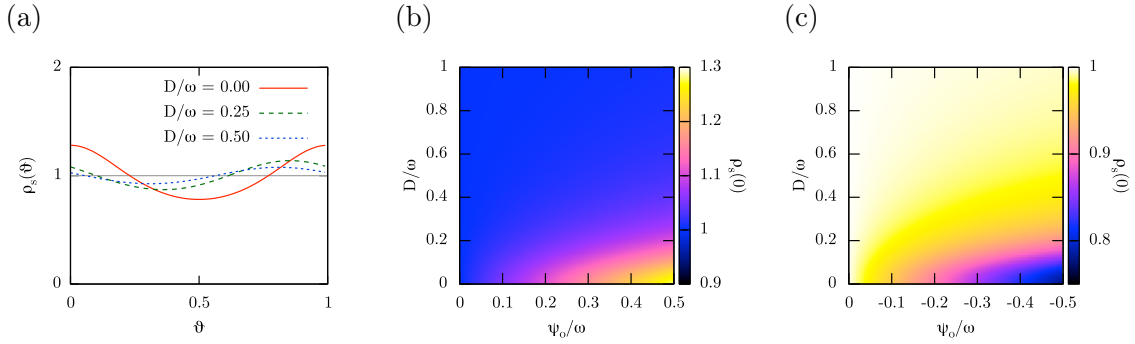

Figure 3.3: (a) Stationary states in networks with symmetric, accelerating type I iPRCs with coupling strength $|\psi_o|/\omega = 0.5$, for various noise strengths $D/\omega \in \{0, 0.25, 0.5\}$. The horizontal line represents the uniform distribution approached in the limit $D/\omega \to \infty$. (b) and (c): Illustration of stationary stimuli $\rho_s(0)$ for various coupling and noise strengths as colour maps for (b), accelerating and (c), delaying symmetric type I iPRCs. Note the different value ranges. The values of ψ_o/ω and D/ω are taken on a 100×100 uniform grid.

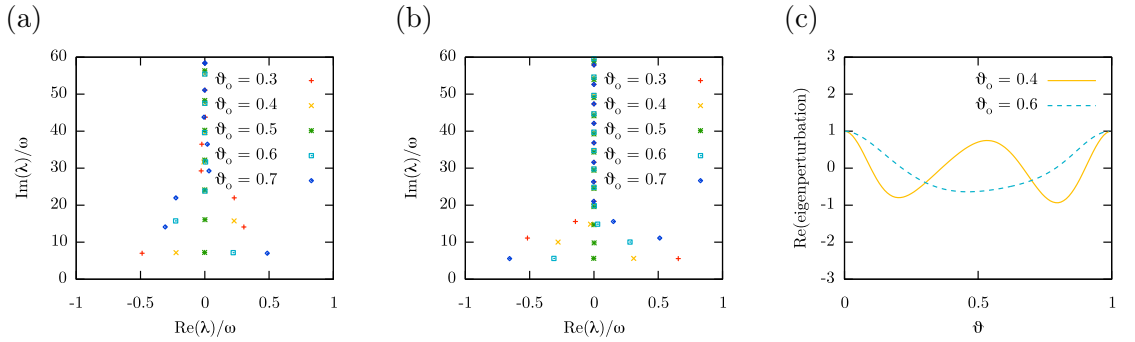

Figure 3.4: (a) and (b): Stability spectra of stationary states in noise-free networks with (a), accelerating and (b), delaying type I iPRCs, for various turning points $\vartheta_o \in \{0.3, 0.4, 0.5, 0.6, 0.7\}$. (c) Leading eigenperturbations (real part) of stationary states in noise-free networks with accelerating type I iPRCs, for various turning points ϑ_o. Leading eigenvalues are $\lambda \approx (0.23 + i \cdot 15.75) \cdot \omega$ (order 2) for $\vartheta_o = 0.4$ and $\lambda \approx (0.22 + i \cdot 7.18) \cdot \omega$ (order 1) for $\vartheta_o = 0.6$. Eigenperturbations are scaled to have value 1 at the origin. Their imaginary part is of similar shape as their real part. Coupling strength is $|\psi_o|/\omega = 0.5$ in all cases.

into $|n|$ synchronized groups. As all eigenvalues and eigenperturbations appear in complex-conjugate pairs, only eigenvalues with non-negative imaginary parts shall be considered from now on.

Since all eigenvalues have zero real part, stationary states in noise-free networks with symmetric type I iPRCs are only (linearly) neutrally stable. As it turns out though, the point spectrum ceases to be purely imaginary as soon as $\vartheta_o \neq 0.5$. In fact for both $\vartheta_o < 0.5$ and $\vartheta_o > 0.5$ some eigenvalues move to the open right half plane, leading to the instability of stationary states. Figures 3.4(a) and (b) show the computed spectra for $|\psi_o|/\omega = 0.5$ and different turning points ϑ_o. Figures 3.5(a) and (b) further illustrate the dependency of the real part of eigenvalues on the turning point ϑ_o. Figure 3.4(c) shows typical leading eigenperturbations in networks with accelerating type I iPRCs. As can be seen, these differ qualitatively for the cases $\vartheta_o < 0.5$ and $\vartheta_o > 0.5$. A similarly abrupt change of leading eigenvalue order also appears for delaying type I iPRCs. As an integration of the Fokker-Planck equation (1.12) reveals, this difference is correlated to a bifurcation in the long term behaviour of the network as ϑ_o traverses the value 0.5. The Fokker-Planck equation was integrated numerically as described in section 3.4.4 for $\vartheta_o \in \{0.3, 0.4, 0.6, 0.7\}$ and $|\psi_o|/\omega \in \{0.1, 0.5\}$. Small perturbations $h \in \mathcal{C}^2_{\mathrm{zm}}(S^1)$ of the stationary state ("small" referring to magnitudes $\|h\|_\infty \approx 0.01$) result in the network splitting up into n oscillator groups, with n being the order of the leading eigenvalue λ_n (e.g. two for $\vartheta_o \lesssim 0.5$,

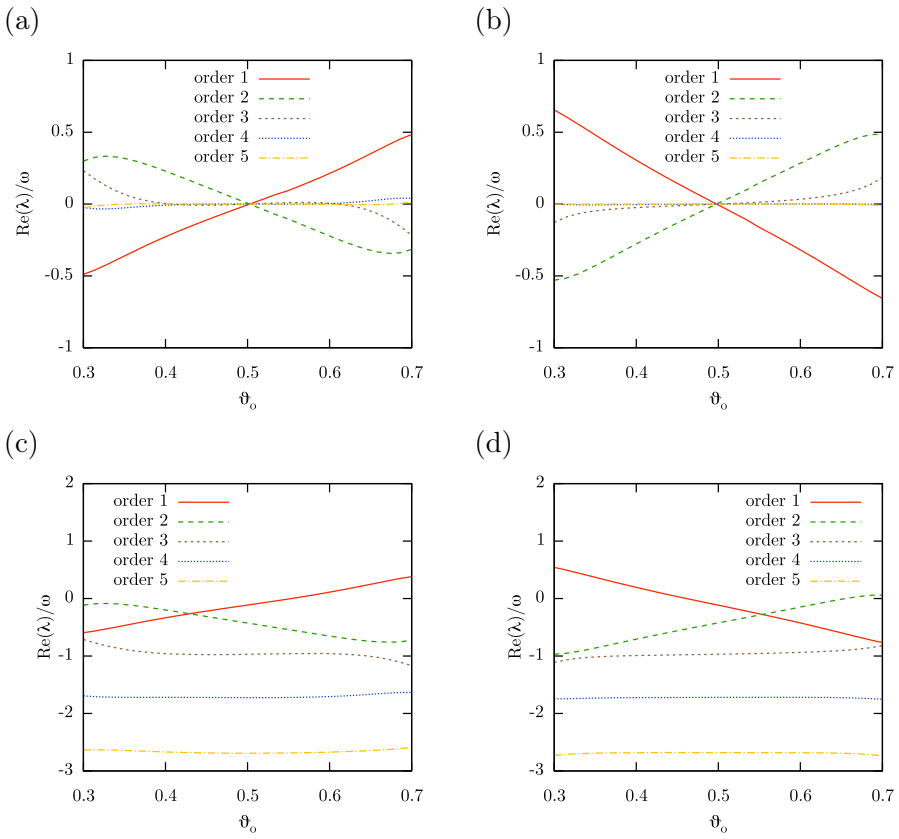

Figure 3.5: Real parts of low-order eigenvalues for type I iPRCs (accelerating in left column, delaying in right column) over varying turning points ϑ_o and for two different noise strengths ($D = 0$ in top row and $D/\omega = 0.0025$ in bottom row). Only the first 5 eigenvalue orders (including the leading ones) are displayed. Increasing the noise shifts all eigenvalues to the left half plane (lower real part), at a rate increasing with the eigenvalue order. Coupling strength is $|\psi_o|/\omega = 0.5$, but similar results have been found for all coupling strengths $|\psi_o|/\omega \in \{0.1, 0.2, .., 0.5\}$.

$\psi_o/\omega = 0.5$ and one for $\vartheta_o \gtrsim 0.5$, $\psi_o/\omega = 0.5$). Eventually, the network settles on a stable limit cycle, on which all oscillators in each of these n equally sized groups are in total synchrony. This splitting of the network into successively firing oscillator groups, results in an oscillation of the network stimulus at a frequency near $\Im(\lambda_n)/(2\pi)$. This limit cycle is approached from all tested perturbations, which included stable and unstable eigenperturbations (or better, numerical approximations of them) up to order 5 as well as random harmonic perturbations of order up to 10. In fact, initial distributions near the uniform one or of a Gaussian nature were also found to eventually converge to this limit cycle, indicating a large basin of attraction. It shall therefore be referred to as the *main attractor*. Figure 3.6(a) shows the results of such a simulation for $\vartheta_o = 0.4$ and $\psi_o/\omega = 0.5$. It demonstrates the splitting of the network into two oscillator groups, within each of which the oscillators tend to synchronize perfectly. Figure 3.6(b) shows the evolution of the corresponding network stimulus, oscillating at an ever increasing amplitude and a frequency approaching $\Im(\lambda_2)/(2\pi)$.

3.5.3 Stability of stationarity in noisy networks

Increasing noise from zero distorts the main attractor, *smoothening* each of the density peaks as noise prevents the emergence of exact synchrony. The width of these peaks increases with increasing noise. Nonetheless, on that attractor the network's stimulus still oscillates at a frequency of approximately $\Im(\lambda_n)/(2\pi)$, with λ_n being the leading eigenvalue at stationarity. The

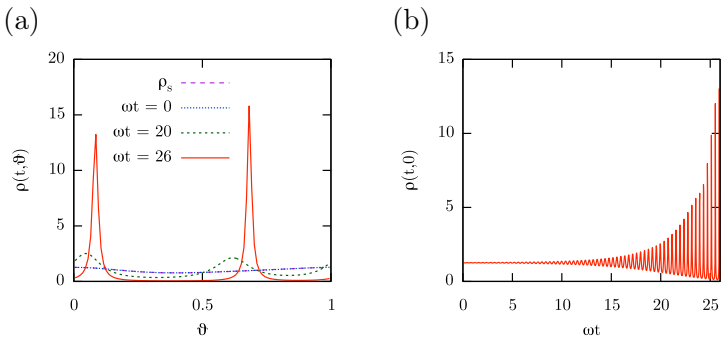

Figure 3.6: (a) Evolution of perturbed stationary state in networks with accelerating type I iPRCs with turning point $\vartheta_o = 0.4$ and zero noise. Perturbation was real part of leading eigenperturbation ($\lambda_2 \approx (0.23 + i \cdot 15.75) \cdot \omega$, order 2) with perturbation stimulus 0.01. Note that the initial and stationary densities seemingly overlap in the graphic. (b) Evolution of the corresponding network stimulus. The network's stimulus eventually oscillates at a frequency $(2.52 \pm 0.05) \cdot \omega \approx \Im(\lambda_2)/(2\pi)$. Coupling strength is $\psi_o/\omega = 0.5$. The Fokker-Planck equation was integrated as described in section 3.4.4 at spectral order 300 and time step $2 \times 10^{-5}\ \omega^{-1}$. Integration was aborted at time $t = 26\ \omega^{-1}$, as the phase density could no longer be adequately spectrally represented by the given order.

attractor's basin of attraction seems to include a neighbourhood of the stationary state (excluding the latter), as all tested perturbations resulted in an eventual settlement on the limit cycle. The latter is also approached when starting from other distributions, such as the uniform one or of a Gaussian nature, though in some cases after a transition close to stationarity. Figures 3.7(a), (b) and (c) show some typical simulation results for a specific accelerating type I iPRC, a fixed noise strength and for various initial distributions. Figures 3.7(d), (e) and (f) show the evolution of the corresponding network stimuli. As can be seen, in all cases the network eventually splits into two approximately equally sized oscillator groups, with two being the order of the leading eigenvalue. These persist for as long as simulations were run (at least 10 times the time periods displayed).

At a particular threshold noise strength, the main attractor merges with the network's stationary state. This point coincides with the local stabilisation of stationarity, suggesting the occurrence of a supercritical Hopf bifurcation. The exact bifurcation noise strength strongly depends on ψ_o/ω and ϑ_o, but for $|\psi_o|/\omega = 0.5$ its order of magnitude ranges between 10^{-3} and 10^{-2}. Figure 3.8 shows the results of an example integration of the Fokker-Planck equation for networks with non-symmetric accelerating type I iPRCs, with sufficiently strong noise so that stationarity has become locally stable.

Figures 3.5(c) and (d) show the stability spectra (real parts) of stationary states in networks with accelerating and delaying type I iPRCs respectively, over varying turning points ϑ_o and for non-zero noise. They show how all eigenvalues move towards the left half plane as noise is increased, a behaviour to be expected based on the simulation results described above. This effect is further illustrated in figures 3.9(a) and (b), which show the real part of leading eigenvalues over varying coupling and noise strengths, for accelerating and delaying type I iPRCs respectively and a fixed iPRC turning point $\vartheta_o = 0.4$. As can be seen, stationarity becomes linearly stable provided that noise exceeds a certain threshold that increases with the coupling strength. These results are complemented by numerical integration of the Fokker-Planck equation (1.12). Figures 3.9(c) and (d) show the final (that is, after a certain fixed time) distance of the network state to stationarity for accelerating and delaying type I iPRCs respectively, over varying coupling and noise strengths and the same turning point ϑ_o. The initial distribution in these simulations was the uniform one, but similar results have been obtained for other initial distributions (e.g. wrapped normal (Mardia & Jupp 2000, §3.5.7) with variance $\sigma^2 = 4 \times 10^{-4}$) as well. Notice the narrow transition bands between orders of magnitude in the final distance to stationarity across

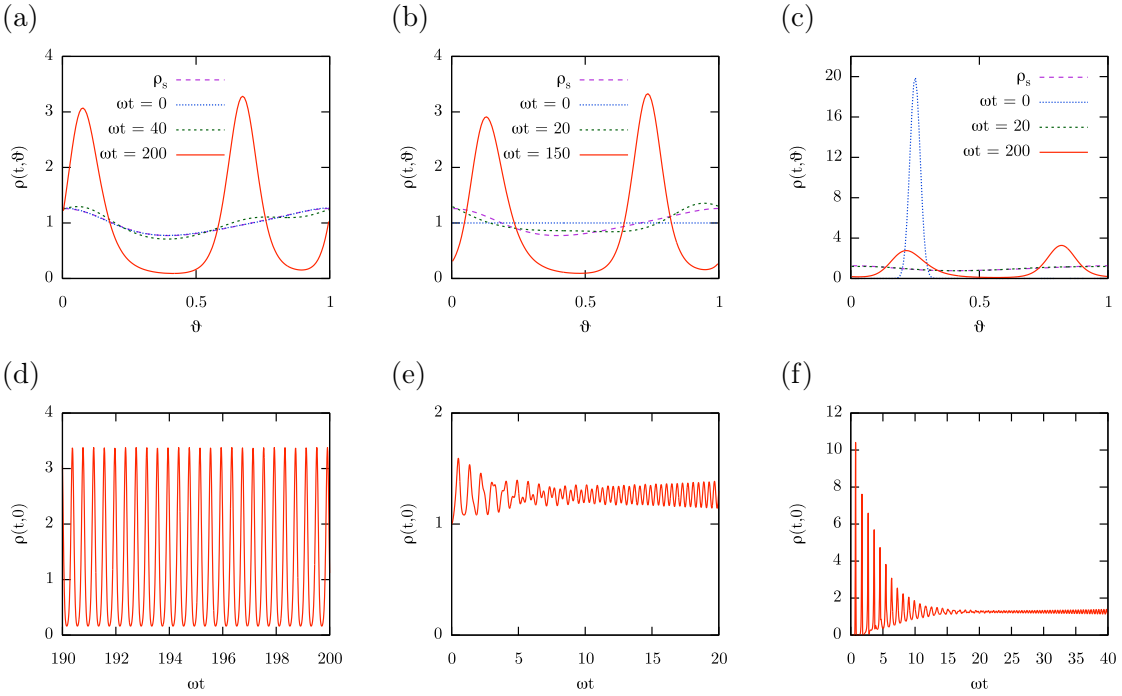

Figure 3.7: Example integration of the Fokker-Planck equation for accelerating type I iPRCs with turning point $\vartheta_o = 0.4$, weak noise and for various initial distributions. Top row: Evolution of the phase density. Bottom row: Evolution of the stimuli (only partially displayed) corresponding to the simulation illustrated on their respective top. (a) and (d): Initial distribution was perturbed stationary state. Perturbation was real part of leading eigenperturbation ($\lambda_2 \approx (0.051 + i \cdot 15.75) \cdot \omega$, order 2) with perturbation stimulus 0.01. (b) and (e): Initial distribution was uniform one. (c) and (f): Initial distribution was wrapped normal distribution with variance $\sigma^2 = 4 \times 10^{-4}$. In all cases stimuli eventually approach the form shown in (d), oscillating at a frequency $(2.51 \pm 0.05) \cdot \omega \approx \Im(\lambda_2)/(2\pi)$. Note that in (a) the initial and stationary densities seemingly overlap. The same is true for the intermediate and stationary densities in (c). Also note the different density scales in (c) compared to (a) and (b). Coupling strength and noise strength are $\psi_o/\omega = 0.5$ and $D/\omega = 10^{-3}$ respectively. The Fokker-Planck equation was integrated as described in section 3.4.4 at spectral order 150 and time step $2 \times 10^{-4}\ \omega^{-1}$.

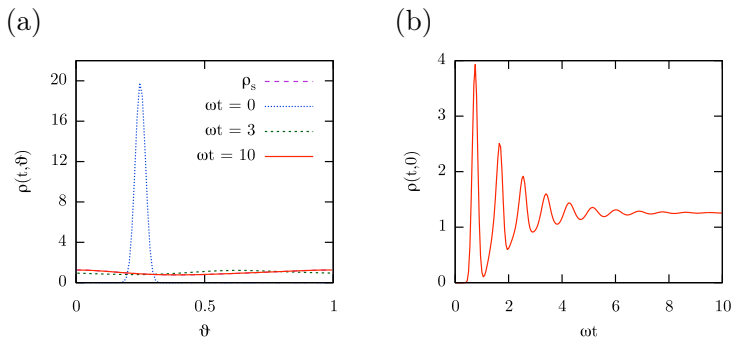

Figure 3.8: Example integration of the Fokker-Planck equation for networks with accelerating type I iPRCs with turning point $\vartheta_o = 0.4$ and strong noise. Initial distribution was wrapped normal distribution with variance $\sigma^2 = 4 \times 10^{-4}$. (a) Evolution of the phase density. (b) Evolution of the network stimulus. Note that in (a) the final and stationary densities seemingly overlap. A similar asymptotic behaviour was observed for all other tested initial densities (e.g. bimodal and uniform) as well. Coupling strength and noise strength are $\psi_o/\omega = 0.5$ and $D/\omega = 0.01$ respectively. The Fokker-Planck equation was integrated as described in section 3.4.4 at spectral order 150 and time step $2 \times 10^{-4}\ \omega^{-1}$.

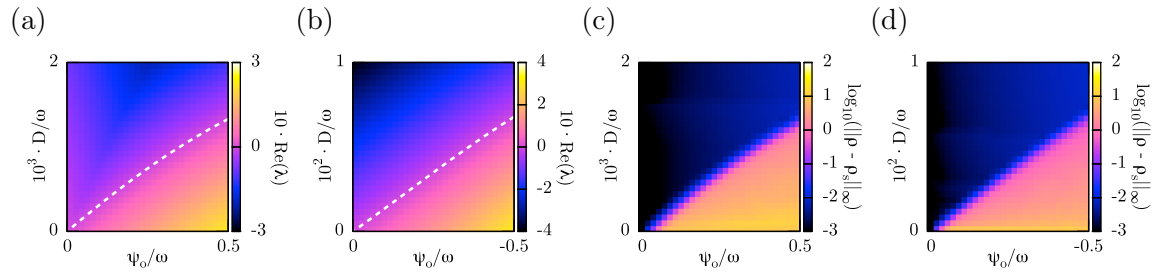

Figure 3.9: (a) and (b): Real part of the leading eigenvalues of linearized dynamics at stationary states, over various coupling and noise strengths. IPRCs are (a), accelerating and (b), delaying type I iPRCs with turning point $\vartheta_o = 0.4$. The white dashed contour is at level zero. Note the different noise scales. In (a) the leading eigenvalue is, at least in the unstable parameter range, of order 2. In (b) the leading eigenvalue is in the whole parameter range of order 1. (c) and (d): Supremum distance (logarithmic scale) of phase density at time $t = 200\ \omega^{-1}$ from stationarity, after integration of the Fokker-Planck equation (1.12) starting from a uniform distribution. IPRCs are in (c) as in (a), in (d) as in (b). Integration time step was $2.5 \times 10^{-4}\ \omega^{-1}$, spectral order was 100. The supremum distance is evaluated on a uniform grid of size 100. The values of the parameters ψ_o/ω and D/ω vary in all four maps on a 30×30 uniform grid.

these maps. These bands closely resemble the transition boundaries in figures 3.9(a) and (b) between linear stability and instability. This suggests that the local stability of stationarity goes along with its global stability. Similar spectra and simulation results have been obtained for all iPRC turning points $\vartheta_o \in \{0.3, 0.4, 0.6, 0.7\}$.

3.6 Type II iPRCs

3.6.1 Stationary states and stationary stimuli

For noise-free networks with symmetric type II iPRCs $\psi(\vartheta) = -\psi_o \cdot \sin(2\pi\vartheta)$, the stationary state equation (3.4) takes the form $\rho_s(0) = \left[1 - (\psi_o \rho_s(0)/\omega)^2\right]^{1/2}$ and has the unique solution

$$\rho_s(0) = \left[1 + (\psi_o/\omega)^2\right]^{-1/2}. \tag{3.47}$$

Stationary states in networks with non-symmetric type II iPRCs or non-zero noise had to be calculated numerically as described in section 3.4.1. Figure 3.10(a) shows some typical stationary states in networks with attracting, symmetric type II iPRCs for various noise strengths. For repulsing, symmetric iPRCs, stationary states qualitatively follow a similar pattern, though with swapped minima and maxima. For non-symmetric iPRCs, stationary states change accordingly. Figures 3.10(b) and (c) illustrate how the stationary stimulus varies with the coupling and noise strengths in networks with symmetric type II iPRCs. Figure 3.10(b) shows that for attracting iPRCs, the network's activity depends (for fixed coupling strength) non-linearly on the noise strength. In fact, a maximum is attained at a non-trivial noise level, an effect that can be interpreted as a *resonance* between the network's dynamics and noise. Figure 3.10(c) shows that for repulsing type II iPRCs, the network's activity depends on the coupling and noise strength in a comparable way. The difference is that the stationary stimulus actually attains (for fixed coupling strength) its minimum at a certain non-trivial noise strength. Similar relations were found to hold for non-symmetric type II iPRCs as well.

3.6.2 Spectral stability analysis of stationarity

For noise-free networks with symmetric type II iPRCs, the eigenvalue equation (3.26) for the linearized dynamics at ρ_s can be solved analytically (see appendix A.4.5), yielding the point

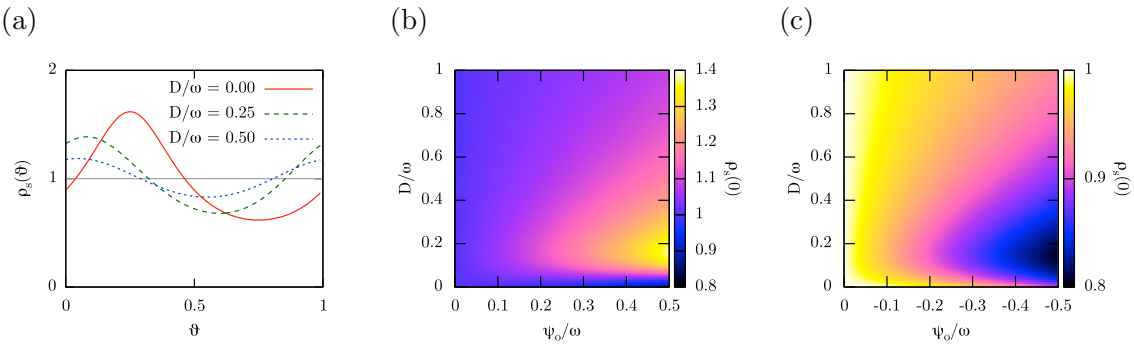

Figure 3.10: (a): Stationary states in networks with attracting, symmetric type II iPRCs with coupling strength $|\psi_o|/\omega = 0.5$ and various noise strengths $D/\omega \in \{0, 0.25, 0.5\}$. The horizontal line represents the uniform distribution approached in the limit $D/\omega \to \infty$. (b) and (c): Illustration of stationary stimuli $\rho_s(0)$ for various coupling and noise strengths as colour maps for (b), attracting and (c), repulsing, symmetric type II iPRCs. Note the different value ranges. The values of ψ_o/ω and D/ω are taken on a 100×100 uniform grid.

spectrum

$$\sigma_p(\mathcal{Q}) = \left\{ \lambda_n := \frac{i2\pi n}{T_s(1)} : n \in \mathbb{Z} \setminus \{0, \pm 1\} \right\} \cup \left\{ \lambda_{\pm 1} := \pi \left[\psi_o \rho_s(0) \pm \sqrt{\psi_o^2 \rho_s^2(0) - 4\omega^2} \right] \right\}. \quad (3.48)$$

All but two (complex conjugate) eigenvalues are purely imaginary, with those two being located on the open right half plane if $\psi_o > 0$ and on the open left half plane if $\psi_o < 0$. The stationary state ρ_s is therefore unstable if $\psi_o > 0$ and (linearly) neutrally stable if $\psi_o < 0$.

It is worth mentioning that the two eigenvalues given in (3.48) having non-zero real part can also be obtained by the special ansatz

$$h(\vartheta) = \frac{1}{v_s^2(\vartheta)} \cdot [a + b\cos(2\pi\vartheta) + c\sin(2\pi\vartheta)] \quad (3.49)$$

for the eigenperturbation h. Here v_s is the stationary velocity introduced in lemma 3.3.1. The corresponding eigenvalue $0 \neq \lambda \in \mathbb{C}$ as well as the constants $a, b, c \in \mathbb{C}$ are determined by the eigenvalue equation $\mathcal{Q}h = \lambda h$. Note that, provided the latter is satisfied, h is indeed in $\mathcal{C}^1_{zm}(S^1)$ since $\mathcal{Q}$ maps $\mathcal{C}^1(S^1)$ into $\mathcal{C}_{zm}(S^1)$. This ansatz was proposed by Ariaratnam (2002, §4.8) for the linear stability analysis of stationary states in the Winfree model with pulses of the shape $I(\vartheta) = 1 + \cos(\vartheta)$. As it turns out, it works equally well for Dirac pulses. It is straightforward to find that

$$a = \frac{h(0) \cdot (\psi_o \omega 2\pi \rho_s(0))^2}{(2\pi\rho_s(0)\psi_o)^2 - \lambda^2 - (2\pi\omega)^2}, \quad b = -\frac{a\lambda}{2\pi\psi_o\rho_s(0)}, \quad c = -\frac{a\omega}{\psi_o\rho_s(0)}, \quad (3.50)$$

and eventually

$$\lambda = \pi \left[\psi_o \rho_s(0) \pm \sqrt{\psi_o^2 \rho_s^2(0) - 4\omega^2} \right], \quad (3.51)$$

in agreement with the point spectrum in (3.48).

Unfortunately, the ansatz (3.49) yields an analytical expression for only two (complex conjugate) eigenperturbations and only for noise-free networks with symmetric iPRCs. For all other cases the spectral stability analysis had to be done numerically, as described in sections 3.4.2 and 3.4.3. Figures 3.11(a) and (b) show typical stability spectra of stationary states in noise-free networks with attracting and repulsing type II iPRCs respectively. They are supplemented by figures 3.12(a) and (b), which show the explicit dependency of these spectra (real part) on the turning point ϑ_o. These figures show that for non-symmetric iPRCs ($\vartheta_o \neq 0.5$) there is always

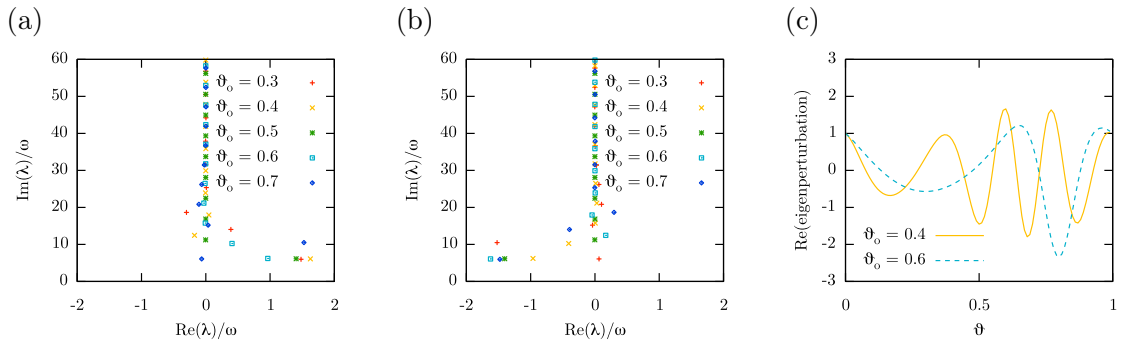

Figure 3.11: (a) and (b): Stability spectra of stationary states in noise-free networks with (a), attracting and (b), repulsing type II iPRCs, for various turning points $\vartheta_o \in \{0.3, 0.4, 0.5, 0.6, 0.7\}$. (c) Leading eigenperturbations (real part) of stationary states in noise-free networks with repulsing type II iPRCs, for various turning points ϑ_o. Leading eigenvalues are $\lambda \approx (0.03 + i \cdot 21.16) \cdot \omega$ (order 4) for $\vartheta_o = 0.4$ and $\lambda \approx (0.17 + i \cdot 12.45) \cdot \omega$ (order 2) for $\vartheta_o = 0.6$. Eigenperturbations are scaled to have value 1 at the origin. Their imaginary part is of similar shape as their real part. Coupling strength is in all cases $|\psi_o| / \omega = 0.5$.

at least one eigenvalue moving to the open right half plane. This shows that stationary states are unstable for all attracting iPRCs, unstable for all non-symmetric, repulsing iPRCs and (linearly) neutrally stable for symmetric, repulsing iPRCs. Also note that the bifurcation occurring at $\vartheta_o \approx 0.5$ is a multiple one, in the sense that multiple (non-conjugate) eigenvalues cross the imaginary axis in different directions. Eigenperturbations corresponding to eigenvalues of order $n \in \mathbb{N}$ have been found to be characterized by n local maxima and n local minima. Figure 3.11(c) shows typical eigenperturbations for noise-free networks with repulsing type II iPRCs. Notice the qualitative difference between the leading eigenperturbations for $\vartheta \lesssim 0.5$ and $\vartheta \gtrsim 0.5$, traced back to their different orders. This is not the case for attracting type II iPRCs, as the leading eigenvalue of order 1 dominates for all turning points close enough to 0.5, at least within the range $[0.4, 0.6]$.

Just as with type I iPRCs, an increased noise eventually results in the local stabilization of stationarity. This is illustrated in figures 3.12(c) and (d), which show the stability spectra (real part) in networks with type II iPRCs over varying turning points and non-zero noise. As can be seen, eigenvalues move to the left half plane as noise is increased, with higher order eigenvalues moving faster than lower order ones. Nonetheless the qualitative shape of eigenperturbations is maintained, at least up to order 5 and as long as they are unstable.

3.6.3 Stability analysis of stationarity by numerical simulation

The stability of stationarity as well as the long-term behaviour of networks have been tested by integrating the Fokker-Planck equation (1.12) as described in section 3.4.4. Parameter values considered are $\vartheta_o \in \{0.3, 0.4, 0.6, 0.7\}$ (as well as $\vartheta_o = 0.5$ for attracting iPRCs), $|\psi_o| / \omega \in \{0.1, 0.5\}$ and $D/\omega \in [0, 1]$. The local stability of stationarity has been tested against leading eigenperturbations h (real part) chosen so small that $\|h\|_\infty \approx 0.01$. Other perturbations applied included random harmonic ones of orders up to 10 with similar amplitudes. Simulations reproduced the predictions of the linear stability analysis.

The observed long-term network behaviour is similar to the one for type I iPRCs. More precisely, the existence of a stable limit cycle (henceforth referred to as the *main attractor*) was found, on which the network's state is characterized by a number (henceforth referred to as the *order* of the attractor) of approximately synchronized and approximately equally sized oscillator groups. These groups succeed each other in firing and cause the network's stimulus to oscillate at a constant amplitude and frequency. The level of synchronization within each of these groups

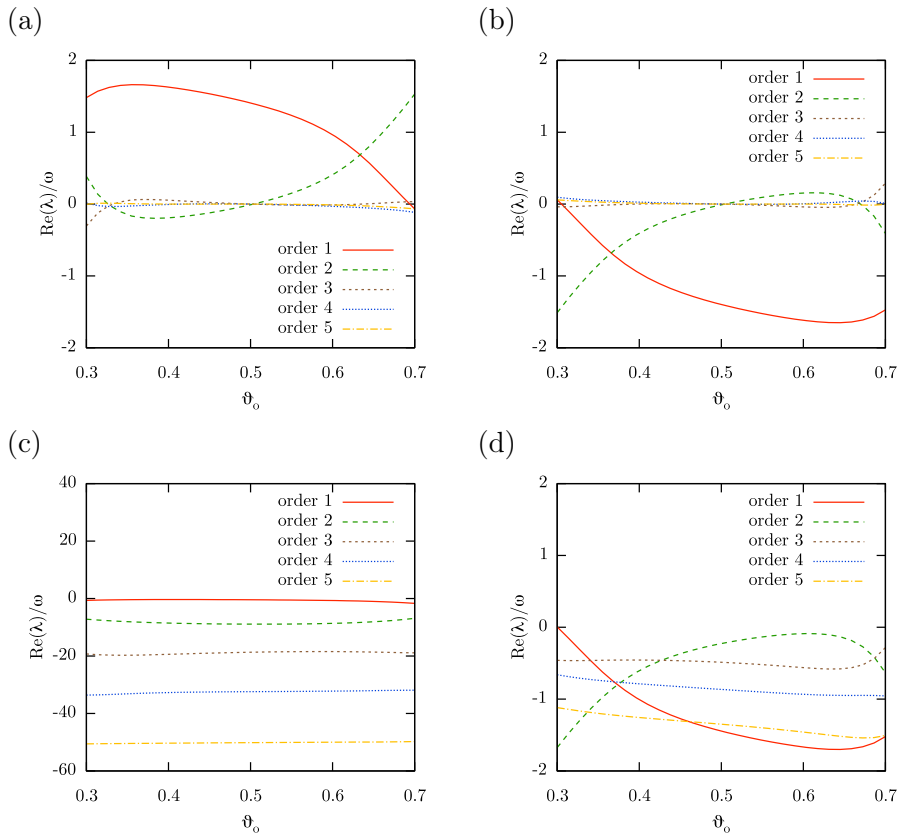

Figure 3.12: Real parts of low-order eigenvalues for type II iPRCs (attracting in left column, repulsing in right column) over varying turning points ϑ_o and for different noise strengths ($D = 0$ in (a) and (b), $D/\omega = 0.05$ in (c) and $D/\omega = 0.001$ in (d)). Only the first 5 eigenvalue orders (including the leading ones) are displayed. Increasing the noise pushes all eigenvalues further to the left half plane (lower real part), at a rate increasing with the eigenvalue order. Coupling strength is $|\psi_o|/\omega = 0.5$, but similar results have been obtained for all coupling strengths $|\psi_o|/\omega \in \{0.1, 0.2, .., 0.5\}$.

increases as noise is reduced. In noise-free networks the main attractor is characterized by a number of perfectly synchronized, equally sized oscillator groups. Simulations indicate that its basin of attraction includes a neighbourhood of the stationary state (excluding the latter) and in certain cases, the uniform distribution as well. The order of the main attractor was found to be equal to the order of the leading stationarity eigenperturbation for attracting iPRCs. For repulsing iPRCs this is true for most but not all cases. When noise strength exceeds a certain threshold, the main attractor merges with the stationary state. This noise threshold coincides with the point at which stationarity becomes linearly stable, that is, the leading eigenvalues have crossed the imaginary axis to the left, as is characteristic for a supercritical Hopf bifurcation.

Figure 3.13 shows typical simulation results for networks with symmetric, attracting type II iPRCs and various noise strengths, starting close to stationarity. In the unstable cases (figures 3.13(a) and (b)) the leading eigenvalue is of order 1, reflected in the fact that oscillators tend to form a single, more or less synchronized cluster. For sufficiently strong noise stationarity becomes locally stable (figure 3.13(c)).

Figure 3.14 shows analogous simulation results for networks with certain non-symmetric, repulsing type II iPRCs and various noise strengths. In the unstable cases (figures 3.14(a) and (b)) the leading eigenvalue is of order 4 and oscillators tend to form four, more or less synchronized clusters. Again, for noise strong enough (figure 3.14(c)) stationarity becomes locally stable.

Figures 3.15(a) and (b) show the real part of leading eigenvalues in networks with attracting and repulsing type II iPRCs respectively, over various coupling and noise strengths and for a

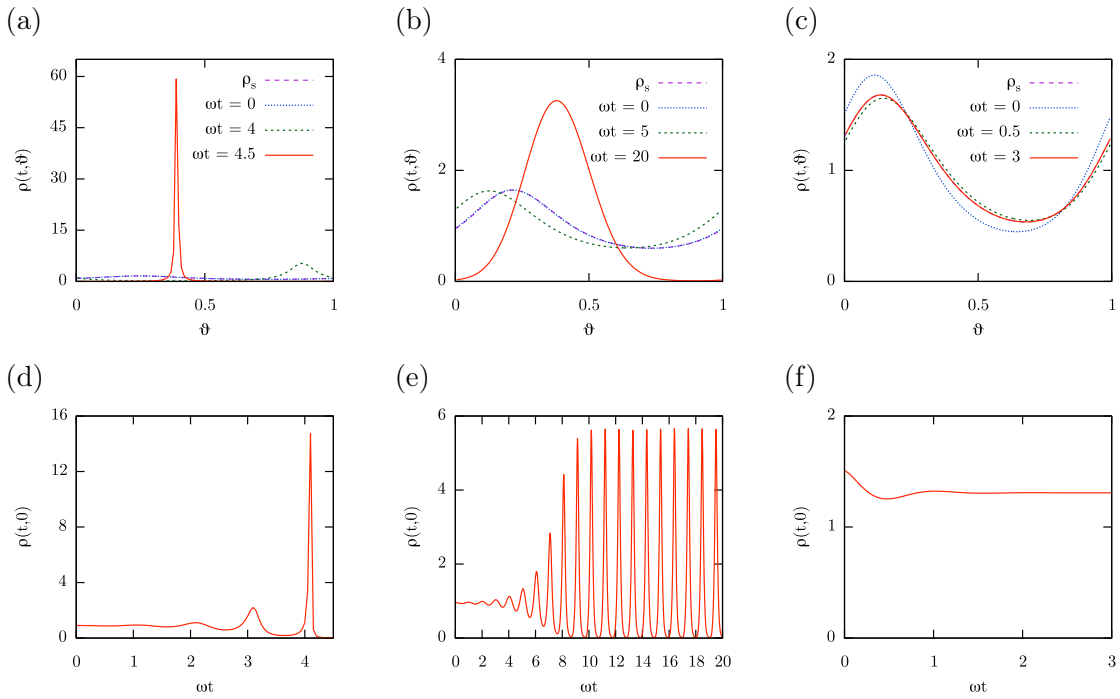

Figure 3.13: Top row: Evolution of perturbed stationary states in networks with symmetric, attracting type II iPRCs for three different noise strengths. Bottom row: Evolution of the stimuli corresponding to the simulation illustrated on their respective top. Noise strength is $D/\omega = 0$ in (a), $D/\omega = 0.02$ in (b) and $D/\omega = 0.1$ in (c). Perturbation was the real part of the leading eigenperturbation (of order 1 in all 3 cases). Perturbation stimuli were 0.01 in (a) and (b), 0.2 in (c). Note that in (a) and (b) the initial and stationary densities seemingly overlap. The same is true for the final and stationary densities in (c). Coupling strength is $|\psi_o|/\omega = 0.5$ in all cases. The Fokker-Planck equation was integrated as described in section 3.4.4 at spectral order 400 with time step $10^{-5}\ \omega^{-1}$ for (a) and at spectral order 200 with time step $2 \times 10^{-4}\ \omega^{-1}$ for (b) and (c).

turning point $\vartheta_o = 0.4$. They demonstrate the fact that increasing noise (while keeping the coupling strength fixed) eventually leads to the local stabilization of stationarity. Nonetheless, the dependence of the corresponding noise threshold on the coupling strength (let alone the whole iPRC) is not at all trivial, as can be seen in figure 3.15(b). These results are complemented by numerical integration of the Fokker-Planck equation (1.12). Figures 3.15(c) and (d) show the final (that is, after a fixed integration time) distance of the network state to stationarity for attracting and repulsing iPRCs respectively, over varying coupling and noise strengths and the same turning point ϑ_o. The initial distribution in these simulations was the uniform one, but similar results have been found for other initial distributions (e.g. wrapped normal with variance $\sigma^2 = 4 \times 10^{-4}$) as well. Notice the narrow transition bands between orders of magnitude in the final distance to stationarity. These bands closely resemble the transition boundaries in figures 3.15(a) and (b) between linear stability and instability of stationarity. This suggests that local stability of stationarity goes along with its global stability. Similar maps and simulation results have been obtained for all iPRC turning points $\vartheta_o \in \{0.3, 0.4, 0.6, 0.7\}$ (as well as $\vartheta_o = 0.5$ for attracting iPRCs).

3.6.4 Multiplicity of attractors

It is noteworthy that for certain attracting type II iPRCs and a non-trivial noise range, a second limit cycle has been found to coexist along with the main attractor described above. This is in particular the case for networks with $\vartheta_o = 0.7$, $\psi_o/\omega = 0.5$ and $D/\omega \in [0, 0.004]$, for which the

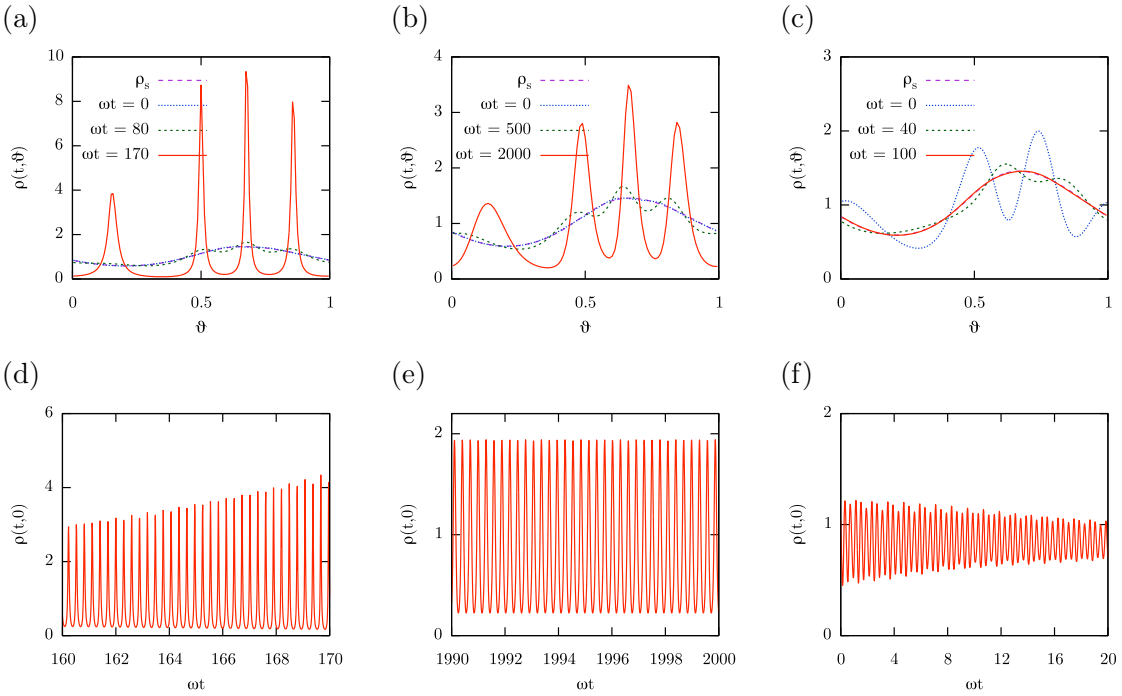

Figure 3.14: Top row: Evolution of perturbed stationary states in networks with repulsing type II iPRCs with turning point $\vartheta_o = 0.4$, for three different noise strengths. Bottom row: Evolution of the stimuli corresponding to the simulation illustrated on their respective top. Noise strengths are (a), $D/\omega = 0$, (b), $D/\omega = 3 \times 10^{-5}$ and (c), $D/\omega = 10^{-4}$. Perturbations were real part of leading eigenperturbations (of order 4 in (a) and (b), order 3 in (c)). Perturbation stimuli were 0.01 in (a) and (b), 0.2 in (c). Note that in (a) and (b) the initial and stationary densities seemingly overlap. The same is true for the final and stationary densities in (b). Coupling strength is $|\psi_o| /\omega = 0.5$. The Fokker-Planck equation was integrated as described in section 3.4.4 at spectral order 200 and time step $10^{-4}\ \omega^{-1}$.

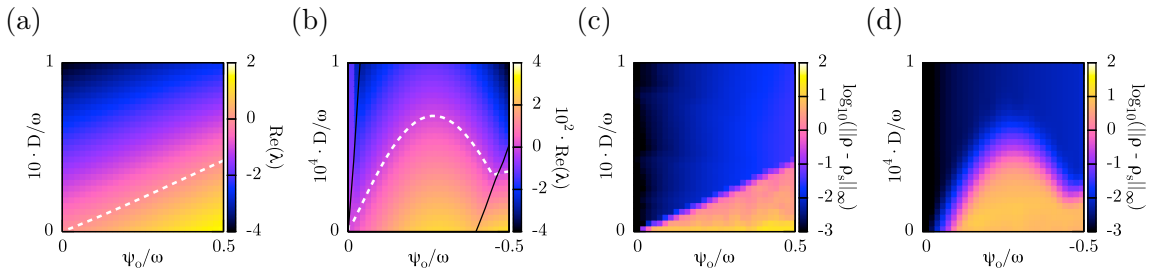

Figure 3.15: (a) and (b): Real part of the leading eigenvalues of linearized dynamics at stationary states over varying coupling and noise strength. IPRCs are (a), attracting and (b), repulsing type II iPRCs with turning point $\vartheta_o = 0.4$. The white dashed contour is at level zero. Note the different noise scales. In (a) the leading eigenvalue is of order 1 in the whole parameter range. In (b) the black contours separate the regions where the leading eigenvalue has order 2 (left-most region), order 3 (centre region) and order 4 (right-most region). (c) and (d): Supremum distance (logarithmic scale) of distribution at time $t = 500\ \omega^{-1}$ from stationary one, after integration of the Fokker-Planck equation (1.12) starting from a uniform distribution. IPRCs are (c), as in (a) and (d), as in (b). Integration time step was $2.5 \times 10^{-4}\ \omega^{-1}$, spectral order was 100. The supremum distance is evaluated on a uniform grid of size 100. The values of the parameters ψ_o/ω and D/ω vary in all figures on a 30×30 uniform grid.

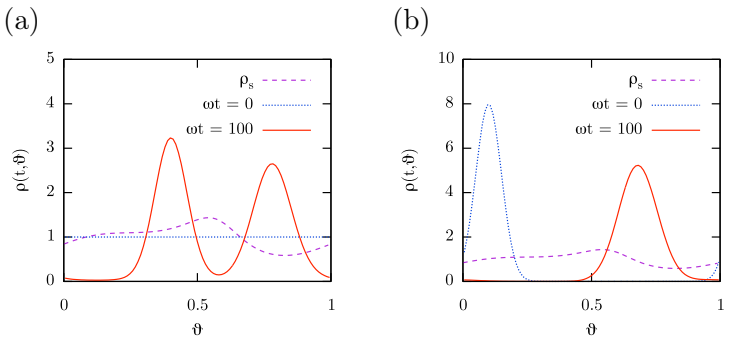

Figure 3.16: Coexistence of two locally stable limit cycles for networks with certain attracting type II iPRCs (see final remark of section 3.6). Both figures show the evolution of the phase density, after an integration of the Fokker-Planck equation (1.12). (a) Network state is initially uniform distribution, eventually settling on the main attractor. The latter is characterized by two approximately synchronized oscillator groups. (b) Phase density is initially wrapped normal one of variance $\sigma^2 = 2 \times 10^{-3}$, eventually settling on the secondary attractor. The latter is characterized by an approximate network synchrony. The purple dashed graph in both figures represents the stationary state for comparison. Parameters are $|\psi_o| / \omega = 0.5$, $\vartheta_o = 0.7$ and $D/\omega = 0.004$. Spectral integration order was 100 with time step $2 \times 10^{-4}\ \omega^{-1}$.

leading stationarity eigenperturbation as well as the main attractor are of order 2. Simulations have revealed the existence of a limit cycle, on which oscillators form a single, more or less synchronized group. On this *secondary attractor* of *order* 1, the extent of synchrony increases as noise is decreased. In particular for zero noise, all oscillators are synchronized and the phase density is formally a time-dependent Dirac distribution. The uniform distribution still lies in the interior of the main attractor's basin of attraction, which also includes a neighbourhood of the stationary state (excluding the latter). On the other hand, unimodal distributions of an adequately small variance (e.g. wrapped normal with variance $\sigma^2 \lesssim 0.002$) are included in the basin of attraction of the secondary attractor. Compare these findings to theorem 2.4.4 for $\#X = 1$, by which network synchrony is indeed predicted to be locally stable, provided the oscillator pulse (in that theorem assumed to be continuous) is adequately concentrated at the origin. The secondary attractor vanishes when noise is strong enough, at a noise level lower than the one needed to destroy the main attractor. See figure 3.16 for an illustration of the main and secondary attractors in networks with the above parameter values. These findings suggest that secondary attractors might exist for other iPRCs as well, at least for noise weak enough. Under which conditions this is the case, and whether they always disappear before the main attractor as noise is increased, remains to be investigated.

3.7 Comparing the Fokker-Planck and Langevin equations

As described in section 1.2, the Fokker-Planck equation (1.12) can be considered a limit of the Winfree model (1.4) for identical, all-to-all coupled networks extended by additive white noise, as the number of oscillators approaches infinity and the emitted pulses approach a Dirac distribution. To examine the validity of this interpretation, the system of coupled Langevin equations (1.7) was numerically integrated in the stochastic processes $\theta_1, .., \theta_N$ on S^1. Various type I and type II iPRCs as well as various noise strengths were considered. As pulse I, wrapped normal distributions were considered, with zero mean and a variance σ_p^2 between 10^{-2} and 10^{-4}. The number of oscillators N ranged from 10^2 to 10^4. An explicit, two-step Runge–Kutta scheme of mean square order 3/2 was used as described by Milstein (1995, §3.4, Theorem 3.3). All random numbers were generated using the libc pseudo-random generator (Apple Inc. 2011). Normally distributed numbers were generated using the Box-Muller transform (Gentle 2003, §5.2.1). The time step was set to $\sigma_\mathrm{p}/(50\omega)$. Further reducing it did not seem to change the outcome of the

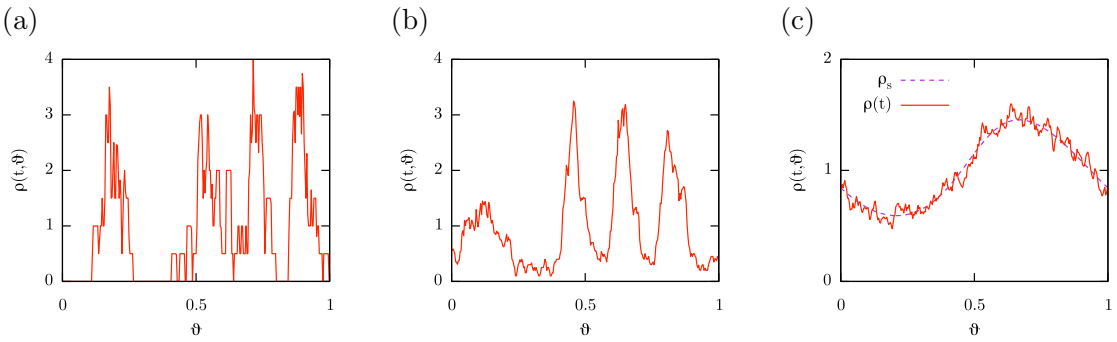

Figure 3.17: Example realisations of the integrated Langevin equation (1.7) at time $t = 10^3\ \omega^{-1}$, for repulsing type II iPRCs with turning point $\vartheta_o = 0.4$. The illustrated phase densities (red graph) are estimated using a box kernel density estimator of width 0.02. Oscillator count and pulse variance are: (a) $N = 10^2$ and $\sigma_p^2 = 10^{-4}$, (b) $N = 10^3$ and $\sigma_p^2 = 10^{-4}$, (c) $N = 10^4$ and $\sigma_p^2 = 10^{-2}$. Phases were initially uniformly and independently distributed on S^1. The dashed curve in (c) represents the stationary state of the Fokker-Planck equation (1.12) for comparison. The splitting of the network into four clusters persisted in simulations (a) and (b) for as long as they ran (at least up to time $t = 10^4\ \omega^{-1}$). The same is true for the seemingly stationary distribution attained in simulation (c). Coupling strength is $|\psi_o|/\omega = 0.5$ and noise strength is $D/\omega = 3 \times 10^{-5}$ in all cases. Time step used was $2 \times 10^{-4}\ \omega^{-1}$ for (a) and (b), 2×10^{-3} for (c). Compare these results to the integration of the corresponding Fokker-Planck equation illustrated in figure 3.14(b).

simulations. IPRC parameters considered were $\vartheta_o \in \{0.3, 0.4, 0.6, 0.7\}$ (as well as $\vartheta_o = 0.5$ for attracting type II iPRCs) and $|\psi_o|/\omega \in \{0.1, 0.5\}$. Noise strengths were taken in the range $D/\omega \in [0, 0.1]$. The phases $\theta_1, .., \theta_N$ were initially uniformly and independently distributed.

The simulation results were compared to the long-term dynamics suggested by the Fokker-Planck equation (1.12), in particular for large N and small pulse variances σ_p^2. Both the Langevin and Fokker-Planck equations were integrated until the network seemed to settle on an attractor. The underlying oscillator phase distribution was estimated from the realizations $\theta_1, .., \theta_N$ using a kernel density estimator (Silverman 1986), based on a box kernel of width 0.02. Preliminary tests revealed a good agreement between the qualitative long-term network behaviours suggested by the two methods, provided N is large enough (typically above 500) and σ_p^2 small enough (typically below 10^{-4}). Figure 3.17 illustrates this for a specific repulsing type II iPRC and noise strength, by displaying the estimated phase densities after an integration of the Langevin equation for various oscillator counts N and pulse variances σ_p^2. Figure 3.14(b) shows an example simulation of the Fokker-Planck equation (1.12) for the same iPRC and noise, where the network eventually settles on its main attractor. The latter is characterized by a splitting into four approximately equally sized and approximately synchronized oscillator groups. As can be seen in figures 3.17(a) and (b), for sufficiently small pulse widths the network indeed settles on an attractor similar to the main attractor predicted by the Fokker-Planck equation. In fact, this is even true for oscillator counts as "low" as $N = 100$. On the other hand, as shown in figure 3.17(c) for an even higher oscillator count ($N = 10^4$), an increased pulse width can lead to a totally different qualitative behaviour, in this case an eventual stationarity of the oscillator phase distribution.

Chapter 4

Conclusions

In this thesis two generalizations of the Winfree model for networks of identical, pulse-coupled phase oscillators are examined. In both models, oscillators are considered to be distributed on a finite Borel measure space over a separable metric space X. The oscillator coupling strength is described by a coupling kernel G. The first model is the field model (1.9), a differential equation in the phase field $\theta(t, x)$. Sufficient conditions are given for the existence and local asymptotic stability of synchrony, which is abundant in many natural systems of interacting oscillating units. These conditions involve (1), the symmetry and connectivity properties of the coupling kernel G and (2), the relation of the iPRC derivative to the oscillator pulse. The second considered model is the fluid model (1.10), defined as a continuity equation for the oscillator phase probability density $\rho(t, x, \vartheta)$. Existence and uniqueness results for solutions to the corresponding initial value problem are given, at least within a certain function class and for certain initial values. Furthermore, the existence and local asymptotic stability of synchrony are proven on conditions involving (1), the stability of synchrony in the corresponding field model and (2), the relation of the iPRC derivative to the oscillator pulse. These results on synchrony support previous findings on finite oscillator networks and verify their validity in the thermodynamic limit.

Following up, infinite networks of identical, all-to-all spike-coupled phase oscillators with additive white noise are studied. This is done by looking at time-independent solutions of the Fokker-Planck equation (1.12) for the phase density $\rho(t, \vartheta)$. It turns out that these so-called *stationary states* are of central importance in large networks of pulse-coupled oscillators with noise, in particular when their pulses can be approximated by a Dirac distribution. For networks with the iPRCs examined in this thesis, stationarity is locally and apparently also globally stable provided that noise is sufficiently strong. The stationary network stimulus itself is found to depend non-linearly on the noise strength, for certain iPRCs even reaching an extremum at a finite, non-trivial noise level. As noise is reduced, for all but a few critical iPRC parameters the stationary state undergoes a supercritical Hopf bifurcation. A stable limit cycle emerges, on which the network splits into one or more groups of approximately synchronized oscillators. From a *macroscopical* point of view, this leads the network stimulus to oscillate at frequencies often much higher than the intrinsic oscillator frequency. This so-called *main attractor* dominates the dynamics of the network, at least when starting in the proximity of stationarity or uniform phase distributions. These effects may need to be taken into consideration when attempting to fit biophysical neuron models to observed oscillatory activity of neural potential fields.

An analogous bifurcation has been reported for certain infinite, noisy, all-to-all coupled oscillator networks by Chawanya et al. (1993). The latter considered so-called *integrate and fire neurons* with constant excitations (Kuramoto 1991) and observed that as noise is decreased, stationarity becomes unstable and oscillators tend to synchronize. My results can, therefore, be seen as an extension to spike-coupled phase oscillators and a larger iPRC class. Furthermore, they demonstrate that even quite simple iPRC shapes can lead to the emergence of high-frequent

oscillatory network behaviour. For certain iPRCs and sufficiently low noise, a second limit cycle was found on which all oscillators are approximately synchronized. This *secondary attractor* appears at a lower noise level than the main attractor, so that certain hysteresis phenomena are to be expected during slow changes of the system's temperature.

Finally, it should be noted that the comparisons performed between the Fokker-Planck equation (1.12) and the finite Winfree model (see section 3.7), are by no means exhaustive. Nonetheless, they suggest that the former is a good starting point for describing large, finite networks of short-pulse-coupled oscillators with external noise. Further comparisons would be advantageous, in particular for iPRCs qualitatively different than the ones considered in this thesis.

An interesting extension to the fluid model considered in section 2.4 would be the addition of white noise effects, similarly to the Fokker-Planck equation (1.12) examined in chapter 3. I expect an analysis of stationary states in this model to be very fruitful, though the corresponding stationary state equations would most likely be of a higher dimension. Furthermore, one could attempt to prove the global uniqueness of stationary states (as suggested by numerical findings, see section 3.4.1), thus strengthening the local uniqueness statements given in section 3.2, at least for all-to-all spike-coupled networks with sufficiently weak coupling. Finally, the appearance of high-order oscillation modes predicted in chapter 3 for spike-coupled networks with certain iPRCs, should be experimentally verified. This might be done by comparing the oscillatory behaviour of single firing neurons subject to somatic current injection, to the temporal patterns of the neural potential field in large neuron populations.

Appendix A

A.1 Comments on the models

A.1.1 On the existence of an iPRC

Obtaining the PRC of an oscillator to incoming stimuli $S \in \mathcal{C}_0(\mathbb{R},\mathbb{R})$ when its iPRC is given, is simply a matter of convolving the stimulus with the iPRC as in (1.2). I show here how the assumption of the existence of an iPRC can be justified, provided PRCs are linear and of a certain smoothness class in the incoming stimulus.

For any given stimulus $S \in \mathcal{C}(\mathbb{R},\mathbb{R})$, let $\dot{\theta}(t) = \mathrm{v}(S,\theta(t),t)$ represent the (non-autonomous) dynamics of a stimulated oscillator, such that $\mathrm{v}(0,\vartheta,t) = \omega$ for some constant, intrinsic oscillator frequency ω. Assume the time-dependence of the dynamics of the stimulated oscillator to be resulting entirely from the time dependence of the stimulus, that is $\mathrm{v}(S(\cdot-\tau),\vartheta,t+\tau) = \mathrm{v}(S,\vartheta,t)$. Let $\Delta(S,\vartheta,t_o,t_1) \in \mathbb{R}$ denote the phase advance of the oscillator at time $t_1 \geq t_o$ with respect to $\vartheta + (t_1 - t_o)\cdot\omega$, if it was at phase $\vartheta \in S^1$ at time t_o. Then by the previous assumption Δ is *stationary*, that is

$$\Delta(S,\vartheta,t_o,t_1) = \Delta(S(\cdot-\tau),\vartheta,t_o+\tau,t_1+\tau) \quad \forall\tau\in\mathbb{R}. \tag{A.1}$$

Assume that $\Delta(S,\vartheta,t_o,t_1)$ only depends on $S|_{[t_o,t_1]}$ and that the mapping $\mathcal{C}_\mathrm{b}([t_o,t_1],\mathbb{R}) \to \mathbb{R}$, $S|_{[t_o,t_1]} \mapsto \Delta(S,\vartheta,t_o,t_1)$ is a bounded, linear functional for any fixed $\vartheta \in S^1$, $t_1 \geq t_o \in \mathbb{R}$. Then by the Riesz representation theorem (see for example Kelley & Srinivasan 1988, chapter 10) there exists a unique, signed, regular Borel measure $\delta(\vartheta,t_o,t_1)$ on $[t_o,t_1]$ of finite variation, such that

$$\Delta(S,\vartheta,t_o,t_1) = \int_{t_o}^{t_1} \delta(\vartheta,t_o,t_1)(dt)\ S(t) \quad \forall S \in \mathcal{C}(\mathbb{R},\mathbb{R}). \tag{A.2}$$

Let us assume a certain smoothness of the PRC with respect to the incoming stimulus, namely that $\delta(\vartheta,t_o,t_1)$ is absolutely continuous with respect to the Lebesgue measure, with continuous density $\psi(\vartheta,t_o,t_1,\cdot) \in \mathcal{C}([t_o,t_1],\mathbb{R})$. I claim that then $\mathrm{v}(S,\vartheta,t) = \omega + \psi(\vartheta)\cdot S(t)$, for a suitable $\psi \in \mathcal{C}(S^1,\mathbb{R})$. To show this, I proceed in several steps.

Note that whenever $t_1 \in [t_o,t_2]$, one has $\psi(\vartheta,t_o,t_1,\cdot) = \psi(\vartheta,t_o,t_2,\cdot)|_{[t_o,t_1]}$. To see this, observe that for any stimulus $S \in \mathcal{C}(\mathbb{R},\mathbb{R})$ such that $S|_{[t_1,t_2]} \equiv 0$, one has

$$\begin{aligned}
&\int_{t_o}^{t_1} dt\ \psi(\vartheta,t_o,t_2,t)\cdot S(t) = \Delta(S,\vartheta,t_o,t_2)\\
=&\Delta(S,\vartheta,t_o,t_1) + \Delta\left(S,\vartheta+(t_1-t_o)\cdot\omega+\Delta(S,\vartheta,t_o,t_1),t_1,t_2\right)\\
=&\Delta(S,\vartheta,t_o,t_1) = \int_{t_o}^{t_1} dt\ \psi(\vartheta,t_o,t_1,t)\cdot S(t).
\end{aligned} \tag{A.3}$$

One can thus define $\psi(\vartheta,t_o,\infty,\cdot) \in \mathcal{C}([t_o,\infty),\mathbb{R})$ so that $\psi(\vartheta,t_o,t_1,t) = \psi(\vartheta,t_o,\infty,t)$ for all $t_o \leq t \leq t_1$. By stationarity (A.1) of the PRC one has

$$\int_{t_o}^{t_1} dt\ \psi(\vartheta,t_o,\infty,t)\cdot S(t) = \int_{t_o}^{t_1} dt\ \psi(\vartheta,t_o+\tau,\infty,t+\tau)\cdot S(t) \tag{A.4}$$

for all stimuli $S \in \mathcal{C}(\mathbb{R}, \mathbb{R})$. Therefore $\psi(\vartheta, t_o, \infty, t)$ only depends on ϑ and the difference $t - t_o$. Denote $\psi(\vartheta, t) := \psi(\vartheta, 0, \infty, t)$ and $\psi(\vartheta) := \psi(\vartheta, 0)$ for $\vartheta \in S^1$ and $t \geq 0$, so that

$$\Delta(S, \vartheta, t_o, t_1) = \int_{t_o}^{t_1} dt\ \psi(\vartheta, t - t_o) \cdot S(t). \tag{A.5}$$

Consequently, one has

$$\mathrm{v}(S, \vartheta, t_o) = \omega + \frac{d}{dt}\Delta(S, \vartheta, t_o, t)\big|_{t=t_o} = \omega + \psi(\vartheta) \cdot S(t_o), \tag{A.6}$$

which was to be shown. □

A.1.2 On the one-oscillator Fokker-Planck equation

I present a motivation of the Fokker-Planck equation (1.8) for the one-oscillator phase density $\rho(t, \vartheta)$ in networks of identical, all-to-all coupled oscillators with additive white noise. Starting point is the N-dimensional Langevin equation (1.7) in the oscillator phases (stochastic processes) $\theta_1, .., \theta_N$. Let us write the latter as $d\theta_i = \mathrm{v}_i(\theta_1, .., \theta_N)dt + \sqrt{2D} \cdot dW_i$, with

$$\mathrm{v}_i(\theta_1, .., \theta_N) := \omega + \frac{\psi(\theta_i)}{N} \cdot \sum_j I(\theta_j). \tag{A.7}$$

Then the N-oscillator probability density $\rho^N(t, \boldsymbol{\vartheta})$ (with $\boldsymbol{\vartheta} = (\vartheta_1, .., \vartheta_N) \in (S^1)^N$) for the vector-valued stochastic process $\boldsymbol{\theta} := (\theta_1, .., \theta_N)$ satisfies the Fokker-Planck equation (Risken 1996, §4.7)

$$\partial_t \rho^N(t, \boldsymbol{\vartheta}) = -\operatorname{div}_{\boldsymbol{\vartheta}} \left[\rho^N(t, \boldsymbol{\vartheta}) \cdot \mathbf{v}(t, \boldsymbol{\vartheta})\right] + D \cdot \Delta_{\boldsymbol{\vartheta}} \rho^N(t, \boldsymbol{\vartheta}), \tag{A.8}$$

with $\mathbf{v}(\boldsymbol{\vartheta}) := (\mathrm{v}_1, .., \mathrm{v}_N)(\boldsymbol{\vartheta})$. For $n \in \{1, .., N-1\}$ denote by

$$\rho^n(t, \vartheta_1, .., \vartheta_n) := \int_{S^1} d\vartheta_{n+1} \ldots \int_{S^1} d\vartheta_N\ \rho^N(t, \vartheta_1, .., \vartheta_N) \tag{A.9}$$

the n-oscillator probability density. Inserting (A.9) into (A.8) yields

$$\begin{aligned}
\partial_t \rho^n(t, \vartheta_1, .., \vartheta_n) &= -\int_{S^1} d\vartheta_{n+1} \ldots \int_{S^1} d\vartheta_N\ \sum_{i=1}^{N} \partial_{\vartheta_i} \left[\rho^N(t, \boldsymbol{\vartheta}) \cdot \mathrm{v}_i(t, \boldsymbol{\vartheta})\right] \\
&\quad + \int_{S^1} d\vartheta_{n+1} \ldots \int_{S^1} d\vartheta_N\ D \cdot \sum_{i=1}^{N} \partial_{\vartheta_i}^2 \rho^N(t, \boldsymbol{\vartheta}) \\
&= -\sum_{i=1}^{n} \partial_{\vartheta_i} \int_{S^1} d\vartheta_{n+1} \ldots \int_{S^1} d\vartheta_N\ \rho^N(t, \boldsymbol{\vartheta}) \cdot \mathrm{v}_i(t, \boldsymbol{\vartheta}) \\
&\quad + D \cdot \sum_{i=1}^{n} \partial_{\vartheta_i}^2 \int_{S^1} d\vartheta_{n+1} \ldots \int_{S^1} d\vartheta_N\ \rho^N(t, \boldsymbol{\vartheta}) \\
&= -\sum_{i=1}^{n} \partial_{\vartheta_i} \int_{S^1} d\vartheta_{n+1} \ldots \int_{S^1} d\vartheta_N\ \rho^N(t, \boldsymbol{\vartheta}) \cdot \mathrm{v}_i(t, \boldsymbol{\vartheta}) \\
&\quad + D \cdot \Delta_{(\vartheta_1, .., \vartheta_n)} \rho^n(t, \vartheta_1, .., \vartheta_n).
\end{aligned} \tag{A.10}$$

Making use of (A.7) in (A.10) gives

$$\begin{aligned}\partial_t \rho^n(t,\vartheta_1,..,\vartheta_n) = &-\frac{1}{N}\sum_{i=1}^{n}\partial_{\vartheta_i}\Big[\psi(\vartheta_i)\cdot\int_{S^1}d\vartheta_{n+1}\ldots\int_{S^1}d\vartheta_N\ \rho^N(t,\boldsymbol{\vartheta})\cdot\sum_{j=n+1}^{N}I(\vartheta_j)\Big]\\ &-\frac{1}{N}\sum_{i=1}^{n}\partial_{\vartheta_i}\Big[\psi(\vartheta_i)\cdot\rho^n(t,\vartheta_1,..,\vartheta_n)\cdot\sum_{j=1}^{n}I(\vartheta_j)\Big]\\ &-\omega\sum_{i=1}^{n}\partial_{\vartheta_i}\rho^n(t,\vartheta_1,..,\vartheta_n)+D\cdot\Delta_{(\vartheta_1,..,\vartheta_n)}\rho^n(t,\vartheta_1,..,\vartheta_n).\end{aligned}\tag{A.11}$$

Due to the equivalence of oscillators, the integral

$$\int_{S^1}d\vartheta_{n+1}\ldots\int_{S^1}d\vartheta_N\ \rho^N(t,\boldsymbol{\vartheta})\cdot I(\vartheta_j)\tag{A.12}$$

must be the same for all $j\in\{n+1,..,N\}$, and in particular equal to

$$\begin{aligned}&\int_{S^1}d\vartheta_{n+1}\ I(\vartheta_{n+1})\int_{S^1}d\vartheta_{n+2}\ldots\int_{S^1}d\vartheta_N\ \rho^N(t,\boldsymbol{\vartheta})\\ =&\int_{S^1}d\vartheta_{n+1}\ I(\vartheta_{n+1})\cdot\rho^{n+1}(t,\vartheta_1,..,\vartheta_{n+1}).\end{aligned}\tag{A.13}$$

Therefore (A.11) takes the form

$$\begin{aligned}\partial_t \rho^n(t,\vartheta_1,..,\vartheta_n) = &-\frac{N-n}{N}\sum_{i=1}^{n}\partial_{\vartheta_i}\Big[\psi(\vartheta_i)\cdot\int_{S^1}d\vartheta_{n+1}\ I(\vartheta_{n+1})\cdot\rho^{n+1}(t,\vartheta_1,..,\vartheta_{n+1})\Big]\\ &-\frac{1}{N}\sum_{i=1}^{n}\partial_{\vartheta_i}\Big[\psi(\vartheta_i)\cdot\rho^n(t,\vartheta_1,..,\vartheta_n)\cdot\sum_{j=1}^{n}I(\vartheta_j)\Big]\\ &-\omega\sum_{i=1}^{n}\partial_{\vartheta_i}\rho^n(t,\vartheta_1,..,\vartheta_n)+D\cdot\Delta_{(\vartheta_1,..,\vartheta_n)}\rho^n(t,\vartheta_1,..,\vartheta_n).\end{aligned}\tag{A.14}$$

Solving the original Fokker-Planck equation (A.8) thus translates to solving the hierarchy (A.14) of coupled differential equations in the n-oscillator probability densities. The second term in (A.14) represents the mutual interaction of the first n oscillators, while the first term represents the influence of oscillators $n+1$ to N on the first n oscillators. Without any further assumptions, (A.14) can not be further simplified.

Let me point out its similarity to the BBGKY hierarchy for the n-particle densities in kinetic gas theory (see for example Wilmanski 2008, §7.2). In the latter, one usually *cuts off* the hierarchy by ignoring any higher-order correlations between particle coordinates, thus obtaining a tractable approximation for the evolution of lower order n-particle densities. I shall proceed in a similar way. Define

$$\kappa(t,\vartheta_1,\vartheta_2) := \rho^2(t,\vartheta_1,\vartheta_2)-\rho^1(t,\vartheta_1)\cdot\rho^1(t,\vartheta_2),\tag{A.15}$$

then (A.14) can for $n=1$ be written as

$$\begin{aligned}\partial_t\rho^1(t,\vartheta) = &-\partial_\vartheta\Big[\rho^1(t,\vartheta)\cdot\Big[\omega+\psi(\vartheta)\cdot\frac{N-1}{N}\int_{S^1}d\varphi\ I(\varphi)\cdot\rho^1(t,\varphi)\Big]\Big]+D\cdot\partial_\vartheta^2\rho^1(t,\vartheta)\\ &-\frac{1}{N}\partial_\vartheta\left[\psi(\vartheta)\cdot\rho^1(t,\vartheta)\cdot I(\vartheta)\right]-\frac{N-1}{N}\cdot\partial_\vartheta\int_{S^1}d\varphi\ \psi(\vartheta)\cdot I(\varphi)\cdot\kappa(t,\vartheta,\varphi).\end{aligned}\tag{A.16}$$

Equation (A.16) is almost the sought one-oscillator Fokker-Planck equation, the greatest difference being two additional terms: One due to self-coupling (penultimate term) and one due to non-vanishing two-oscillator correlations (last term). The first one scales down as $\sim 1/N$. The latter would vanish if oscillator phases were to be statistically independent for all times.

Suppose all oscillator phases at time $t = 0$ to be independently distributed on S^1, according to the probability density $\rho^1(0, \cdot)$. The assumption of so-called *propagation of chaos* (Dawson 1983, Crawford & Davies 1999) now states that $\kappa \to 0$ as $N \to \infty$, that is, two-oscillator correlations vanish if the network becomes large enough. Adopting it for the model at hand and taking the thermodynamic limit, finally leads to the evolution equation

$$\partial_t \rho^1(t,\vartheta) = -\,\partial_\vartheta \left[\rho^1(t,\vartheta) \cdot \left[\omega + \psi(\vartheta) \cdot \int_{S^1} d\varphi \; I(\varphi) \cdot \rho^1(t,\varphi) \right] \right] + D \cdot \partial_\vartheta^2 \rho^1(t,\vartheta) \tag{A.17}$$

for the one-oscillator probability density $\rho^1(t, \cdot)$. Note that even if propagation of chaos may appear intuitive, it is in fact at this point a pure postulate. Nonetheless, its validity has been proven for numerous similar dynamical systems, a prominent example being the Kuramoto model (Bonilla 1987, Bonilla et al. 1992, Acebrón et al. 2005). See Hildebrand et al. (2007) for estimating the error corresponding to this approximation in finite networks.

A.2 Supplementary proofs to chapter 1

A.2.1 Proof of lemma 1.4.4

Let $G_{\max} := \sup_{x \in X} \|G(x,\cdot)\|_{L^1(\mu)}$. Since for any $\rho \in \Omega_o$ and $x \in X$

$$\int_X d\mu(y) \;\; |G(x,y)| \int_K d\kappa(\varphi) \;\; |\rho(y,\varphi) \cdot I(y,\varphi)| \leq G_{\max} \cdot \|I\|_\infty \,, \tag{A.18}$$

the stimulus $S : X \times \Omega_o \to \mathbb{K}$ is well-defined and bounded.

1. For any $\rho \in \Omega_o$ and $x_1, x_2 \in X$ one can by Hölder estimate

$$\begin{aligned} |S(x_1,\rho) - S(x_2,\rho)| \leq & \|G(x_1,\cdot) - G(x_2,\cdot)\|_{L^1(\mu)} \cdot \|I\|_\infty \\ \leq & \omega_G(d(x_1,x_2)) \cdot \|I\|_\infty \,, \end{aligned} \tag{A.19}$$

   with ω_G being the modulus of continuity of the mapping $x \mapsto G(x,\cdot) \in L^1(\mu)$. Therefore $S(\cdot,\rho) \in \mathcal{C}_{\mathrm{u,b}}(X, \mathbb{K})$. Now fix $x \in X$ and let $(\rho_n)_n \subseteq \Omega_o$ be a sequence converging to $\rho \in \Omega_o$. By Brézis & Lieb (1983) one knows that $\|\rho_n(y,\cdot) - \rho(y,\cdot)\|_{L^1(\kappa)} \overset{n\to\infty}{\longrightarrow} 0$ for every $y \in X$. This implies that

$$\int_K d\kappa(\varphi) \;\; \rho_n(y,\varphi) \cdot I(y,\varphi) \overset{n\to\infty}{\longrightarrow} \int_K d\kappa(\varphi) \;\; \rho(y,\varphi) \cdot I(y,\varphi) \tag{A.20}$$

   for every $y \in X$. Since $\left| \int_K d\kappa(\varphi) \;\; \rho_n(y,\varphi) \cdot I(y,\varphi) \right| \leq \|I\|_\infty$ and $G(x,\cdot) \in L^1(\mu)$, by Lebesgue's dominated convergence theorem this implies that $S(x,\rho_n) \overset{n\to\infty}{\longrightarrow} S(x,\rho)$.

2. For any $x_1, x_2 \in X$ and $\rho_1, \rho_2 \in \Omega_o$ one can estimate

$$\begin{aligned} & |S(x_1,\rho_1) - S(x_2,\rho_2)| \\ \leq & \int_X d\mu(y) \;\; |G(x_1,y)| \int_K d\kappa(\varphi) \;\; |\rho_1(y,\varphi) - \rho_2(y,\varphi)| \cdot |I(y,\varphi)| \\ & + \int_X d\mu(y) \;\; |G(x_1,y) - G(x_2,y)| \int_K d\kappa(\varphi) \;\; |\rho_2(y,\varphi) \cdot I(y,\varphi)| \\ \leq & G_{\max} \cdot \|I\|_\infty \cdot \kappa(K) \cdot \|\rho_1 - \rho_2\|_\infty + \omega_G(d(x_1,x_2)) \cdot \|I\|_\infty \,, \end{aligned} \tag{A.21}$$

   which shows that $S \in \mathcal{C}_{\mathrm{u,b}}(X \times \Omega_o, \mathbb{K})$. It also shows that S is Lipschitz continuous in Ω_o with Lipschitz constant $L_S := G_{\max} \cdot \|I\|_\infty \cdot \kappa(K)$. □

A.3 Supplementary proofs to chapter 2

A.3.1 On strictly positive measures

I show the following claim: If X is a separable metric space and μ a Borel measure on it, then there exists a closed subset $X_o \subseteq X$ of full measure, such that the restriction of μ on the subspace $(X_o, \mathscr{B}(X_o))$ is strictly positive. Indeed, let Z be the union of all open subsets of X having zero measure. As X is separable, it is hereditarily Lindelöf. Thus Z is a countable union of open sets of zero measure. Therefore $\mu(Z) = 0$. Define $X_o := X \setminus Z$, then X_o is a closed set with full measure. On it, μ is strictly positive, that is $\mu(U_o) > 0$ for any open subset $\emptyset \neq U_o \subseteq X_o$ (that is with $U_o = X_o \cap U$ for some open subset $U \subseteq X$). Indeed, were it not the case, one would have $\mu(U) = \mu(X_o \cap U) + \mu(Z \cap U) = 0$ and thus $U \subseteq Z$, therefore $U_o = \emptyset$, a contradiction. □

A.3.2 Proof of lemma 2.3.2

As a preliminary, let the following be remarked:

1. $(\mathcal{H}_{1,o}, \mathcal{H}_{2,o})$ generates on $V_1 \times V_2$ a flow $(U_{1,o}, U_{2,o})$. To see this, note that by assumptions (4) and (5) $\mathcal{H}_{1,o}(v_1) = \mathcal{H}_1(v_1, 0)$ for all $v_1 \in V_1$. By assumption (1) $\mathcal{H}_{1,o}$ is Lipschitz-continuous so that the flow $U_{1,o}(t, t_o) : V_1 \to V_1$ is well-defined. Since $\mathcal{H}_{2,o} : V_1 \times V_2 \to V_2$ is by assumption (3) continuous, for each fixed $v_1 \in V_1$ and $t_o \in \mathbb{R}$ the mapping $(t, v_2) \mapsto \mathcal{H}_{2,o}(U_{1,o}(t, t_o)(v_1))v_2$ is continuous. Furthermore, by assumption (3) the mapping $(t, v_2) \mapsto \mathcal{H}_{2,o}(U_{1,o}(t, t_o)(v_1))v_2$ is Lipschitz continuous in the second argument, with a time-independent Lipschitz constant. Therefore, the propagator $U_{2,o}(t, t_o)(v_1, \cdot) : V_2 \to V_2$ is for each $v_1 \in V_1$ and $t_o \leq t \in \mathbb{R}$ well-defined and a bounded, linear operator on V_2.

2. Since $\mathcal{H}_2(v_1, 0) = 0$ for all $v_1 \in V_1$, the sub-space $V_1 \times \{0\}$ is indeed U-invariant, that is $(U_1, U_2)(t, t_o)(v_1, 0) \in V_1 \times \{0\}$ for any $v_1 \in V_1$ and $t_o \leq t \in \mathbb{R}$. Thus $U_1(t, t_o)(v_1, 0) = U_{1,o}(t, t_o)(v_1)$. Consequently, Kv_2 is simply $U_{2,o}(t_o + T, t_o)(v_1, v_2)$ for any arbitrary $v_1 \in V_1$.

By autonomy of the flow one may without loss of generality fix the initial time t_o. Then one has

$$[(U_1, U_2)(t, t_o)(v_1, v_2) - (U_{1,o}, U_{2,o})(t, t_o)(v_1, v_2)] \in o(v_2) \tag{A.22}$$

as $v_2 \to 0$, uniformly in $v_1 \in V_1$ and $t \in [t_o, t_o + T]$.

> **Proof of claim.** Define $\eta_1 := \mathcal{H}_1 - \mathcal{H}_{1,o}$ and $\eta_2 := \mathcal{H}_2 - \mathcal{H}_{2,o}$. By Lipschitz continuity of $(\mathcal{H}_1, \mathcal{H}_2)$ there exists a constant $C > 0$, depending only on T and the Lipschitz-constant of $(\mathcal{H}_1, \mathcal{H}_2)$, such that
>
> $$\begin{aligned} \|(U_1, U_2)(t, t_o)(v_1, v_2) - (U_1, U_2)(t, t_o)(v_1, 0)\| &\leq C \cdot \|(v_1, v_2) - (v_1, 0)\| \\ &= C \cdot \|v_2\| . \end{aligned} \tag{A.23}$$
>
> for all $(v_1, v_2) \in V_1 \times V_2$ and $t \in [t_o, t_o + T]$. By flow invariance of $V_1 \times \{0\}$ in particular
>
> $$\|U_2(t, t_o)(v_1, v_2)\| \leq C \cdot \|v_2\| . \tag{A.24}$$
>
> One can therefore estimate
>
> $$\|\eta_i((U_1, U_2)(t, t_o)(v_1, v_2))\| \in o(v_2) \tag{A.25}$$
>
> for $i \in \{1, 2\}$, uniformly in $v_1 \in V_1$ and $t \in [t_o, t_o + T]$. Let $\Omega \subseteq V_2$ be an open neighbourhood of the origin such that $(\mathcal{H}_{1,o}, \mathcal{H}_{2,o})$ is Lipschitz continuous on $V_1 \times \Omega$

with Lipschitz constant L_o. Such an Ω exists by assumptions (2) and (3). Any solution $(v_1(t), v_2(t))$ to the ODE $\frac{d}{dt}(v_1(t), v_2(t)) = (\mathcal{H}_1, \mathcal{H}_2)(v_1(t), v_2(t))$ in $V_1 \times V_2$ satisfies

$$\frac{d}{dt}(v_1(t), v_2(t)) = (\mathcal{H}_{1,o}, \mathcal{H}_{2,o})(v_1(t), v_2(t)) + (\eta_1, \eta_2)(v_1(t), v_2(t)). \tag{A.26}$$

Using Grönwall's inequality it is easy to see that this implies

$$\begin{aligned} &\|(U_1, U_2)(t, t_o)(v_1, v_2) - (U_{1,o}, U_{2,o})(t, t_o)(v_1, v_2)\| \\ \leq &T \cdot e^{TL_o} \cdot \sup_{s \in [t_o, t_o+T]} \|(\eta_1, \eta_2)((U_1, U_2)(s, t_o)(v_1, v_2))\| \end{aligned} \tag{A.27}$$

for all $t \in [t_o, t_o + T]$ and $(v_1, v_2) \in V_1 \times V_2$, as long as both $(U_1, U_2)(t, t_o)(v_1, v_2)$ and $(U_{1,o}, U_{2,o})(t, t_o)(v_1, v_2)$ are within $V_1 \times \Omega$ for all $t \in [t_o, t_o + T]$. By (A.24) it can be guaranteed that $(U_1, U_2)(t, t_o)(v_1, v_2) \in V_1 \times \Omega$ for all $t \in [t_o, t_o + T]$ and all $v_1 \in V_1$ by choosing v_2 arbitrarily small. On the other hand, one can estimate $\|U_{2,o}(t, t_o)(v_1, v_2)\| \leq e^{TM}\|v_2\|$ for all $t \in [t_o, t_o + T]$, with $M := \sup_{u \in V_1} \|\mathcal{H}_{2,o}(u)\| < \infty$. One can thus also guarantee $(U_{1,o}, U_{2,o})(t, t_o)(v_1, v_2) \in V_1 \times \Omega$ for all $t \in [t_o, t_o + T]$ and all $v_1 \in V_1$ by choosing v_2 adequately small. Thus the estimate (A.27) holds for all $v_1 \in V_1$ and $t \in [t_o, t_o + T]$ provided that v_2 is chosen adequately small. By (A.25) the supremum on the right hand side of (A.27) is of order $o(v_2)$, uniformly in $v_1 \in V_1$.

Define $f := U_2(t_o + T, t_o) - U_{2,o}(t_o + T, t_o)$, then $U_2(t_o + T, t_o)(v_1, v_2) = Kv_2 + f(v_1, v_2)$ with $K \in \mathcal{L}(V_2)$ being uniformly exponentially stable (see for example Eisner 2010, Chapter II). Since $f(v_1, v_2) \in o(v_2)$ uniformly in v_1, it follows easily that uniform exponential stability in V_2 is also valid for $U_2(t_o + T, t_o)$: There exist constants $\tilde{A}, \beta, \tilde{\delta} > 0$ such that whenever $\|v_2\| \leq \tilde{\delta}$, one has

$$\|U_2(t_o + nT, t_o)(v_1, v_2)\| \leq \tilde{A}e^{-\beta \cdot nT} \cdot \|v_2\| \tag{A.28}$$

for any $v_1 \in V_1$ and all $n \in \mathbb{N}_0$. Choose $\delta := \tilde{\delta}/(C + 1)$ and $A := C\tilde{A}e^{\beta T}$, then for any $n \in \mathbb{N}_0$, $\tau \in [0, T]$, $v_1 \in V_1$ and $v_2 \in V_2$ with $\|v_2\| \leq \delta$ one has

$$\begin{aligned} &\|U_2(t_o + nT + \tau, t_o)(v_1, v_2)\| \\ \overset{(1)}{=} &\|U_2(t_o + nT, t_o) \circ (U_1(t_o + \tau, t_o), U_2(t_o + \tau, t_o))(v_1, v_2)\| \\ \overset{(2)}{\leq} &\tilde{A}e^{-\beta \cdot nT} \cdot \|U_2(t_o + \tau, t_o)(v_1, v_2)\| \\ \overset{(3)}{\leq} &C\tilde{A}e^{-\beta \cdot nT} \cdot \|v_2\| \leq Ae^{-\beta \cdot (nT+\tau)} \cdot \|v_2\|. \end{aligned} \tag{A.29}$$

In step (1), use has been made of the autonomy of the flow U. In step (2), the estimates (A.24) and (A.28) were used. In step (3), the estimate (A.24) was used. This finishes the proof. □

A.3.3 Proof of lemma 2.4.1

As a preliminary, let the following fact be remarked: *Let $[t_o, t_1] \subseteq \mathbb{R}$ be a compact interval. Let $\{f_\alpha\}_{\alpha \in A} \subseteq \mathcal{C}([t_o, t_1], \mathbb{R})$ be a family of equicontinuous functions differentiable on (t_o, t_1). Let $f := \sup_{\alpha \in A} f_\alpha$ be defined pointwise (not necessarily finite). Suppose that there exists some $M \in \mathbb{R}$, such that whenever $f(t) < M$ for some $t \in [t_o, t_1]$ one has $\frac{d}{dt} f_\alpha(t) \leq 0$ for all $\alpha \in A$. Then if $f(t_o) < M$, one has $f(t) < M$ for all $t \in [t_o, t_1]$.* This follows from the fact that the supremum of equicontinuous functions is continuous. Use shall be made of it below.

Without loss of generality assume $A_o \geq 1$. Without loss of generality one can assume $r \leq \frac{1}{4}$ and $A_o e^{-\beta_o T} \leq \frac{1}{4}$ (otherwise increase T). One may also assume $A_o \cdot \delta_o \leq \varepsilon/8$ (otherwise decrease δ_o). One may even assume that there exists a constant $C_o > 0$, such that $\|\mathcal{E}(\gamma_o)\| \leq C_o \cdot D_{\mathrm{loc}}(\gamma_o)$ whenever $D_{\mathrm{loc}}(\gamma_o) \leq \delta_o$ (otherwise decrease δ_o). Note that $A_o \geq 1$. In the following, let us denote by $\Theta_o(t) = (\Theta_{o1}(t), \Theta_{o2}(t))$ solutions of the ODE $\frac{d}{dt}\Theta_o(t) = \mathcal{H}_o(\Theta_o(t))$ in V. Let us fix some orbit $(\gamma(t))_{t\geq 0} \in \Gamma$ and write $f(t)$ instead of $f(\gamma(t))$ for any function f defined on Γ_o, as for example $\Theta(t) := (\Theta_1(t), \Theta_2(t)) := (\Theta_1(\gamma(t)), \Theta_2(\gamma(t)))$.

Since $\mathcal{H}_o$ is Lipschitz continuous there exists a constant $C \geq 1$, depending only on the Lipschitz constant of $\mathcal{H}_o$, the period T and C_o, such that for all $0 \leq t_o \leq t \leq t_o + T$ one has

$$\|\Theta(t) - \Theta_o(t)\| \leq C \cdot \sup_{s\in[t_o,t]} D_{\mathrm{loc}}(s), \tag{A.30}$$

provided that $\Theta(t_o) = \Theta_o(t_o)$ and $\sup_{s\in[t_o,t]} D_{\mathrm{loc}}(s) \leq \delta_o$. Choose some $0 < \delta_1 < \delta_o/(4C)$.
Claim 01: *Suppose $\Theta(t_o) = \Theta_o(t_o)$, $D_{\mathrm{loc}}(t_o) < \delta_1$ and $\|\Theta_2(t_o)\| \leq \delta_o$ for some $t_o \geq 0$. Then $\|\Theta(t) - \Theta_o(t)\| \leq \delta_o/4$ for all $t \in [t_o, t_o + T]$.*

> **Proof of claim.** Suppose the contrary. Then by continuity of $\Theta(t)$ and $\Theta_o(t)$ in t, there exists a $t_1 \in [t_o, t_o + T]$ such that $\|\Theta(t) - \Theta_o(t)\| < \delta_o/4$ for all $t \in [t_o, t_1)$ and $\|\Theta(t_1) - \Theta_o(t_1)\| = \delta_o/4$. Since $\|\Theta_{o2}(t_o)\| = \|\Theta_2(t_o)\| \leq \delta_o$, by condition (C3) one has $\|\Theta_{o2}(t)\| \leq \varepsilon/8$ for all $t \in [t_o, t_1]$. This implies
>
> $$\|\Theta_2(t)\| \leq \|\Theta_{o2}(t)\| + \|\Theta_2(t) - \Theta_{o2}(t)\| \leq \frac{\varepsilon}{8} + \frac{\delta_o}{4} \leq \frac{\varepsilon}{4} \tag{A.31}$$
>
> for all $t \in [t_o, t_1]$. Thus whenever $D_{\mathrm{loc}}(t) \leq \delta_1 \leq \varepsilon/8$ with $t \in [t_o, t_1]$, one has by (A.31) $D_{\mathrm{gl}}(t) \leq \varepsilon$ and therefore by condition (C1) $\frac{d}{dt}D_\alpha(t) \leq 0\ \forall \alpha \in A$. Consequently the initial condition $D_{\mathrm{loc}}(t_o) < \delta_1$ implies by the preliminary remark above that $D_{\mathrm{loc}}(t) < \delta_1$ for all $t \in [t_o, t_1]$. By (A.30) this implies $\|\Theta(t) - \Theta_o(t)\| \leq C\delta_1 < \delta_o/4$ for all $t \in [t_o, t_1]$, a contradiction.

Claim 02: *Suppose $D_{\mathrm{loc}}(t_o) < \delta_1$ and $\|\Theta_2(t_o)\| \leq \delta_o$ for some $t_o \geq 0$. Then $D_{\mathrm{gl}}(t) \leq \varepsilon$ for all $t \in [t_o, t_o + T]$.*

> **Proof of claim.** Set $\Theta_o(t_o) = \Theta(t_o)$. By condition (C3) one then has $\|\Theta_{o2}(t)\| \leq \varepsilon/8$ for all $t \in [t_o, t_o + T]$. Since by claim 01 also $\|\Theta(t) - \Theta_o(t)\| \leq \varepsilon/8$ for all $t \in [t_o, t_o + T]$, this implies $\|\Theta_2(t)\| \leq \varepsilon/4$ for all $t \in [t_o, t_o + T]$. Thus whenever $D_{\mathrm{loc}}(t) \leq \delta_1 \leq \varepsilon/8$ with $t \in [t_o, t_o + T]$, one has $D_{\mathrm{gl}}(t) \leq \varepsilon$ and therefore by condition (C1) $\frac{d}{dt}D_\alpha(t) \leq 0\ \forall \alpha \in A$. The initial condition $D_{\mathrm{loc}}(t_o) < \delta_1$ implies by the preliminary remark above that $D_{\mathrm{loc}}(t) < \delta_1$ for all $t \in [t_o, t_o + T]$. Thus $D_{\mathrm{gl}}(t) = 2\|\Theta_2(t)\| + 2D_{\mathrm{loc(t)}} \leq \varepsilon$ for all $t \in [t_o, t_o + T]$.

In the following, suppose $D_{\mathrm{loc}}(t_o) < \delta_1$ and $\|\Theta_2(t_o)\| \leq \delta_o$ at some time $t_o \geq 0$. Then by claim 02 and condition (C1) $D_{\mathrm{loc}}(t)$ is non-increasing on $[t_o, t_o + T]$, so that also $D_{\mathrm{loc}}(t_o + T) < \delta_1$. By condition (C3) $\|\Theta_{o2}(t_o + T)\| \leq A_o e^{-\beta_o T}\|\Theta_{o2}(t_o)\| \leq \delta_o/4$ and by claim 01 $\|\Theta_2(t_o + T) - \Theta_{o2}(t_o + T)\| \leq \delta_o/4$ if one sets $\Theta_o(t_o) = \Theta(t_o)$. Therefore $\|\Theta_2(t_o + T)\| \leq \delta_o/2 \leq \delta_o$. By induction one concludes that $D_{\mathrm{loc}}(t_o + nT) < \delta_1$ as well as $\|\Theta_2(t_o + nT)\| \leq \delta_o$ for all $n \in \mathbb{N}_0$ and by claim 02 $D_{\mathrm{gl}}(t) \leq \varepsilon$ for all $t \geq t_o$. By condition (C1) this implies that all $D_\alpha(t)$ ($\alpha \in A$) are non-increasing with t and by condition (C2) that $D_\alpha(t_o + (n+1)T) \leq D_\alpha(t_o + nT)/4$ for all $n \in \mathbb{N}_0$ and $\alpha \in A$.

Through similar reasoning as above and by using estimate (A.30), one finds that

$$\begin{aligned}\|\Theta_2(t_o + (n+1)T)\| \leq& A_o e^{-\beta_o T}\|\Theta_2(t_o + nT)\| + C \cdot D_{\mathrm{loc}}(t_o + nT)\\ \leq& \frac{1}{4}\|\Theta_2(t_o + nT)\| + C \cdot D_{\mathrm{loc}}(t_o + nT).\end{aligned} \tag{A.32}$$

Denote $a_n := \|\Theta_2(t_o + nT)\|$ and $b_n := 4CD_{\mathrm{loc}}(t_o + nT)$, then inequality (A.32) reads

$$a_{n+1} \leq \frac{a_n}{4} + \frac{b_n}{4}. \tag{A.33}$$

Note that also $b_{n+1} \leq \frac{a_n}{4} + \frac{b_n}{4}$, so that $(a_{n+1} + b_{n+1}) \leq (a_n + b_n)/2$ and therefore $(a_n + b_n) \leq (a_o + b_o)/2^n$. Consequently

$$\begin{aligned} \frac{1}{2} D_{\mathrm{gl}}(t_o + nT) \leq & \|\Theta_2(t_o + nT)\| + 4C \cdot D_{\mathrm{loc}}(t_o + nT) \\ \leq & \frac{1}{2^n} \cdot \big(\|\Theta_2(t_o)\| + 4C \cdot D_{\mathrm{loc}}(t_o) \big) \leq \frac{2C}{2^n} \cdot D_{\mathrm{gl}}(t_o), \end{aligned} \tag{A.34}$$

where use has been made of the fact that $C \geq 1$. Similarly to (A.32), one may for any $n \in \mathbb{N}_0$ and $\tau \in [0, T]$ estimate

$$\begin{aligned} D_{\mathrm{gl}}(t_o + nT + \tau) = & 2D_{\mathrm{loc}}(t_o + nT + \tau) + 2 \|\Theta_2(t_o + nT + \tau)\| \\ \leq & 2D_{\mathrm{loc}}(t_o + nT) + 2A_o e^{-\beta_o \tau} \cdot \|\Theta_2(t_o + nT)\| \\ & + 2C \cdot D_{\mathrm{loc}}(t_o + nT) \\ \leq & A_1 \cdot D_{\mathrm{gl}}(t_o + nT), \end{aligned} \tag{A.35}$$

with $A_1 > 0$ being some constant only depending on C and A_o. By combining (A.34) with (A.35) one finds that

$$D_{\mathrm{gl}}(t) \leq A e^{-\beta \cdot (t - t_o)} \cdot D_{\mathrm{gl}}(t_o) \tag{A.36}$$

for all $t \geq t_o$, with $\beta := \frac{1}{T} \ln 2$ and $A > 0$ being some constant only depending on C and A_1. Choosing $\delta := \delta_1$ finishes the proof. □

A.4 Supplementary proofs to chapter 3

A.4.1 Proof of proposition 3.2.2

Define two auxiliary functions $\zeta, \eta : \mathbb{R} \to \mathbb{R}_+$ by

$$\begin{aligned} \zeta(s) &:= \int_0^1 d\varphi \; e^{-s\varphi} = \frac{1}{s} \left[1 - e^{-s} \right], \\ \eta(s) &:= \int_0^1 d\varphi \; e^{-s\varphi} \varphi = \frac{1}{s^2} \left[1 - e^{-s} - s \cdot e^{-s} \right], \end{aligned} \tag{A.37}$$

the expressions on the right hand side being for $s = 0$ understood as their respective limits. Note that for $0 \leq s_1 \leq s_2$ one has

$$\frac{\zeta(s_1)}{\zeta(s_2)} \leq \frac{s_2}{s_1} \quad , \quad \frac{\eta(s_1)}{\zeta(s_2)} \leq \frac{s_2}{s_1^2}. \tag{A.38}$$

Denote by $M(\rho_{\mathrm{s}}(0))$ and $N(\rho_{\mathrm{s}}(0))$ the numerator and denominator on the right hand side of (3.15) respectively, so that $A_D = M/N$. It is straightforward to obtain for $r, r_1, r_2 \geq 0$ the estimates

$$\begin{aligned} & |M(r)| \leq \zeta \left[\frac{\omega}{D} (1 - \mathcal{E} r) \right], \\ & \zeta \left[\frac{\omega}{D} (1 + \mathcal{E} r) \right] \leq |N(r)| \leq \zeta \left[\frac{\omega}{D} (1 - \mathcal{E} r) \right], \\ & |M(r_1) - M(r_2)| \leq \frac{\|\psi\|_\infty}{D} \cdot \eta \left[\frac{\omega}{D} \left[1 - \mathcal{E} \cdot \max(r_1, r_2) \right] \right] \cdot |r_1 - r_2|, \\ & |N(r_1) - N(r_2)| \leq \frac{\|\psi\|_\infty}{D} \cdot \eta \left[\frac{\omega}{D} \left[1 - \mathcal{E} \cdot \max(r_1, r_2) \right] \right] \cdot |r_1 - r_2|. \end{aligned} \tag{A.39}$$

Combining them leads to the estimate

$$|A_D(r)| \leq \frac{\zeta\left[\frac{\omega}{D}(1-\mathcal{E}r)\right]}{\zeta\left[\frac{\omega}{D}(1+\mathcal{E}r)\right]} \tag{A.40}$$

and (assuming $r_1 \geq r_2$) furthermore to

$$\begin{aligned} |A_D(r_1) - A_D(r_2)| \leq & \frac{\left[\,|N(r_2)|\cdot|M(r_1)-M(r_2)| + |N(r_1)-N(r_2)|\cdot|M(r_2)|\,\right]}{|N(r_1)\cdot N(r_2)|} \\ \leq & 2\mathcal{E}\cdot\frac{\eta\left[\frac{\omega}{D}(1-\mathcal{E}r_1)\right]\cdot\zeta\left[\frac{\omega}{D}(1-\mathcal{E}r_2)\right]}{\zeta\left[\frac{\omega}{D}(1+\mathcal{E}r_1)\right]\cdot\zeta\left[\frac{\omega}{D}(1+\mathcal{E}r_2)\right]}\cdot\frac{\omega}{D}\cdot|r_1-r_2|\,. \end{aligned} \tag{A.41}$$

Now let $\beta \geq 2$ and assume $\mathcal{E} \leq 1/4\beta$. Then $\mathcal{E}r < 1$ for all $r \in J_\beta$. By applying (A.38) to (A.40) one finds that

$$|A_D(r)| \leq \frac{1+\mathcal{E}r}{1-\mathcal{E}r} \leq \frac{1+\mathcal{E}\beta}{1-\mathcal{E}\beta} \leq \frac{5}{3} \tag{A.42}$$

for all $r \in J_\beta$, so that indeed $A_D(J_\beta) \subseteq J_{5/3}$. Similarly, by applying (A.38) to (A.41) one finds

$$\begin{aligned} |A_D(r_1) - A_D(r_2)| \leq & 2\mathcal{E}\cdot\frac{1+\mathcal{E}r_1}{(1-\mathcal{E}r_1)^2}\cdot\frac{1+\mathcal{E}r_2}{1-\mathcal{E}r_2}\cdot|r_1-r_2| \\ \leq & \frac{1}{2\beta}\cdot\frac{(1+\mathcal{E}\beta)^2}{(1-\mathcal{E}\beta)^3}\cdot|r_1-r_2| \leq \frac{25}{27}\cdot|r_1-r_2| \end{aligned} \tag{A.43}$$

for all $r_1, r_2 \in J_\beta$. □

A.4.2 Proof of proposition 3.2.3

The proof is based on the following, easily verifiable fact: If $f \in \mathcal{C}([0,1],\mathbb{R})$ is (right-)differentiable in 0 with $f'(0) > 0$ and such that 0 is a unique, global minimum of f, then

$$\lim_{D\to 0^+}\left\{\int_0^1 d\varphi\ \exp\left[-\frac{1}{D}f(\varphi)\right]\right\}^{-1}\cdot\int_0^1 d\varphi\ \exp\left[-\frac{1}{D}\left[f(0)+f'(0)\cdot\varphi\right]\right] = 1. \tag{A.44}$$

For each $\vartheta \in [0,1]$ consider the function $f_\vartheta : [0,1] \to \mathbb{R}$ defined as $f_\vartheta(\varphi) := \omega\varphi + \Psi(\vartheta, \vartheta+\varphi)\cdot r$. Then f_ϑ satisfies the assumptions of the above assertion with $f'_\vartheta(0) = \omega + \psi(\vartheta)\cdot r > 0$. By (A.44) this implies that

$$\begin{aligned} \lim_{D\to 0^+} A_D(r) = & \left\{\int_0^1 d\vartheta\ \lim_{D\to 0^+}\left[\int_0^1 d\varphi\ \exp\left[-\frac{1}{D}\left[\omega+\psi(0)\cdot r\right]\cdot\varphi\right]\right]^{-1}\right. \\ & \left.\cdot\int_0^1 d\varphi\ \exp\left[-\frac{1}{D}\left[\omega+\psi(\vartheta)\cdot r\right]\cdot\varphi\right]\right\}^{-1} \\ = & \left\{\int_0^1 d\vartheta\ \lim_{D\to 0^+}\zeta\left[\frac{\omega}{D}\right]^{-1}\cdot\zeta\left[\frac{1}{D}\left[\omega+\psi(\vartheta)\cdot r\right]\right]\right\}^{-1} \\ = & \left[\omega\cdot\int_0^1\frac{d\vartheta}{\omega+\psi(\vartheta)\cdot r}\right]^{-1} = A_0(r), \end{aligned} \tag{A.45}$$

with $\zeta : \mathbb{R}_+ \to \mathbb{R}_+$ being the auxiliary function introduced in (A.37). Note that Lebesgue's dominated convergence theorem has been used to swap the limit with the ϑ-integral. The theorem

can be applied due to the estimate

$$\begin{aligned}
&\left\{\int_0^1 d\varphi\ \exp\left[-\frac{1}{D}\left[\omega\varphi+\Psi(0,\varphi)\cdot r\right]\right]\right\}^{-1}\cdot\int_0^1 d\varphi\ \exp\left[-\frac{1}{D}\left[\omega\varphi+\Psi(\vartheta,\vartheta+\varphi)\cdot r\right]\right]\\
\leq&\left\{\int_0^1 d\varphi\ \exp\left[-\frac{1}{D}\left[\omega+\|\psi\|_\infty\cdot r\right]\cdot\varphi\right]\right\}^{-1}\cdot\int_0^1 d\varphi\ \exp\left[-\frac{1}{D}\left[\omega-\|\psi\|_\infty\cdot r\right]\cdot\varphi\right] \qquad (A.46)\\
=&\frac{\zeta\left[\frac{\omega}{D}\left[1-\mathcal{E}r\right]\right]}{\zeta\left[\frac{\omega}{D}\left[1+\mathcal{E}r\right]\right]}<\infty,
\end{aligned}$$

holding uniformly in ϑ. □

A.4.3 An upper bound for the imaginary part of eigenvalues

I show that the eigenvalue equation

$$\chi(\lambda):=1-e^{-\lambda T_{\rm s}(1)}\left[1+\omega T_{\rm s}(1)\cdot\int_0^1 d\varphi\ \rho_{\rm s}'(\varphi)\cdot e^{\lambda T_{\rm s}(\varphi)}\right]=0 \qquad (A.47)$$

(see the proof of lemma 3.3.1(1)) can not be satisfied if $\Re(\lambda)\neq 0$ and

$$|\Im(\lambda)|>\tilde{M}\cdot\left[1-e^{-|\Re(\lambda)|\cdot T_{\rm s}(1)}\right]^{-1}, \qquad (A.48)$$

with $\tilde{M}$ given by

$$\tilde{M}:=\frac{1}{T_{\rm s}(1)}\cdot\left[\frac{2}{\omega}\cdot|\psi'(0)|+\left\|\left(\frac{\psi'}{{\rm v_s}}\right)'\right\|_\infty\right]. \qquad (A.49)$$

Using $\rho_{\rm s}(\varphi)=1/(T_{\rm s}(1)\cdot{\rm v_s}(\varphi))$ one can write $\chi(\lambda)$ as

$$\chi(\lambda)=1-e^{-\lambda T_{\rm s}(1)}\left[1-\frac{1}{T_{\rm s}(1)}\cdot\int_0^1 d\varphi\ \frac{\psi'(\varphi)}{{\rm v_s}^2(\varphi)}\cdot e^{\lambda T_{\rm s}(\varphi)}\right]. \qquad (A.50)$$

Let us estimate the integral $C:=\int_0^1 d\varphi\ \psi'(\varphi)\cdot e^{\lambda T_{\rm s}(\varphi)}/{\rm v_s}^2(\varphi)$ appearing in (A.50). For $\lambda\neq 0$ one has

$$C=\frac{1}{\lambda}\int_0^1 d\varphi\ \frac{\psi'(\varphi)}{{\rm v_s}(\varphi)}\frac{d}{d\varphi}e^{\lambda T_{\rm s}(\varphi)}=\frac{1}{\lambda}\frac{\psi'(0)}{{\rm v_s}(0)}\left[e^{\lambda T_{\rm s}(1)}-1\right]-\frac{1}{\lambda}\int_0^1 d\varphi\ e^{\lambda T_{\rm s}(\varphi)}\frac{d}{d\varphi}\frac{\psi'(\varphi)}{{\rm v_s}(\varphi)}, \qquad (A.51)$$

Define $\chi_o(\lambda):=1-\chi(\lambda)$, so that

$$|\chi_o(\lambda)|=e^{-\Re(\lambda)\cdot T_{\rm s}(1)}\cdot|1-C/T_{\rm s}(1)|. \qquad (A.52)$$

Now suppose that $|\Im(\lambda)|>\tilde{M}\cdot\left[1-e^{-|\Re(\lambda)|\cdot T_{\rm s}(1)}\right]^{-1}$. Consider the case $\Re(\lambda)<0$, then using (A.51) one can estimate

$$|C|\leq\frac{1}{|\Im(\lambda)|}\cdot\left[2\cdot\frac{|\psi'(0)|}{{\rm v_s}(0)}+\left\|\left(\frac{\psi'}{{\rm v_s}}\right)'\right\|_\infty\right]=\frac{\tilde{M}\cdot T_{\rm s}(1)}{|\Im(\lambda)|}. \qquad (A.53)$$

Applying (A.53) to (A.52) yields

$$|\chi_o(\lambda)|\geq e^{-\Re(\lambda)\cdot T_{\rm s}(1)}\cdot\left(1-|C|/T_{\rm s}(1)\right)\geq e^{-\Re(\lambda)\cdot T_{\rm s}(1)}\cdot\left(1-\tilde{M}/|\Im(\lambda)|\right)>1, \qquad (A.54)$$

a contradiction to the eigenvalue equation. Now consider the case $\Re(\lambda) > 0$. From (A.51) one can estimate

$$|C| \leq \frac{1}{|\Im(\lambda)|} \cdot \left[2 \cdot \frac{|\psi'(0)|}{\mathrm{v_s}(0)} + \left\| \left(\frac{\psi'}{\mathrm{v_s}} \right)' \right\|_\infty \right] \cdot e^{\Re(\lambda) \cdot T_\mathrm{s}(1)} = \frac{\tilde{M} \cdot T_\mathrm{s}(1)}{|\Im(\lambda)|} \cdot e^{\Re(\lambda) \cdot T_\mathrm{s}(1)}. \tag{A.55}$$

Applying (A.55) to (A.52) yields

$$|\chi_o(\lambda)| \leq e^{-\Re(\lambda) \cdot T_\mathrm{s}(1)} \cdot (1 + |C| \, / T_\mathrm{s}(1)) \leq e^{-\Re(\lambda) \cdot T_\mathrm{s}(1)} + \frac{\tilde{M}}{|\Im(\lambda)|} < 1, \tag{A.56}$$

again a contradiction to the eigenvalue equation. □

A.4.4 The point spectrum for symmetric type I iPRCs

I consider noise-free networks with symmetric type I iPRCs $\psi(\vartheta) = \frac{\psi_o}{2} [1 - \cos(2\pi\vartheta)]$. I present an analytical treatment of the eigenvalue equation (3.26) for the linearized dynamics at the stationary state ρ_s. Let us assume $\psi_o \neq 0$, since otherwise the point spectrum is easily found to be given by (3.46). The corresponding stationary stimulus $\rho_\mathrm{s}(0)$ is given by (3.45). The eigenvalue equation takes the form

$$\int_0^1 \frac{d\vartheta \; e^{\lambda T_\mathrm{s}(\vartheta)}}{\left[\omega + \frac{\psi_o}{2} \rho_\mathrm{s}(0) \left[1 - \cos(2\pi\vartheta) \right] \right]^2} = 0, \tag{A.57}$$

with the travel time $T_\mathrm{s}(\vartheta)$ introduced in lemma 3.3.1 is for $\vartheta \in [0, 1]$ given by

$$T_\mathrm{s}(\vartheta) = \frac{1}{\pi\omega\sqrt{1 + \frac{\psi_o}{\omega}\rho_\mathrm{s}(0)}} \cdot \arctan\left[\sqrt{1 + \frac{\psi_o}{\omega}\rho_\mathrm{s}(0)} \cdot \tan(\pi\vartheta) \right]. \tag{A.58}$$

Note that arctan() is evaluated so that $T_\mathrm{s}(0) = 0$ and $T_\mathrm{s}(\vartheta)$ is continuous in $\vartheta \in [0, 1]$. The left hand side of (A.57) evaluates to

$$\frac{Q(\lambda)}{4\omega\lambda} \cdot \frac{e^{\lambda/(\rho_\mathrm{s}(0)\omega)} - 1}{\lambda^2 + 2\pi^2\psi_o\rho_\mathrm{s}(0)\omega + (2\pi\omega)^2}, \tag{A.59}$$

with

$$Q(\lambda) := (2\lambda)^2 + 2\psi_o\rho_\mathrm{s}(0)\omega(2\pi)^2 + (4\pi\omega)^2 \tag{A.60}$$

and provided that $\lambda \neq 0$ and $\lambda^2 + 2\pi^2\psi_o\rho_\mathrm{s}(0)\omega + (2\pi\omega)^2 \neq 0$, that is $\lambda \notin \{0, \pm i2\pi\omega\rho_\mathrm{s}(0)\}$. Clearly, $\lambda = 0$ does not satisfy the eigenvalue equation (A.57). It is straightforward to show that

$$\lim_{\lambda \to \pm i2\pi\omega\rho_\mathrm{s}(0)} \frac{e^{\lambda/(\rho_\mathrm{s}(0)\omega)} - 1}{\lambda^2 + 2\pi^2\psi_o\rho_\mathrm{s}(0)\omega + (2\pi\omega)^2} = \mp \frac{1}{\rho_\mathrm{s}(0)^2\omega^2} \cdot \frac{i}{4\pi}. \tag{A.61}$$

Consequently, the left hand side of (A.57) tends with $\lambda \to \pm i2\pi\omega\rho_\mathrm{s}(0)$ to

$$-\frac{Q(\pm i2\pi\omega\rho_\mathrm{s}(0))}{4\omega \cdot i2\pi\omega\rho_\mathrm{s}(0)} \cdot \frac{1}{\rho_\mathrm{s}(0)^2\omega^2} \cdot \frac{i}{4\pi}, \tag{A.62}$$

which is non-zero if $\psi_o \neq 0$. Since the left hand side of the eigenvalue equation (A.57) is continuous in λ, one concludes that $\pm i2\pi\omega\rho_\mathrm{s}(0)$ are no eigenvalues of $\mathcal{Q}$. Consequently, the point spectrum $\sigma_\mathrm{p}(\mathcal{Q})$ is given by the solutions of

$$Q(\lambda) \cdot \left[e^{\lambda/(\rho_\mathrm{s}(0)\omega)} - 1 \right] = 0 \tag{A.63}$$

other than $\{0, \pm i2\pi\omega\rho_\mathrm{s}(0)\}$. One finally arrives at the point spectrum (3.46).

A.4.5 The point spectrum for symmetric type II iPRCs

I consider noise-free networks with symmetric type II iPRCs $\psi(\vartheta) = -\psi_0 \cdot \sin(2\pi\vartheta)$. I present an analytical evaluation of the eigenvalue equation (3.26). Let us assume $\psi_o \neq 0$, since otherwise the point spectrum is easily found to be given by (3.48). The corresponding stationary stimulus $\rho_s(0)$ is given by (3.47). The eigenvalue equation takes the form

$$\int_0^1 \frac{d\vartheta \; e^{\lambda T_s(\vartheta)}}{[\omega - \psi_o \rho_s(0) \sin(2\pi\vartheta)]^2} = 0. \tag{A.64}$$

The travel time $T_s(\vartheta)$ introduced in lemma 3.3.1 is for $\vartheta \in [0,1]$ given by

$$T_s(\vartheta) = -\frac{1}{\pi\omega\sqrt{1-(\psi_o\rho_s(0)/\omega)^2}} \cdot \arctan\left[\frac{\psi_o\rho_s(0) - \omega\tan(\pi\vartheta)}{\sqrt{\omega^2 - \psi_o^2\rho_s^2(0)}}\right] + C_s, \tag{A.65}$$

with the constant C_s chosen and arctan() evaluated so that $T_s(0) = 0$ and $T_s(\vartheta)$ is continuous in $\vartheta \in [0,1]$. The left hand side of (A.64) evaluates to

$$\frac{1}{\lambda\omega} \cdot \frac{\lambda^2 + (2\pi\omega)^2 - 2\pi\psi_o\rho_s(0)\lambda}{\lambda^2 + (2\pi)^2(\omega^2 - \psi_o^2\rho_s^2(0))} \cdot \left[e^{\lambda/(\rho_s(0)\omega)} - 1\right], \tag{A.66}$$

provided that $\lambda^2 + (2\pi)^2(\omega^2 - \psi_o^2\rho_s^2(0)) \neq 0$ and $\lambda \neq 0$, that is $\lambda \notin \{0, \pm 2\pi i/T_s(1)\}$. Note that use has been made of the fact that $T_s(1) = 1/(\rho_s(0)\omega)$. It is easy to see that

$$\lim_{\lambda \to \pm(2\pi i\rho_s(0)\omega)} \frac{e^{\lambda/(\rho_s(0)\omega)} - 1}{\lambda^2 + (2\pi)^2(\omega^2 - \psi_o^2\rho_s^2(0))} = \mp\frac{1}{\omega^2\rho_s^2(0)} \cdot \frac{i}{4\pi}. \tag{A.67}$$

Applying (A.67) to the representation (A.66) one finds that the left hand side of (A.64) tends to

$$-\frac{1}{2\pi i\rho_s(0)\omega} \cdot \frac{1}{\omega^2\rho_s^2(0)} \cdot \frac{i}{4\pi} \cdot \frac{\psi_o\omega(2\pi)^2(\psi_o \mp i\omega)}{\omega^2 + \psi_o^2} \neq 0 \tag{A.68}$$

as $\lambda \to \pm 2\pi i/T_s(1)$. As it is continuous in λ, one concludes that $\{\pm 2\pi i/T_s(1)\}$ are no eigenvalues of $\mathcal{Q}$. Clearly, $\lambda = 0$ does not solve (A.64). Thus, the eigenvalues of $\mathcal{Q}$ are the solutions of

$$\left[\lambda^2 + (2\pi\omega)^2 - 2\pi\psi_o\rho_s(0)\lambda\right] \cdot \left[e^{\lambda/(\rho_s(0)\omega)} - 1\right] = 0 \tag{A.69}$$

other than $\{0, \pm 2\pi i/T_s(1)\}$. Solving (A.69) finally yields the point spectrum (3.48).

A.5 A short time propagator for the spectral method

In this section I describe the numerical integration scheme used for the hierarchy (3.44) of bounded order N, that is, with spectral components of order higher than N explicitly set to zero. Let us write the latter as a non-linear, ordinary differential equation

$$\frac{d\boldsymbol{\rho}(t)}{dt} = -\hat{\Omega}\boldsymbol{\rho}(t) + S(\boldsymbol{\rho}(t)) \cdot \hat{\Psi}\boldsymbol{\rho}(t) \tag{A.70}$$

in the vector $\boldsymbol{\rho}(t) := (\rho_n(t))_{|n|\leq N} \in \mathbb{C}^{2N+1}$. The matrices $\hat{\Omega}, \hat{\Psi} \in \mathbb{C}^{(2N+1)\times(2N+1)}$ are defined as

$$\hat{\Omega}_{nm} := \left[in2\pi\omega + (n2\pi)^2 D\right] \cdot \delta_{nm}, \quad \hat{\Psi}_{nm} := -in2\pi \cdot \mathcal{F}_{n-m}(\psi), \tag{A.71}$$

with δ_{nm} being the Kronecker symbol and the indices n, m ranging within $\{-N, .., N\}$. The *stimulus* $S(\boldsymbol{\rho}(t))$ is defined as

$$S(\boldsymbol{\rho}(t)) := \langle 1, \boldsymbol{\rho}(t)\rangle := \sum_{|n|\leq N} \rho_n(t). \tag{A.72}$$

Note that any solution $\boldsymbol{\rho}(t)$ to (A.70), should it exist, is of class $\mathcal{C}^\infty$. Furthermore, one has

$$\boldsymbol{\rho}(t_o+\delta t) = \exp\left[-\delta t\cdot\hat{\Omega} + R(\delta t,\boldsymbol{\rho}(t_o))\cdot\hat{\Psi}\right]\boldsymbol{\rho}(t_o) \tag{A.73}$$

for any *start time* $t_o\in\mathbb{R}$ and *time step* $\delta t\geq 0$, where $R(\delta t,\boldsymbol{\rho}(t_o)) := \int_{t_o}^{t_o+\delta t} dt\; S(\boldsymbol{\rho}(t))$. Note that $R(\delta t,\boldsymbol{\rho}(t_o))$ depends on δt and the initial value $\boldsymbol{\rho}(t_o)$ but not on the initial time t_o, since the differential equation (A.70) is autonomous. Using the Zassenhaus formula (Magnus 1954) and the fact that $R(\delta t,\boldsymbol{\rho}(t_o))\in O(\delta t)$ as $\delta t\to 0^+$, one can write (A.73) as

$$\begin{aligned}\boldsymbol{\rho}(t_o+\delta t) &= e^{-\delta t\cdot\hat{\Omega}}\cdot e^{R(\delta t,\boldsymbol{\rho}(t_o))\cdot\hat{\Psi}}\cdot\exp\left[\delta t\cdot R(\delta t,\boldsymbol{\rho}(t_o))\cdot\frac{1}{2}[\hat{\Omega},\hat{\Psi}]\right]\boldsymbol{\rho}(t_o)+O(\delta t^3)\\ &= e^{-\delta t\cdot\hat{\Omega}}\cdot\left[1+R(\delta t,\boldsymbol{\rho}(t_o))\cdot\hat{\Psi}+R^2(\delta t,\boldsymbol{\rho}(t_o))\cdot\frac{1}{2}\hat{\Psi}^2\right]\\ &\quad\cdot\left[1+\delta t\cdot R(\delta t,\boldsymbol{\rho}(t_o))\cdot\frac{1}{2}[\hat{\Omega},\hat{\Psi}]\right]\boldsymbol{\rho}(t_o)+O(\delta t^3),\end{aligned} \tag{A.74}$$

with $[\hat{\Omega},\hat{\Psi}] := \hat{\Omega}\hat{\Psi}-\hat{\Psi}\hat{\Omega}$ denoting the commutator between $\hat{\Omega}$ and $\hat{\Psi}$. Note that

$$R(\delta t,\boldsymbol{\rho}(t_o)) = S(\boldsymbol{\rho}(t_o))\cdot\delta t + \left.\frac{dS(\boldsymbol{\rho}(\cdot))}{dt}\right|_{t_o}\cdot\frac{\delta t^2}{2}+O(\delta t^3), \tag{A.75}$$

where

$$\left.\frac{dS(\boldsymbol{\rho}(\cdot))}{dt}\right|_{t_o} = \sum_{|n|\leq N}\left.\frac{d\rho_n}{dt}\right|_{t_o} = \left\langle 1,-\hat{\Omega}\boldsymbol{\rho}(t_o)+\langle 1,\boldsymbol{\rho}(t_o)\rangle\cdot\hat{\Psi}\boldsymbol{\rho}(t_o)\right\rangle. \tag{A.76}$$

Inserting (A.76) and (A.75) into (A.74) yields $\boldsymbol{\rho}(t_o+\delta t) = \hat{U}_{\mathrm{s}}(\delta t,\boldsymbol{\rho}(t_o))+O(\delta t^3)$, with the non-linear *short time propagator* $\hat{U}_{\mathrm{s}}(\delta t,\;\cdot\,):\mathbb{C}^{2N+1}\to\mathbb{C}^{2N+1}$ defined by

$$\begin{aligned}\hat{U}_{\mathrm{s}}(\delta t,\boldsymbol{\rho}(t_o)) :=& e^{-\delta t\cdot\hat{\Omega}}\cdot\left[1+R_s(\delta t,\boldsymbol{\rho}(t_o))\cdot\hat{\Psi}+R_s^2(\delta t,\boldsymbol{\rho}(t_o))\cdot\frac{1}{2}\hat{\Psi}^2\right]\\ &\times\left[1+\delta t\cdot R_s(\delta t,\boldsymbol{\rho}(t_o))\cdot\frac{1}{2}[\hat{\Omega},\hat{\Psi}]\right]\boldsymbol{\rho}(t_o),\\ R_s(\delta t,\boldsymbol{\rho}(t_o)) :=& \langle 1,\boldsymbol{\rho}(t_o)\rangle\cdot\delta t+\left\langle 1,-\hat{\Omega}\boldsymbol{\rho}(t_o)+\langle 1,\boldsymbol{\rho}(t_o)\rangle\cdot\hat{\Psi}\boldsymbol{\rho}(t_o)\right\rangle\cdot\frac{\delta t^2}{2}.\end{aligned} \tag{A.77}$$

Setting $\boldsymbol{\rho}^{(0)} := \boldsymbol{\rho}(0)$ as start value and defining the step $\boldsymbol{\rho}^{(n+1)} := \hat{U}_s(\delta t,\boldsymbol{\rho}^{(n)})$, one obtains an explicit fixed-time-step numerical integration scheme for (A.70) of order 2 in δt, with $\boldsymbol{\rho}^{(n)}$ approximating $\boldsymbol{\rho}(n\cdot\delta t)$. The technique follows the ideas of the celebrated Feynman path integral method for the Schrödinger equation (Feynman & Hibbs 1965, Schulman 1981, Wehner & Wolfer 1983).

List of symbols and abbreviations

ODE	Ordinary differential equation.
EOM	Equation of motion.
PRC	Phase Response Curve. See section 1.1.
iPRC	Infinitesimal Phase Response Curve. See section 1.1.
W.l.o.g.	Without loss of generality.
$\mathbb{R}_+$	$:= [0, \infty)$
$\mathbb{K}$	Either $\mathbb{R}$ or $\mathbb{C}$.
Θ	Either S^1 or $\mathbb{R}$.
$\mathbb{N}_0$	$:= \mathbb{N} \cup \{0\}$.
S^1	One-dimensional circle, identified with the quotient group $\mathbb{R}/\mathbb{Z}$.
$\mathbb{T}^m$	m-dimensional torus, identified with the quotient group $\mathbb{R}^m/\mathbb{Z}^m$.
1_A	Indicator function of the set A.
$\Re$	Real part.
$\Im$	Imaginary part.
z^*	Complex conjugate of $z \in \mathbb{C}$.
Π_w	Wrapping operator from functions defined on $\mathbb{R}$ to functions defined on S^1. See definition 1.4.1.
Π_c	Canonical projection $\mathbb{R} \to \mathbb{R}/\mathbb{Z} = S^1$.
$\lvert J \rvert$	$:= \sup J - \inf J$ for any real interval $J \subseteq \mathbb{R}$.
$\#R$	Cardinality of set R.
$\delta(\cdot)$	Dirac distribution.
$\Delta_{\boldsymbol{\vartheta}}$	$:= \sum_{i=1}^n \partial^2_{\vartheta_i}$, Laplace operator in the coordinate $\boldsymbol{\vartheta} = (\vartheta_1, .., \vartheta_n)$.
$\mathscr{B}(Q)$	Borel σ-algebra of the topological space Q.
$\mathcal{L}(E, F)$	Linear space of bounded, linear operators $E \to F$ between the normed spaces E, F.
$\mathcal{L}(E)$	$:= \mathcal{L}(E, E)$.
$r(\mathcal{H})$	Spectral radius of linear operator $\mathcal{H}$ defined on some normed space.
$\sigma(\mathcal{H})$	Spectrum of linear operator $\mathcal{H}$ defined on some linear space.
$\sigma_\mathrm{p}(\mathcal{H})$	Point spectrum of linear operator $\mathcal{H}$ defined on some linear space.
$\lVert\mathcal{H}\rVert$	Operator norm of linear operator $\mathcal{H}$ defined between two normed spaces.
Id	Identity operator.
$\mathrm{span}_\mathbb{K}\{v_i : i \in I\}$	$\mathbb{K}$-Linear hull of vectors $\{v_i\}_{i \in I}$.
$(K, \mathcal{K}, \kappa)$	Measure space over K, with measure κ and σ-algebra $\mathcal{K}$.
$L^q(\kappa)$	Complex L^q-space defined on some measure space $(K, \mathcal{K}, \kappa)$.
$\lVert\cdot\rVert_{L^q(\kappa)}$	L^q-norm on $L^q(\kappa)$.
$(X, \mathscr{B}(X), \mu)$	Finite, strictly positive Borel measure space on the separable metric space X. Introduced in section 1.2 and used in chapter 2.
$\kappa(f)$	$:= \int_K d\kappa\ f$, for any measurable function $f : K \to \mathbb{K}$ defined on some measure space $(K, \mathcal{K}, \kappa)$.

$B_\varepsilon(x)$	Closed ball of radius $\varepsilon \geq 0$ and centre x.
J_β	$:= [0, \beta]$, for $\beta \geq 2$. See proposition 3.2.2.
d	Metric on the space in the given context.
ω	Intrinsic oscillator frequency (strictly positive). See section 1.1.
G	Coupling matrix (for finite networks) or coupling kernel (for networks on metric spaces). See sections 1.1 and 1.2.
D	Diffusion coefficient for oscillator networks with white noise. See section 1.1.
I	Oscillator pulse in pulse-coupled oscillators. See section 1.1.
ρ	Oscillator-phase probability density, identified with the network state. See sections 1.1 and 1.2.
ρ_s	Stationary oscillator phase density. See chapter 3.
A_0	Fixed-point operator in stationary state equation for noise-free networks. See lemma 3.2.1.
A_D	Fixed-point operator in stationary state equation for noisy networks. See proposition 3.2.2.
$\mathcal{Q}$	Evolution operator for linearized dynamics at stationary state in all-to-all spike-coupled noise-free networks. Defined in (3.25), section 3.3.
$\mathcal{Q}_D$	Evolution operator for linearized dynamics at stationary state in all-to-all spike-coupled noisy networks. Defined in (3.39), section 3.3.
$\mathrm{v_s}$	Stationary oscillator phase velocity. See lemma 3.26.
T_s	Stationary travel time. See lemma 3.26.
ψ	iPRC of considered oscillator models. See sections 1.1 and 1.2.
$\Psi(\vartheta_1, \vartheta_2)$	$:= \int_{\vartheta_1}^{\vartheta_2} d\varphi\ \psi(\varphi)$ for $\vartheta_1, \vartheta_2 \in \mathbb{R}$. See section 3.2, page 37.
ζ	Auxiliary function defined in (A.37).
η	Auxiliary function defined in (A.37).
$\operatorname{diam} A$	$:= \sup_{x,y \in A} d(x, y)$, for any subset A of some metric space (X, d).
$\omega_f(\varepsilon)$	$:= \sup \{d(f(x_1), f(x_2)) : x_1, x_2 \in X,\ d(x_1, x_2) \leq \varepsilon\}$, modulus of continuity of function $f : X \to Y$ between two metric spaces X, Y.
$\operatorname{supp} f$	Closure of the set $\{f \neq 0\}$ for any function $f : Q \to \mathbb{K}$ on a topological space Q.
$\operatorname{supp}_{S^1} f$	Closure of $\bigcup_{r \in R} \operatorname{supp} f(r, \cdot)$ for any function $f : R \times S^1 \to \mathbb{K}$ and any set R.
$\operatorname{supp}_{\mathbb{R}} f$	Closure of $\bigcup_{r \in R} \operatorname{supp} f(r, \cdot)$ for any function $f : R \times \mathbb{R} \to \mathbb{K}$ and any set R.
$\operatorname{diam} f$	$:= \operatorname{diam} \operatorname{supp} f$, for any function $f : S^1 \to \mathbb{K}$ or $f : \mathbb{R} \to \mathbb{K}$.
$\operatorname{diam} f$	$:= \operatorname{diam} \operatorname{supp}_{S^1} f$, for any function $f : Y \times S^1 \to \mathbb{K}$ and any set Y.
$\operatorname{diam} f$	$:= \operatorname{diam} \operatorname{supp}_{\mathbb{R}} f$, for any function $f : Y \times \mathbb{R} \to \mathbb{K}$ and any set Y.
$Q_1 \times \cdots \times Q_n$	Cartesian product of topological spaces $Q_1, .., Q_n$, endowed with the product topology.
$X_1 \times \cdots \times X_n$	Cartesian product of metric spaces $(X_1, d_1), .., (X_n, d_n)$, endowed with the product metric $d((x_1, .., x_n), (y_1, .., y_n)) := \sum_{i=1}^n d_i(x_i, y_i)$.
$V_1 \times \cdots \times V_n$	Cartesian product of normed spaces $(V_1, \|\cdot\|_1), .., (V_n, \|\cdot\|_n)$ endowed with the product norm $\|(v_1, .., v_n)\| := \sum_{i=1}^n \|v_i\|$.
$V_1 \oplus \cdots \oplus V_n$	Direct sum of vector spaces $V_1, .., V_n$.
$\mathscr{M}_1 \otimes \cdots \otimes \mathscr{M}_n$	Product σ-algebra on the cartesian product $M_1 \times \cdots \times M_n$, for measurable spaces $(M_1, \mathscr{M}_1), .., (M_n, \mathscr{M}_n)$.
$[\vartheta_1, \vartheta_2]$	Circular arc between $\vartheta_1 \in S^1$ and $\vartheta_2 \in S^1$ (inclusive), covered as one traverses S^1 from ϑ_1 to ϑ_2 in the positive sense. By convention $[\vartheta_1, \vartheta_1] := \{\vartheta_1\}$.

$\|\cdot\|_\infty$	Supremum norm.
$d_\infty(f,g)$	$:= \sup_{s\in S} d(f(s),g(s))$, supremum distance between functions $f,g : R \to Y$ mapping some set R into some metric space (Y,d).
$\mathcal{C}(Q,P)$	Class of continuous functions $f : Q \to P$ between topological spaces Q,P.
$\mathcal{C}_\mathrm{b}(Q,Y)$	Class of bounded, continuous functions $f : Q \to Y$ from the topological space Q to the metric space Y. By default endowed with the supremum metric.
$\mathcal{C}^k(M,\mathbb{K})$	Class of k-times continuously differentiable, real (or complex) functions on some smooth manifold M.
$\mathcal{C}^k(M)$	$:= \mathcal{C}^k(M,\mathbb{C})$.
$\mathcal{C}^k(M,\mathbb{R}_+)$	Class of k-times continuously differentiable, real functions on some smooth manifold M with values in $\mathbb{R}_+$.
$\mathcal{C}^k_\mathrm{zm}(S^1)$	$:= \{f \in \mathcal{C}^k(S^1,\mathbb{C}) : \int_{S^1} d\varphi\ f(\varphi) = 0\}$.
$\mathcal{C}_0(Q,\mathbb{K})$	Class of continuous functions $f : Q \to \mathbb{K}$ on a topological space Q with compact support.
$\mathcal{C}_\mathrm{u}(X,Y)$	Class of uniformly continuous functions $X \to Y$ between two metric spaces X,Y.
$\mathcal{C}_\mathrm{u,b}(X,Y)$	Class of bounded, uniformly continuous functions $X \to Y$ between two metric spaces X,Y. By default endowed with the supremum metric.
$\mathcal{M}(M,N)$	Class of measurable functions $M \to N$ between two measurable spaces $(M,\mathscr{M}),(N,\mathscr{N})$.
$\mathcal{M}_\mathrm{b}(M,Y)$	Class of measurable, bounded functions $M \to Y$ from a measurable space $(M,\mathscr{M})$ into a metric space Y. By default endowed with the supremum metric.
Ω_{o,S^1}	Function space defined in (1.22).
$\Omega_{o,\mathbb{R}}$	Function space defined in (1.22).
Ω_{S^1}	Function space defined in (1.23).
$\Omega_\mathbb{R}$	Function space defined in (1.23).
$\mathcal{F}_n(f)$	$:= \int_{S^1} d\varphi\ f(\varphi)\cdot e^{-in2\pi\cdot\varphi}$, n-th Fourier component of $f : S^1 \to \mathbb{K}$.
$f * g$	Convolution of two measurable functions $f,g : K\times K \to \mathbb{K}$ on some σ-finite measure space $(K,\mathcal{K},\kappa)$, defined as $(f*g)(x,y) := \int_K d\kappa(z)\ f(x,z)\cdot g(z,y)$.

Bibliography

Abbott L & van Vreeswijk C 1993 *Phys. Rev. E* **48**(2), 1483.

Acebrón J, Bonilla L, Vicente C, Ritort F & Spigler R 2005 *Rev. Mod. Phys.* **77**(1), 137.

Achuthan S & Canavier C 2009 *J. Neurosci.* **29**(16), 5218–5233.

Ambrosio L, Da Prato G & Mennucci A 2011 *Introduction to Measure Theory and Integration* PPUNTI Lecture Notes Springer.

An Z, Zhu H, Li X, Xu C & Xu Y 2011 *IEEE T. Ind. Electron.* **58**(6).

Anderson E, Bai Z, Bischof C, Blackford S, Demmel J, Dongarra J, Du Croz J, Greenbaum A, Hammarling S, McKenney A & Sorensen D 1999 *LAPACK Users' Guide* third edn Society for Industrial and Applied Mathematics Philadelphia, PA.

Appell J, Kalitvin A & Zabreko P 2000 *Partial Integral Operators and Integro-Differential Equations* Pure and Applied Mathematics M. Dekker.

Apple Inc. 2011 'Random, part of bsd libc' Standard C Library, Darwin 10.8.0.

Arenas A, Díaz-Guilera A, Kurths J, Moreno Y & Zhou C 2008 *Phys. Rep.* **469**(3), 93–153.

Ariaratnam J 2002 Collective Dynamics of the Winfree Model of Coupled Nonlinear Oscillators PhD thesis Cornell University.

Ariaratnam J & Strogatz S 2001 *Phys. Rev. Lett.* **86**(19), 4278–4281.

Basnarkov L & Urumov V 2009 *J. Stat. Mech.* **2009**(10), P10014.

Berge C 1976 *Graphs and Hypergraphs* North-Holland Mathematical Library North-Holland Publishing Company.

Beurle R 1956 *Philos. T. R. Soc. B* **240**(669), 55–94.

Bogachev V 2006 *Measure Theory* Vol. 1 & 2 Springer.

Bonilla L 1987 *J. Stat. Phys.* **46**(3), 659–678.

Bonilla L L, Neu J C & Spigler R 1992 *J. Stat. Phys.* **67**, 313–330.

Brézis H 2010 *Functional Analysis, Sobolev Spaces and Partial Differential Equations* Springer.

Brézis H & Lieb E 1983 *P. Am. Math. Soc.* **88**(3), 486–490.

Burden R & Faires J 2001 *Numerical Analysis* Brooks Cole.

Chawanya T, Aoyagi T, Nishikawa I, Okuda K & Kuramoto Y 1993 *Biol. Cybern.* **68**(6), 483–490.

Crawford J D & Davies K 1999 *Physica D* **125**(1-2), 1 – 46.

Cui J, Canavier C C & Butera R J July 2009 *J. Neurophysiol.* **102**(1), 387–398.

Dawson D A 1983 *J. Stat. Phys.* **31**, 29–85.

Deimling K 1977 *Ordinary Differential Equations in Banach Spaces* Lecture Notes in Mathematics Springer.

Desmaisons D, Vincent J & Lledo P 1999 *J. Neurosci.* **19**(24), 10727–10737.

Drachman D 2005 *Neurology* **64**(12), 2004–2005.

Eckhardt B, Ott E, Strogatz S H, Abrams D M & McRobie A 2007 *Phys. Rev. E* **75**, 021110.

Eisner T 2010 *Stability of Operators and Operator Semigroups* Operator Theory: Advances and Applications Birkhäuser.

Ermentrout B 1996 *Neural Comput.* **8**(5), 979–1001.

Ermentrout G & Kopell N 1990 *SIAM J. Appl. Math.* pp. 125–146.

Feynman R & Hibbs A 1965 *Quantum Mechanics and Path Integrals* International Series in Pure and Applied Physics McGraw-Hill.

Frank T 2005 *Nonlinear Fokker-Planck Equations: Fundamentals and Applications* Springer.

Frobenius G 1912 *Über Matrizen aus Nicht Negativen Elementen* Königliche Akademie der Wissenschaften.

Galán R, Ermentrout G & Urban N 2005 *Phys. Rev. Lett.* **94**(15), 158101.

Gentle J 2003 *Random Number Generation and Monte Carlo Methods* Statistics and Computing Springer.

Giannuzzi F, Marinazzo D, Nardulli G, Pellicoro M & Stramaglia S 2007 *Phys. Rev. E* **75**, 051104.

Goel P & Ermentrout B 2002 *Physica D* **163**(3-4), 191–216.

Granada A, Hennig R, Ronacher B, Kramer A & Herzel H 2009 *Method. Enzymol.* **454**, 1–27.

Griffith J 1963 *B. Math. Biol.* **25**(1), 111–120.

Grobler J J 1987 *in* 'Indagationes Mathematicae (Proceedings)' Vol. 90 Elsevier pp. 381–391.

Guckenheimer J 1975 *J. Math. Biol.* **1**, 259–273.

Guckenheimer J & Holmes P 1990 *Nonlinear Oscillations, Dynamical Systems, and Bifurcations of Vector Fields* Applied Mathematical Sciences Springer.

Hansel D, Mato G & Meunier C 1995 *Neural Comput.* **7**(2), 307–337.

Hildebrand E J, Buice M A & Chow C C 2007 *Phys. Rev. Lett.* **98**, 054101.

Hollinger H 1962 *J. Chem. Phys.* **36**, 3208.

Jalife J & Antzelevitch C 1979 *Science* **206**(4419), 695–697.

Jalife J & Moe G 1979 *Circ. Res.* **45**(5), 595–608.

Jalife J, Slenter V, Salata J & Michaels D 1983 *Circ. Res.* **52**(6), 642–656.

Kandel E, Schwartz J & Jessell T 2000 *Principles of Neural Science* McGraw-Hill, Health Professions Division.

Katriel G 2005 *Discret. Contin. Dyn. B* **5**(2), 353–364.

Kelley J 1955 *General Topology* Graduate Texts in Mathematics Springer.

Kelley J & Srinivasan T 1988 *Measure and Integral* Graduate Texts in Mathematics Springer.

Kiss I Z, Zhai Y & Hudson J L 2005 *Phys. Rev. Lett.* **94**, 248301.

Kolmogoroff A 1931 *Math. Ann.* **104**, 415–458.

Kuramoto Y 1975 *in* 'International Symposium on Mathematical Problems in Theoretical Physics' Springer pp. 420–422.

Kuramoto Y 1991 *Physica D* **50**(1), 15–30.

Kuramoto Y & Arakai H 1984 *Chemical Oscillations, Waves and Turbulence* Springer.

Lagier S, Carleton A & Lledo P 2004 *J. Neurosci.* **24**(18), 4382–4392.

Lago-Fernández L F, Corbacho F J & Huerta R 2001 *Neural Networks* **14**, 687 – 696.

Laing C 2009 *Physica D* **238**(16), 1569–1588.

Langer R E 1931 *Bull. Amer. Math. Soc.* **37**, 213–239.

Lax P 2002 *Functional Analysis* Pure and Applied Mathematics Wiley.

Lee W S, Restrepo J G, Ott E & Antonsen T M 2011 *Chaos* **21**, 023122–023122–14.

Levy M, Martin P, Iano T & Zieske H 1970 *Am. J. Physiol.* **218**(5), 1256–1262.

Louca S & Atay F M n.d.*a* Spatially structured networks of pulse-coupled phase oscillators on metric spaces. To be published.

Louca S & Atay F M n.d.*b* Stationary states in infinite networks of spiking oscillators with noise. To be published.

Magnus W 1954 *Comm. Pure Appl. Math.* **7**(4), 649–673.

Mardia K & Jupp P 2000 *Directional Statistics* Wiley Series in Probability and Statistics Wiley.

Meiss J 2007 *Differential Dynamical Systems* number 1 *in* 'Mathematical Modeling and Computation' Society for Industrial and Applied Mathematics.

Michel A, Hou L & Liu D 2008 *Stability of Dynamical Systems: Continuous, Discontinuous, and Discrete Systems* Systems & Sontrol Birkhaüser.

Milstein G 1995 *Numerical Integration of Stochastic Differential Equations* Vol. 313 Springer.

Netoff T, Acker C, Bettencourt J & White J 2005 *J. Comput. Neurosci.* **18**(3), 287–295.

Nicolaescu L 2007 *Lectures on the Geometry of Manifolds* World Scientific.

Ota K, Omori T, Watanabe S, Miyakawa H, Okada M & Aonishi T 2011 *Phys. Rev. E* **84**, 041902.

Perez C & Ritort F 1997 *J. Phys. A* **30**, 8095.

Perron O 1907 *Math. Ann.* **64**(2), 248–263.

Pólya G 1918 *Math. Z.* **2**(3), 352–383.

Press W, Teukolsky S, Vetterling W & Flannery B 1997 *Numerical Recipes in C: The Art of Scientific Computing* Cambridge University Press.

Preyer A J & Butera R J 2005 *Phys. Rev. Lett.* **95**, 138103.

Quinn D D, Rand R H & Strogatz S H 2007 *Phys. Rev. E* **75**, 036218.

Risken H 1996 *The Fokker-Planck Equation: Methods of Solution and Applications* Vol. 18 Springer.

Sakaguchi H 1988 *Prog. Theor. Phys.* **79**(1), 39–46.

Schaefer H 1974 *Banach Lattices and Positive Operators* Grundlehren der Mathematischen Wissenschaften Springer.

Schulman L 1981 *Techniques and Applications of Path Integration* Wiley-Interscience Publication Wiley.

Schultheiss N W, Edgerton J R & Jaeger D 2010 *J. Neurosci.* **30**(7), 2767–2782.

Shiogai Y & Kuramoto Y 2003 *Prog. Theor. Phys. Supp.* **150**, 435–438.

Silverman B 1986 *Density Estimation for Statistics and Data Analysis* Monographs on Statistics and Applied Probability Chapman and Hall.

Smeal R, Ermentrout G & White J 2010 *Philos. T. Roy. Soc. B* **365**(1551), 2407–2422.

Sompolinsky H, Golomb D & Kleinfeld D 1991 *Phys. Rev. A* **43**, 6990–7011.

Strogatz S 2000 *Physica D* **143**(1-4), 1–20.

Strogatz S H, Abrams D M, McRobie A, Eckhardt B & Ott E 2005 *Nature* **438**, 43–44.

Strogatz S H & Mirollo R E 1991 *J. Stat. Phys.* **63**, 613–635.

Strogatz S & Stewart I 1993 *Sci. Am.* **269**(6), 102–109.

Swade R 1969 *J. Theor. Biol.* **24**(2), 227–239.

Tateno T & Robinson H 2007 *Biophys. J.* **92**(2), 683–695.

Trees B R, Saranathan V & Stroud D 2005 *Phys. Rev. E* **71**, 016215.

Wang D 1995 *IEEE T. Neural Networ.* **6**(4), 941–948.

Watts D J & Strogatz S H 1998 *Nature* **393**, 440–442.

Wehner M & Wolfer W 1983 *Phys. Rev. A* **27**(5), 2663.

Wiesenfeld K, Colet P & Strogatz S H 1998 *Phys. Rev. E* **57**, 1563–1569.

Wilmanski K 2008 *Continuum Thermodynamics: Foundations* Series on Advances in Mathematics for Applied Sciences World Scientific.

Winfree A 1967 *J. Theor. Biol.* **16**(1), 15–42.

Winfree A 2001 *The Geometry of Biological Time* Interdisciplinary Applied Mathematics: Mathematical Biology Springer.

Wu C W 2005 *Nonlinearity* **18**(3), 1057.

Zaanen A 1997 *Introduction to Operator Theory in Riesz Spaces* Springer.

List of Figures

Index